ถังปฏิกรณ์ชีวภาพอากาศยกเชิงแสงแบบแผ่นเรียบขนาดใหญ่ เพื่อการเพาะเลี้ยงเซลล์เวเจทเททีฟ ความหนาแน่นสูงของฮีมาโทคอคคัส พลูเวียลิส

นายกีรติ อิสระพายัพ

วิทยานิพนธ์นี้เป็นส่วนหนึ่งของการศึกษาตามหลักสูตรปริญญาวิศวกรรมศาสตรดุษฎีบัณฑิต
สาขาวิชาวิศวกรรมเคมี ภาควิชาวิศวกรรมเคมี
คณะวิศวกรรมศาสตร์ จุฬาลงกรณ์มหาวิทยาลัย
ปีการศึกษา 2554

LARGE SCALE FLAT PANEL AIRLIFT PHOTOBIOREACTOR FOR HIGH DENSITY CULTIVATION OF VEGETATIVE CELL, *Haematococcus pluvialis*

Mr. Kerati Issarapayup

A Dissertation Submitted in Partial Fulfillment of the Requirements
for the Degree of Doctor of Engineering Program in Chemical Engineering
Department of Chemical Engineering
Faculty of Engineering
Chulalongkorn University
Academic Year 2011

Thesis Title	LARGE SCALE FLAT PANEL AIRLIFT PHOTOBIOREACTOR FOR HIGH DENSITY CULTIVATION OF VEGETATIVE CELL, *Haematococcus pluvialis*
By	Mr. Kerati Issarapayup
Field of Study	Chemical Engineering
Thesis Advisor	Associate Professor Prasert Pavasant, Ph.D.
Thesis Co-advisor	Sorawit Powtongsook, Ph.D.

Accepted by the Faculty of Engineering, Chulalongkorn University in Partial Fulfillment of the Requirements for the Doctoral Degree

…… Dean of the Faculty of Engineering
(Associate Professor Boonsom Lerdhirunwong, Dr.lng)

THESIS COMMITTEE

…….. Chairman
(Associate Professor Muenduen Phisalaphong, Ph.D.)

…….……. Thesis Advisor
(Associate Professor Prasert Pavasant, Ph.D.)

…….……. Thesis Co-advisor
(Sorawit Powtongsook, Ph.D.)

…….. Examiner
(Associate Professor Artiwan Shotipruk, Ph.D.)

…….. Examiner
(Associate Professor Sarawut Rimdusit, Ph.D.)

…….. External Examiner
(Assistant Professor Marasri Ruengjitchatchawalya, Ph.D.)

กีรติ อิสระพายัพ : ถังปฏิกรณ์ชีวภาพอากาศยกเชิงแสงแบบแผ่นเรียบขนาดใหญ่เพื่อการเพาะเลี้ยงเซลล์เวเจทเททีฟความหนาแน่นสูงของฮีมาโทคอคคัส พลูเวียลิส (LARGE SCALE FLAT PANEL AIRLIFT PHOTOBIOREACTOR FOR HIGH DENSITY CULTIVATION OF VEGETATIVE CELL, *Haematococcus pluvialis*)
อ. ที่ปรึกษาวิทยานิพนธ์หลัก: รศ.ดร. ประเสริฐ ภวสันต์, อ.ที่ปรึกษาวิทยานิพนธ์ร่วม: ดร. สรวิศ เผ่าทองศุข, 119 หน้า.

งานวิจัยนี้ทำการศึกษาการเพาะเลี้ยงเซลล์จุลสาหร่ายฮีมาโทคอคคัส พลูเวียลิส (NEIS-144) ในถังปฏิกรณ์ชีวภาพเชิงแสงแบบอากาศยกชนิดแผ่นเรียบ (Flat panel airlift photobioreactor) ปริมาตร 17 50 90 และ 200 ลิตร โดยดำเนินการทดลองในห้องควบคุมอุณภูมิไอน้ำ (27±3 องศาเซลเซียส) และสภาวะการเพาะเลี้ยง โดยการป้อนอากาศที่ผสมก๊าซคาร์บอนไดอกไซด์ 1 เปอร์เซนต์โดยปริมาตรเข้าสู่ระบบ ที่ความเร็ว 0.4 เซนติเมตรต่อวินาที และ สัดส่วนของพื้นที่ไม่ให้อากาศต่อพื้นที่ให้อากาศเท่ากับ 0.4 นอกจากนั้นยังได้ทำการศึกษาอุทกพลศาสตร์ของระบบถังปฏิกรณ์ชีวภาพเชิงแสงแบบอากาศยกชนิดแผ่นเรียบ อาทิ เช่น ค่าความเร็วของของเหลว และค่าการถ่ายเทมวลสารระหว่างก๊าซและของเหลว เป็นต้น ซึ่งผลของการศึกษาอุทกพลศาสตร์ในถังปฏิกรณ์ขนาด 17 ลิตร พบว่าค่าสัดส่วนของพื้นที่ไม่ให้อากาศต่อพื้นที่ให้อากาศเท่ากับ 0.4 ส่งผลให้ค่าความเร็วของของเหลวในระบบน้อยที่สุด (1.2 - 6.3 เซนติเมตรต่อวินาที) ในทางตรงกันข้ามส่งผลต่อค่าการถ่ายเทมวลสารระหว่างก๊าซและของเหลวในระบบสูงที่สุด (0.000358 – 0.0066 ต่อวินาที) ซึ่งเป็นสภาวะที่เหมาะสมต่อการเพาะเลี้ยงเซลล์จุลสาหร่าย ฮีมาโทคอคคัส พลูเวียลิส ในระยะเซลล์เวเจทเททีฟ การศึกษาการเพาะเลี้ยงเซลล์จุลสาหร่ายชนิดนี้ นอกจากการทดลองเพื่อหาสภาวะที่เหมาะสมเพื่อเพิ่มมวลการผลิตของจุลสาหร่ายแล้ว ยังได้รวมการวิเคราะห์ค่าความคุ้มทุนทางเศรษฐศาสตร์ของการเพาะเลี้ยงเซลล์จุลสาหร่ายอีกด้วย การทดลองที่ผ่านมาพบว่ากระบวนการเพาะเลี้ยงเซลล์จุลสาหร่ายนี้ต้องใช้พลังงานสูงในการดำเนินการผลิต ซึ่งส่งผลให้ต้นทุนการผลิตสูง งานวิจัยนี้จึงได้เสนอวิธีช่วยลดต้นทุนดังกล่าวคือ ดำเนินการเพาะเลี้ยงในถังปฏิกรณ์ขนาด 50 ลิตร โดยใช้แสงธรรมชาติแทนการใช้หลอดไฟฟลูออเรสเซนต์ ซึ่งพบว่าสามารถลดรายจ่ายของกระบวนการผลิตต่อปีได้ถึง 307 ดอลล่าร์ต่อสาหร่ายแห้ง 0.5 กิโลกรัม อย่างไรก็ตาม การใช้แสงธรรมชาติส่งผลให้ความหนาแน่นสูงสุดของเซลล์ลดลง (387 x 10^4 เป็น 140 x 10^4 เซลล์ต่อมิลลิลิตร) และอัตราการเจริญเติบโตจำเพาะลดลง (จาก 0.63 เป็น 0.53 ต่อวัน) นอกจากนั้น การขยายขนาดถังปฏิกรณ์เพื่อเพิ่มปริมาณเซลล์ผลผลิต พบว่าการขยายขนาดจาก 17 เป็น 200 ลิตร สามารถลดรายจ่ายของกระบวนการผลิต โดยการดำเนินการในถังปฏิกรณ์ขนาด 17 ลิตร เพื่อให้ได้ผลผลิตเซลล์แห้งที่ต้องการ 0.5 กิโลกรัมนั้น มีค่ารายจ่ายต่อปี เท่ากับ 197 ดอลล่าร์ ในขณะที่ดำเนินการในถังปฏิกรณ์ขนาด 200 ลิตร มีค่ารายจ่ายต่อปี ลดลงเท่ากับ 121 ดอลล่าร์ อย่างไรก็ตาม การดำเนินการผลิตในถังปฏิกรณ์ขนาด 200 ลิตร ส่งผลให้ความหนาแน่นสูงสุดของเซลล์ลดลง (290 x 10^4 เป็น 147 x 10^4 เซลล์ต่อมิลลิลิตร) และอัตราการเจริญเติบโตจำเพาะลดลง (จาก 0.49 เป็น 0.47 ต่อวัน) เมื่อเทียบกับการดำเนินการผลิตในถังปฏิกรณ์ขนาด 17 ลิตร แนวทางสุดท้ายคือการนำสารอาหารกลับมาใช้เพาะเลี้ยงเซลล์สาหร่ายใหม่ ผลการประเมินพบว่าวิธีการนี้มีประสิทธิภาพไม่เพียงพอที่จะช่วยลดค่าใช้จ่ายของกระบวนการผลิตอย่างมีนัยสำคัญ โดยสามารถลดรายจ่ายของกระบวนการผลิตต่อปีได้เพียง 8 ดอลล่าร์ต่อสาหร่ายแห้ง 0.5 กิโลกรัม ในขณะที่อัตราการเจริญเติบโตของเซลล์ลดลงถึง 30 เปอร์เซ็นต์

ภาควิชา วิศวกรรมเคมี ลายมือชื่อนิสิต.....
สาขาวิชา วิศวกรรมเคมี ลายมือชื่อ อ.ที่ปรึกษาวิทยานิพนธ์หลัก.....
ปีการศึกษา 2554 ลายมือชื่อ อ.ที่ปรึกษาวิทยานิพนธ์ร่วม.....

5171840021: MAJOR CHEMICAL ENGINEERING
KEYWORDS: PHOTOBIOREACTOR / BIOREACTOR / MICROALGA

KERATI ISSARAPAYUP: LARGE SCALE FLAT PANEL AIRLIFT PHOTOBIOREACTOR FOR HIGH DENSITY CULTIVATION OF VEGETATIVE CELL, *Haematococcus pluvialis*. ADVISOR: ASSOC. PROF. PRASERT PAVASANT, Ph.D., CO-ADVISOR: SORAWIT POWTONGSOOK, Ph.D., 119 pp.

The cultivation of green vegetative cells of *Haematococcus pluvialis* NIES-144 was carried out in flat panel airlift photobioreactors (FP-ALPBRs) of different sizes, i.e. 17, 50, 90 and 200L, operated in the evaporative room where the temperature was controlled at 27±3 ^{o}C. Normal cultivation was carried out with a superficial gas velocity (U_{sg}) of 0.4 cm s^{-1} mixed with 1%vol CO_2, and a ratio of downcomer and riser cross sectional area (A_d/A_r) of 0.4. The hydrodynamic characteristics for FP-ALPBR system, i.e. liquid velocity and overall volumetric gas-liquid mass transfer, were also investigated. The hydrodynamic study reveals that the system with A_d/A_r of 0.4 provided the lowest liquid velocity for 17L ALPBR system (U_l ranged from 1.2-6.3 cms^{-1}), and the greatest amount of overall volumetric mass transfer coefficient (K_La ranged from 0.000358 to 0.0066 s^{-1}). This condition provides the lowest shear stress which makes it suitable for the green vegetative stage of *H. pluvialis*. Several alternative growth options were proposed in order to enhance mass production of green vegetative cell of *H. pluvialis* and also to cut down the total operating cost for such algal cultivation. The use of natural lighting was inevitable to avoid the high electricity cost, and replacing artificial lighting with natural light was found to decrease the total production cost by as much as 307 US$ per 0.5 kg dry cell in the 50L FP-ALPBR. Nevertheless, the lack of control of diurnal light intensity resulted in a drop in the growth performance with cell density decreasing from 387 x 10^4 to 140 x 10^4 cell mL^{-1}, and specific growth rate from 0.63 to 0.53 day^{-1}. Reactor sizes (under natural light operation) appeared to be significant for the profitability of the system, and enlarging the FP-ALPBR from 17 to 200L required significantly lower total costs of production per year (121 US$ per 0.5 kg dry cell for 200L culture when compared to 197 US$ per 0.5 kg dry cell for the 17L system). Unfortunately this had to be compensated by a drop in the growth performance with cell density decreasing from 290 x 10^4 to 147 x 10^4 cell mL^{-1} and specific growth rate from 0.49 to 0.47 day^{-1}. Finally, the reuse of spent medium (under natural light operation) with proper replenishment of nutrients caused an unexpected around 30 % drop in the growth rate and did not seem to provide an attractive response as the total cost per 0.5 kg dry cell was only saved by 8 US$ a year.

Department: Chemical Engineering Student's Signature.....
Field of Study: Chemical Engineering Advisor's Signature.....
Academic Year: 2011 Co-advisor's Signature.....

ACKNOWLEDGEMENTS

This small confined page means overwhelmingly a lot to me because here I am allowed to portray all my attitudes toward those who profited me to draw the vividly successful works. Without further ado, almost 4 years that I have spent that time pursuing the Ph.D. program in Chemical Engineering, Chulalongkorn University have been such a productive moment I have ever had. During that time, I was introduced to meet a variety of states of life where was such a memorable moment. Thus far, having been flooded by considerably sophisticated experiences, I gradually become a mature and solid person with inquisitive mind. Now, I myself was proven that this logic has been ever existence **"There are nothings that perseverance cannot win"**. In fact, I can't be what I really am today unless I received a lot of hands from those significant persons.

I would particularly like to single out the best advisor ever, **Associate Professor Prasert Pavasant**, who not only did provide enthusiastic encouragement but also, over half decade, has kept his concentration onto my work and never held it against me on my passed mistakes. Having him as a navigator, I never once feared to lose my future track. Thank you sir

Another particularly significant person for my issue is **Dr. Sorawit Powtongsook**, the best co-advisor ever, who has properly harnessed the power of his useful knowledge to broaden my eyes and never mounted pressure on me. Also, thank you for his understanding, invaluable supports and kind guidance throughout my Ph.D. program.

This research has been supported and funded by **Thailand Graduate Institute of Science and Technology (TGIST).** Moreover, I would like to thank the Center of Excellence for Marine Biotechnology (at Chulalongkorn University) National Center of Genetic Engineering and Biotechnology for allowing me to setup the experimental apparatus and using the accessories. I thank them all.

Special thanks could also be directed towards my special persons. I would like to thank **Dr. Porntip Wongsuchoto** and **Dr. Tansiphon Janhom** for kind helps and warms for taking care of me as like as my sister. I could hardly have completed the thesis without my faithful friends: **Puchong Sri-Uam**, **Chenwit Linthong**, **Watadta Ritcharoen**, **Dr.Duangkamol Ruen-ngam**, **Panu Panitchakarn**, **Chattip Prommuak**, and **Woradej Poonkum**. Thank you for being such wonderful and close friends who were always available when I needed helps. Most of all, I would like to express love and thanks to my family, especially **My grandmother**, for their precious love, inspiration and supports that have propelled me to the completion of this epic work and all achievements to come in my life.

CONTENTS

Page

Page

Page

List of Tables

List of Figures

CHAPTER I
INTRODUCTION

1.1 Motivations

Apart from the traditional raceway pond, the enhancement of algal mass production conducted in a specified photobioreactor has been widely achieved. Particularly, an airlift photobioreactor (ALPBR) is a gas-liquid contacting device in which its broad application in biotechnology perspectives has recently grown significantly. The advantageous performances, for instance, low and homogeneous distribution of hydrodynamic shear, simple construction, well defined fluid flow pattern and high mass transfer rate, have made the airlift quite attractive as an alternative photobioreactor. Thus, ALPBRs were used to cultivate several types of single cell algae, e.g. sea water diatom *Chaetoceros calcitrans* (used as shrimp larvae live feed) (Krichnavaruk et al., 2005 and 2007), *Skeletonema costatum* (Monkunsit et al., 2011), *Entomoneis sp.* (used as shrimp larvae feed) and a green alga, *Chlorella sp* (used as fish larvae feed). Moreover, airlift was also proven suitable for boosting the mass cell production of *Haematococcus pluvialis* in green vegetative stage (Harker et al., 1996a; Vega-Estrada et al., 2005; Garcia et al., 2006; Kaewpintong et al., 2006 and Ranjbar et al., 2008;) as it generates low shear stress which, on the other hand, is inherited from conventional stirred tank photobioreactors (Choi et al., 2003).

H. pluvialis is an outstanding microorganism capable of producing an antioxidant compound, astaxanthin. As much as 1.5-3.0% by weight, astaxanthin could be accumulated in the cells if proper inductive conditions are applied (Lorenz and Cysewski, 2000). Astaxanthin produced from *H. pluvialis* is proved to be naturally compatible to human acceptability and its versatile applications, thus leading to high market price (approximately $2,500-3,000 per kg). Research perspective for the production of astaxanthin from *H.pluvialis* is generally separated into two categories. The first part is to deal with the cultivation of high density culture and the

second involves the induction and harvesting. The focus of this work was on the development of the high efficiency photobioreactor for *H. pluvialis* mass cultivation. Recent work has shown that *H.pluvialis* could be successfully cultivated in an airlift photobioreactor where a high growth rate could be achieved in a semi-continuous operation (Issarapayup et al., 2009). However, the work was only limited to a small scale airlift system. There was evidently found at that time that the management of the large scale airlift for such culture was inevitable if this is to be moved on further to a commercial scale system.

In fact, the studies of enhancement in *H. pluvialis* mass production in large scale system have been scarce. Most of the works have put their interest on the optimization of stress/inductive conditions in order to convert the green vegetative cells to the red cyst, and also the evaluation of extraction methods to release astaxanthin from cyst. There are a few successful cases on the implementation of ALPBR for the mass cultivation of green vegetative *H. pluvialis*, unfortunately all were confined to small scale reactors. The highest cell density reported was available from Ranjbar et al. (2008) who achieved the highest cell density of 70 x 10^5 cell mL^{-1} from 1L ALPBR, but the attained specific growth rate from their work was quite slow at 0.2 d^{-1}. Kaewpintong et al. (2006) successfully achieved the cultivation of vegetative cells of *H. pluvialis* in the small scale 3L ALPBR with a maximum cell density of 7.7 x 10^5 cell mL^{-1} and with the maximum specific growth rate of 0.45 d^{-1}. Similarly, Vega-Estrada et al. (2005) accomplished the maximum cell density of 11 x 10^5 cell mL^{-1} with specific growth rate of 0.26 d^{-1} in 2L split-cylinder internal loop ALPBR. Recently, Issarapayup et al. (2009) reported the optimized growth conditions for the cultivation of *H. pluvialis* in a 17L developed photobioreactor defined as flat panel airlift photobioreactors (FP-ALPBRs) operated in evaporative room with artificial light supplement. This was performed with a maximum growth rate and cell density of 0.52 d^{-1} and 4.1 x 10^5 cell mL^{-1}, respectively.

The goal of this research was set out to develop a large scale cultivation system for the vegetative cell of *H.pluvialis*. The performance was measured in terms of maximum cell density and high specific growth rate. The flat panel airlift

photobioreactors (FP-ALPBRs) was proposed as a target airlift type of photobioreactor for this study. FP-ALPBR has been designed as a rectangular column and was separated internally by a plate to riser and downcomer. The length of this FP-ALPBR could be freely adjusted to accommodate the requirement for desired volumes (17, 50, 90 and 200L). Besides, the investigation of the hydrodynamic properties of FP-ALPBRs was also carried out (overall volumetric mass transfer coefficient, liquid velocity, and gas hold up) to find the relationship between the system behavior and the cell growth. In addition, a variety of operating conditions for improving an algal growth (in vegetative stage of *H. pluvialis*) was proposed. Finally, a break down of economical evaluation of each operating conditions for algal mass production was deliberately computed. In addition, several options on how to save cost during the cultivation of the alga were scrutinized. For example, the use of natural and artificial light as a light source for algal growth and the recycle of algal medium in consequent batches (with and without replenishment of nutrients) were thoroughly investigated.

1.2 Objectives

The objective of this work was specifically set to investigate the cultivation of *H. pluvialis* in a large scale volume of flat panel airlift photobioreactors (FP-ALPBRs). These mainly included three strategies:

(i) to study hydrodynamics characteristics of FP-ALPBR (liquid circulation, gas holdup and mass transfer) of the FP-ALPBR

(ii) to examine the efficiency of FP-ALPBR on the production of high density vegetative cells of *H. pluvialis*

(iii) to evaluate economic assessment and to propose alternative possibilities that reduce the production costs and improve the economics of this system

1.3 Scopes of this work

1) Hydrodynamics characteristics (liquid circulation, gas holdup and mass transfer)

- The flat panel airlift bioreactors employed in this work were 17, 90 and 200L in volume.
- The ratio between the downcomer and riser cross sectional area (A_d/A_r) was varied from 0.4, 1.5, and 3.0, respectively.
- The superficial gas velocity (U_{sg}) was approximately controlled at 0.2, 0.4, 1.5, and 3.0 cm.s^{-1}, respectively.
- F1 medium was used as liquid phase and ambient air as gas phase.
- All experiments were performed at controlled temperature in the evaporative room in which the temperature was in range of 27±3 ^{o}C.

2) The optimal conditions for sustained high production of vegetative cells of *H. pluvialis*

- The ratio between the downcomer and riser cross sectional area (A_d/A_r) was at 0.4 (the optimal ratio previously determined by Issarapayup et al., 2009).
- The superficial gas velocity was controlled at approximately 0.4 cm s^{-1} (Issarapayup et al., 2009).
- The CO_2 enriched air was mixed with air before entering into the system where the concentration of CO_2 was 1% by volume (Issarapayup et al., 2009).
- All experiments were performed at evaporative room (27±3 ^{o}C).

2.1) In case of using the artificial light supplement (fluorescent lamps) for algal growth

- The supplement of artificial light for algal growth was constantly at 30 µmol photon.m^{-2}.s^{-1}
- The artificial light was subject to the system for algal growth for 24 h through the end of cultivation.
- The 17 and 50L FP- ALPBRs were performed.

2.2) In case of using the natural light supplement (sunlight) for algal growth

- The supplement of natural light for algal growth was contributed light intensity of approximately 100 to 500 µmol photon.m^{-2}.s^{-1}.
- The contribution of natural light was naturally controlled by ratio of light and dark cycle (average of 12 h:12 h).
- The 17, 50, 90, and 200L FP-ALPBRs were employed for investigation of large scale production for *H. pluvialis* cultivation.
- The 17L FP-ALPBR was conducted for examination of reused algal medium for *H. pluvialis* cultivation.

3) The evaluation of the economic assessment of the cultivation process of *H. pluvialis*

3.1) The evaluation of an economic assessment was based on the availability of light source.

- Artificial light supplement (17 and 50L FP-ALPBRs)
- Natural light supplement (17, 50, 90, and 200L FP-ALPBRs)

3.2) This study also evaluated an economic assessment based on the possibility of reusing the algal growth medium

- Natural light supplement (17L FP-ALPBR)

CHAPTER II
AIRLIFT PHOTOBIOREACTORS

2.1 Airlift photobioreactors (ALPBRs)

Airlift photobioreactors (ALPBRs) are generally classified as pneumatic reactor without any mechanical stirring arrangements. The circulation in a defined cyclic pattern through a loop of conduits ensures an adequate circulation of the liquid. The possibility of providing the required aeration with low energy consumption input and low shear force is absolutely major reasons for the interests in ALPBRs. Moreover, the advantages of ALPBRs over the other conventional reactors are perfectly penetration of light as well as liquid circulation which is enhanced by liquid flow from a riser region to an annular space leading to an enhancement of liquid recirculation in airlift system. All of beneficial strategies could therefore result in better performance for the enhancement of the algal cultivation for cell biomass and also the production of secondary metabolites. Up to now, many kinds of ALPBRs have been used widely to study not only to determine the hydrodynamic behavior of the airlift systems (liquid circulation, gas holdup and mass transfer) but, they were also used as applications for cultivation of other potential microorganisms to regain the high cell biomass and/or the high value secondary metabolite products. For instance, a concentric tube airlift photobioreactor (Ranjbar et al., 2008), a split-cylinder internal loop airlift photobioreactor (Vega-Estrada et al., 2005), an inclined-tube airlift reactor and a triangle airlift reactor (Vunjak-Novakovic et al., 2005), an internal loop airlift photobioreactor (Wongsuchoto et al., 2004; Kaewpintong et al., 2006 and Ruen-ngam et al., 2008), an airlift tubular photobioreactor (Garcia et al., 2006) and a double-layered airlift photobioreactor (Lee et al., 2005 and Suh et al., 2006).

An internal and external airlift photobioreactors are two main schematic characteristic of ALPBRs (as displayed in Figure 2.1) which have essentially the same

region and function: a riser (gas injection produces a highly turbulent region with high gas hold up), a gas separator (a large portion of gas disperses out at the liquid surface and creates heavier fluid), a downcomer (the liquid returns to the bottom after separating from the gas bubbles that disengage in the gas separator). The difference in the gas holdups between the two regions produces the difference in the appearance of fluid density that drives the liquid circulation. In terms of gas-liquid flow configurations, the riser and separator sections are mostly in bubbly or bubbly turbulent flow regimes, whereas, the liquid in the downcomer usually shows a near plug flow behavior (Vunjak-Novakovic et al., 2005).

The airlift can also be designed as a rectangular column which is separated internally by a plate. The length of the column can be adjusted to accommodate the requirement for different volumes (17, 90, and 200L) referred to in this work as a flat panel airlift photobioreactor (FP-ALPBR), as shown in Figure 2.2. The success of this work allows an easy and simple way of up-scaling the ALPBRs.

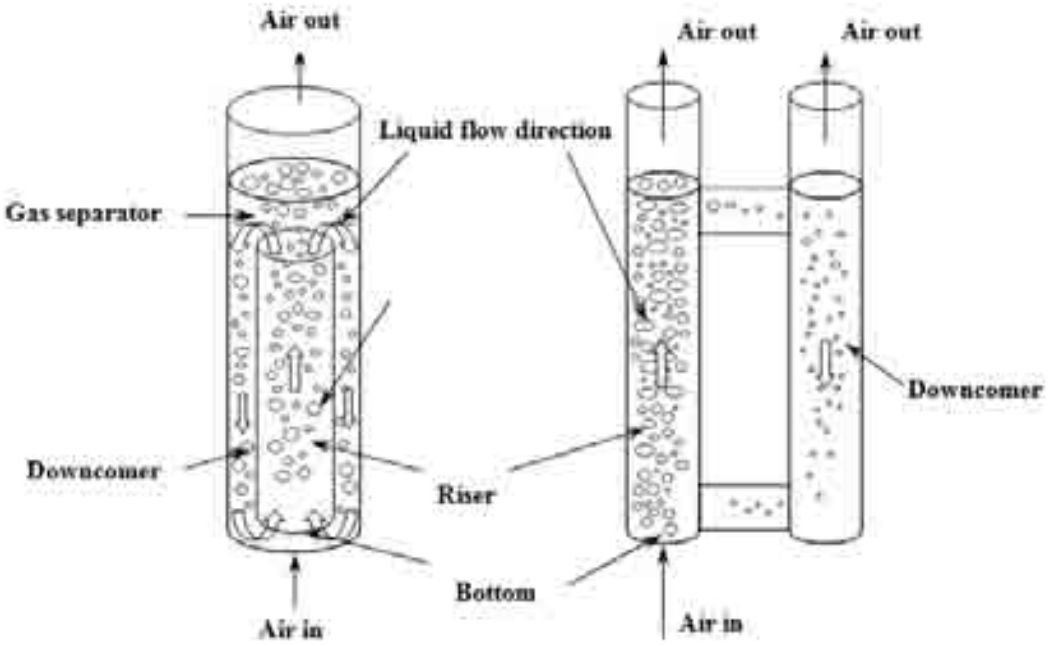

(a) **(b)**

Figure 2.1 Classification of airlift photobioreactor: (a) internal loop (b) external loop (Kaewpintong et al, 2006 and Issarapayup et al, 2009)

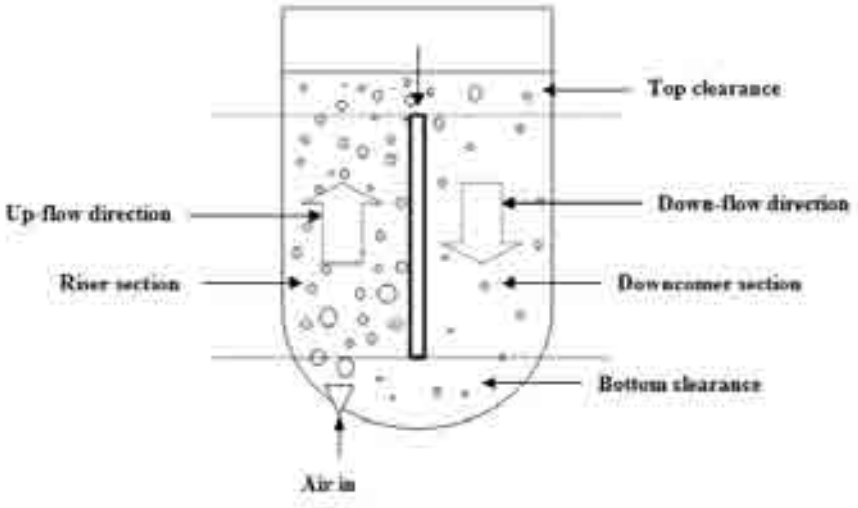

Figure 2.2 Various sections of the flat plate airlift system (Issarapayup et al., 2009)

2.2 Gas-liquid hydrodynamics and mass transfer in airlift systems

Liquid circulation, gas holdup and mass transfer are the major parameters underlining the behavior of the airlift systems. Such hydrodynamic and gas-liquid mass transfer behaviors are described in this section.

2.2.1 Gas-liquid hydrodynamics

2.2.1.1 Gas holdup

Gas holdup is described as the fraction of the reaction volume taken by the gas. Estimated as the volume of liquid displaced by the gas (expansion of liquid volume) due to aeration, gas holdup is very important in photobioreactor design as it affects the circulation rate, the gas residence time, as well as the overall mass transfer rate ($k_L a$) (Ugwu et al., 2008).

The volume fraction of the gas-phase in the gas-liquid dispersion is known as the gas void fraction or the gas holdup. The overall gas holdup (ε) is ratio between volume of gas phase and the total volume of reactor can be expressed as:

$$\varepsilon = \frac{V_G}{V_G + V_L} \tag{2.1}$$

where: V_G is gas volume

V_L is liquid volume.

In airlift contactors, gas holdups are different in the various parts of the system. In general, gas holdups are described using the three quantities, i.e. overall gas holdup, riser gas holdup and downcomer gas holdup. The three holdups can be correlated as follows:

$$\varepsilon = \frac{A_r \varepsilon_r + A_d \varepsilon_d}{A_r + A_d} \tag{2.2}$$

where: ε_r is riser gas holdup

ε_d is downcomer gas holdup

A_r is riser cross sectional area

A_d is downcomer cross sectional area.

The overall gas holdup from experimental can be determined by this equation:

$$\varepsilon_o = 1 - \frac{h_L}{h_D} \tag{2.3}$$

where: ε_o is overall gas holdup

h_L is unaerated liquid height

h_D is dispersed liquid height.

Wongsuchoto et al. (2003), Tunthikul et al. (2006) and Ruen-ngam et al. (2008) used this empirical correlation to determine gas holdup in internal loop airlift

contactor. Downcomer gas holdup is determined from pressure drop between the two vertical points of the column and calculated from:

$$\varepsilon_d = 1 - \frac{\Delta Z_{manometer}}{\Delta H} \tag{2.4}$$

where: ΔZ is pressure difference of defined liquid level

ΔH is distance between the two vertical points in the airlift column

Riser gas holdup can then be calculated from the overall and downcomer gas holdups according to:

$$\varepsilon_r = \varepsilon_o + (\frac{A_d}{A_r})(\varepsilon_o - \varepsilon_d) \tag{2.5}$$

2.2.1.2 Liquid velocity

Liquid velocity is a measure of liquid flow and degree of turbulence in photobioreactors. Some degree of turbulence is required in photobioreactors to ensure that all the cells are frequently exposed to light (Pruvost et al., 2006).

Liquid velocity in the airlift system is described using the velocities in riser and downcomer. The liquid velocity in riser is induced from the input gas sparger at the bottom of airlift contactors whereas the liquid velocity in downcomer is influenced by the different fluid densities between bottom and top of airlift contactors. As the air is supplied into the riser section, the apparent density of the fluid in this section is lower than that of the liquid. The fluid therefore moves upwards. Having reached the gas separating section, the bubbles in the fluid separated from the liquid at the top surface. The heavy liquid moves down in the downcomer section where no aeration is supplied. In this manner, the liquid circulation takes place in the airlift systems.

Generally, liquid velocity is measured in terms of linear liquid velocity

defined as:

$$u_L = \frac{x_L}{t} \tag{2.6}$$

where: u_L is liquid velocity

x_L is the liquid path length

t is time for liquid complete movement.

u_L is often called superficial velocity as it is calculated from the assumption of non-obstructed flow in the column. However, the actual liquid velocity, v_L, must be calculated, taken into account the obstruction. The obstruction in this case is caused by the existence of gas bubbles. The superficial liquid velocity and the linear liquid velocity can be related as:

$$v_{Lr} = \frac{u_{Lr}}{1-\varepsilon_r} \tag{2.7}$$

and

$$v_{Ld} = \frac{u_{Ld}}{1-\varepsilon_d} \tag{2.8}$$

where: v_{Lr} and v_{Ld} are actual linear liquid velocity in riser and downcomer, respectively

u_{Lr} and u_{Ld} are superficial liquid velocity in riser and downcomer, respectively.

The relationship of superficial liquid velocity in riser and in downcomer can be expressed as:

$$u_{Lr}A_r = u_{Ld}A_d \tag{2.9}$$

2.2.2 Gas-liquid mass transfer

Gas-liquid mass transfer is probably one of the most important characters for

gas-liquid contacting systems. The mechanisms of gas-liquid mass transfer can be generalized into four steps as follows:

1. the transport in a gas film inside the bubble
2. the transfer at the gas-liquid interface
3. the transfer in a liquid film at the gas-liquid interface
4. the transport in the bulk liquid

The liquid side film often has a much higher mass transfer resistance than that in the gas side. Therefore the overall mass transfer resistance is controlled by the resistance of the liquid film.

The overall volumetric mass transfer coefficient *(k_La)* is most commonly used parameters for assessing the performance of photobioreactors. The term k_La is generally used to describe the overall volumetric mass transfer coefficient in photobioreactors. The volumetric mass transfer coefficient *(k_La)* of photobioreactors depends on various factors such as agitation rate, the type of sparger, surfactants/antiform agents and temperature (Ugwu et al., 2008).

The overall volumetric mass transfer coefficient *(k_La)* is a combination of two quantities, i.e. k_L and a where k_L is a gas-liquid mass transfer coefficient and a is specific surface area that the transfer takes place. Such two parameters are difficult to determine separately. Conventionally these two parameters are combined and called "overall volumetric mass transfer coefficient" which can be determined from:

$$\frac{dC_L}{dt} = k_L a(C_L^* - C_L) - r_{o_2} \tag{2.10}$$

where: C_L is the dissolved oxygen concentration

C_L^* is the dissolved oxygen concentration in equilibrium with partial pressure of oxygen in the air

r_{O_2} is the rate of oxygen used per unit mass of organisms

For systems without reaction, r_{O_2} disappears and Equation (2.10) becomes

$$\frac{dC_L}{dt} = k_L a(C_L^* - C_L) \tag{2.11}$$

Previous research showed that an increase in the superficial gas velocity could decrease the liquid film and increased overall mass transfer coefficient. In contrast, when A_d/A_r increased, the overall mass transfer coefficient often decreased (Al-Masry, 1999).

Ruen-ngam et al. (2008), Vega-Estrada et al. (2005) and Wongsuchoto et al. (2003) demonstrated that k_La increased with u_{sg} but decreased with an increase in A_d/A_r, whilst the influence of number of holes in sparger on k_La was negligible.

2.3 Large scale airlift contactors

In 1997, Heijnen et al. designs a simple model to predict hydrodynamics behavior of a three phase internal loop airlift contactors. Three different scales of the airlift were used in this work, i.e. laboratory-scale with the volume of 19L, pilot-scale with the volume of 400L, and a large scale with 284,000L, the ratio between downcomer and riser cross sectional areas or A_d/A_r was set at the same ratio (about 1.04-1.47). The result showed that, at the same superficial gas flow rate, the larger scale airlift contactors had a higher liquid velocity than smaller scale because the smaller scale was subject to a higher wall friction.

In 2004, Blazej et al. studied the effect of reactor scale on hydrodynamic properties in three internal loop airlift reactors of different scales with a working volume of 10.5, 32 and 200L, respectively. The three reactors were of similar geometry, i.e. with the same ratio between riser and downcomer cross-sectional areas, and similar aspect ratio of the column and the shape of the column bottom (the same

A_d/A_r and *H/D* ratio). The average of the liquid circulation velocities increased with increasing reactor scale for the same superficial gas velocity. The value of the driving force ($\varepsilon_R - \varepsilon_D$) was found to be important only for lower values of gas flow rate, because at higher values, the circulation velocity seemed to be governed only by friction in the reactor wall.

In reality, liquid circulation of large scale airlift contactors is vitally concerned. It has been shown that, in particular, the airlift with large riser inherited internal liquid circulation within the riser itself. Wongsuchoto et al. (2004) examined the internal liquid circulation in annulus sparged airlift contactors with a volume of 13L at different A_d/A_r (i.e. 0.067, 0.431, 0.540 and 1.540) and demonstrated that, for the case of large riser, the measured liquid velocity in riser was always observed to have a greater value than the calculated value. This meant that there must be an existence of a down-flow of liquid in the riser to counterbalance the excess liquid up-flow. This presentation of the internal liquid circulation caused the airlift contactors to possess bubble column behavior. In addition, the past studies revealed that up-scaling of airlift photobioreactors resulted in an increasing of liquid circulation but the trend of mass transfer coefficient was opposite (as shown in Table 2.1). Therefore, it becomes a research problem in tackling the scale up the airlift systems without causing a reduction in the gas-liquid mass transfer rate.

Table 2.1 Hydrodynamic study in airlift system

References	Details			K_La (s^{-1})	Liquid velocity (m s^{-1})	System	Sparger
	Type	Volume	A_d/A_r				
Ruen-ngam et al., 2008	Internal loop airlift	17 L	0.661	0.085		air-water	perforated ring sparger with 30 holes of 1 mm diameter
Blazej et al., 2004	Internal loop airlift	10.5 L	1.23		0.35	air-water	plate sparger (teflon) with 25 holes of 0.5 mm diamete
		32 L	0.95		0.4		plate sparger (teflon) with 25 holes of 0.5 mm diameter
		200 L	1.01		0.45		plate sparger (stainless steel) with 90 holes of 1.0 mm diameter
Wongsuchoto et al., 2004	Internal loop airlift	130 L	0.07		0.3	air-water	perforated ring sparger with 14 holes of 1 mm diameter
			0.43		0.3		
			1		0.5		
			1.54		0.5		

Table 2.1 (cont.) Hydrodynamic study in airlift system

References	Details			K_La (s^{-1})	Liquid velocity (m s^{-1})	System	Sparger
	Type	Volume	A_d/A_r				
Wongsuchoto et al., 2003	Internal loop airlift	15 L	0.07	0.045	0.2	air-water	perforated ring sparger with 14 holes of 1 mm diameter
			0.43	0.035	0.35		
			1	0.035	0.27		
Wang et al., 2003	External loop airlift	20 mL	0.36		0.15	air-gluconate buffer	glass plate with pore size of 40-100 micron
Baten et al., 2003	Internal loop airlift	35 L	1.25		0.9	air-water	perforated ring sparger with 625 holes of 0.5 mm diameter
		48 L	2.03		1.2		
		882 L	1.25		1.2		

Table 2.1 (cont.) Hydrodynamic study in airlift system

References	Details			K_La (s^{-1})	Liquid velocity (m s^{-1})	System	Sparger
	Type	Volume	A_d/A_r				
Al-Mary et al., 1999	External loop airlift	60 L	0.25	0.045	0.35	air-water	plate sparger with 1 mm diamete
		350 L	0.44	0.033	0.6		
		700 L	1	0.015	0.8		
Tung et al., 1998	Internal loop airlift (4 net draft tubes)	132 L		0.08		air-water	perforated ring sparger
Heijnen et al., 1997	Internal loop airlift	19 L		0.3		air-water	
		400 L		0.7			
		284,000 L		0.9			

CHAPTER III
HAEMATOCOCCUS PLUVIALIS

3.1 *Haematococcus pluvialis*

3.1.1 Biological information

Haematococcus pluvialis is a freshwater unicellular green alga. *H. pluvialis* reproduces asexually by division from a single cell into and/or four motile cells (Droop, 1995). The taxonomy of *H. pluvialis* is as follows (Smith, 1950).

Domain	:	Eukaryota
Kingdom	:	Viridiplantae
Division	:	Chlorophyta
Class	:	Chlorophyceae
Order	:	Volvocales
Family	:	Chlamydomondaceae
Genus	:	*Haematococcus*
Species	:	*Haematococcus pluvialis*

3.1.2 Growth stages of *H. pluvialis*

The growth stages of *H. pluvialis* can be generally classified into three stages as described below:

- **Vegetative green cell** (Fig. 3.1 A)

Under suitable growth conditions, most cells remain in green vegetative forms, capable of moving with two flagella. The cells produce chlorophylls a and b and primary carotenoids, especially β - carotene and lutein (Rockette, 1970). Astaxanthin is not generated in this stage. The shape of these cells is typically spherical or

ellipsoid with a diameter of approximately 10-20 µm. The cells are enclosed with cell walls within which consist of golgi apparatus, chloroplast, polysaccharidic envelope, pyrenoid, and fragility zone (Gudin and Chaumont, 1991).

- **Immature cell** (Fig. 3.1 B)

Once the cells are exposed to unfavorable conditions such as depletion of essential elements, e.g. carbon, nitrogen, phosphorous, light induction, etc., astaxanthin is then partially created within cytoplasm of the cells. Cell growth is generally ceased and some of the cells start to lose their flagella and grow larger in size.

- **Cyst (Aplanospore)** (Fig. 3.1 C)

Under such conditions vegetative motile green cells enter a process of encystment. The formation of astaxanthin-replete aplanospores begins which is still spherical in shape. However, they lose flagella and generate an extremely resistant cell wall that cannot be easily digested (Mendes-Pinto et al., 2001; Hagen and Braune, 2002). The diameter of algal cells increases dramatically from 10-20 µm to 40-50 µm. Besides, they produce secondary carotenoids such as echinenone, canthaxanthin and astaxanthin while the chlorophyll and primary carotenoids are decreasing (Droop, 1954; Lee et al., 1991). Growth rate of *H. pluvialis* in this state decreases whereas an abundance of astaxanthin is generated in almost cells. Up to now, the exact mechanism pathway on how the cell generates astaxanthin has not well known (Christiansen and Torrissen., 1997). Fully cysts contain up to 5% dry weight astaxanthin (Renstrom et al., 1981; Bubrick, 1991).

10 µm

(A)

30 µm

(B)

50 µm

(C)

Figure 3.1 *H. pluvialis* cells in different stages of growth in autotrophic condition (Issarapayup et al., 2009)

3.2 What is astaxanthin?

Astaxanthin is one of most important carotenoids in marine organisms, responsible for the pigmentation of skin and flesh of fish, mainly salmonids, and it also influences the survival and growth of fish larvae. Currently, having gained much interest owing to its versatile applications as its good biological function such as antioxidant activity, astaxanthin has been used for immune response enhancement and cancer protection (Kobayashi et al., 1991). Astaxanthin price is relatively high (2,500 US$ per kg) compared with other antioxidants and the annual market size of astaxanthin was around 200 million US$ in 2000 (Lorenz and Cysewski, 2000).

3.2.1 Chemical properties of astaxanthin

Astaxanthin (3,3'- dihydroxy - β - β - carotene - 4,4' - dione) is an oxycarotenoid with a molecular formula $C_{40}H_{52}O_4$ and a molecular weight of 596.86. It can be dissolved at room temperature in non-polar solvents such as dimethyl-sulfoxide and acetone. There are two different pathways for astaxanthin biosynthesis. The first one starts with the oxidation of β-carotenoid of β-carotene with echinenone, canthaxanthin and adonirubin taking part as intermediates. The second one starts with β-carotene hydroxylation with β-cryptoxanthin, zeaxanthin and adonixanthin as intermediates (Schoefs et al., 2001) (as shown in Figure 3.2). The astaxanthin molecule has two asymmetric carbons located at the 3 and 3′ positions of benzenoid rings on either end of molecule with three configurations as demonstrated in Figure 3.3.

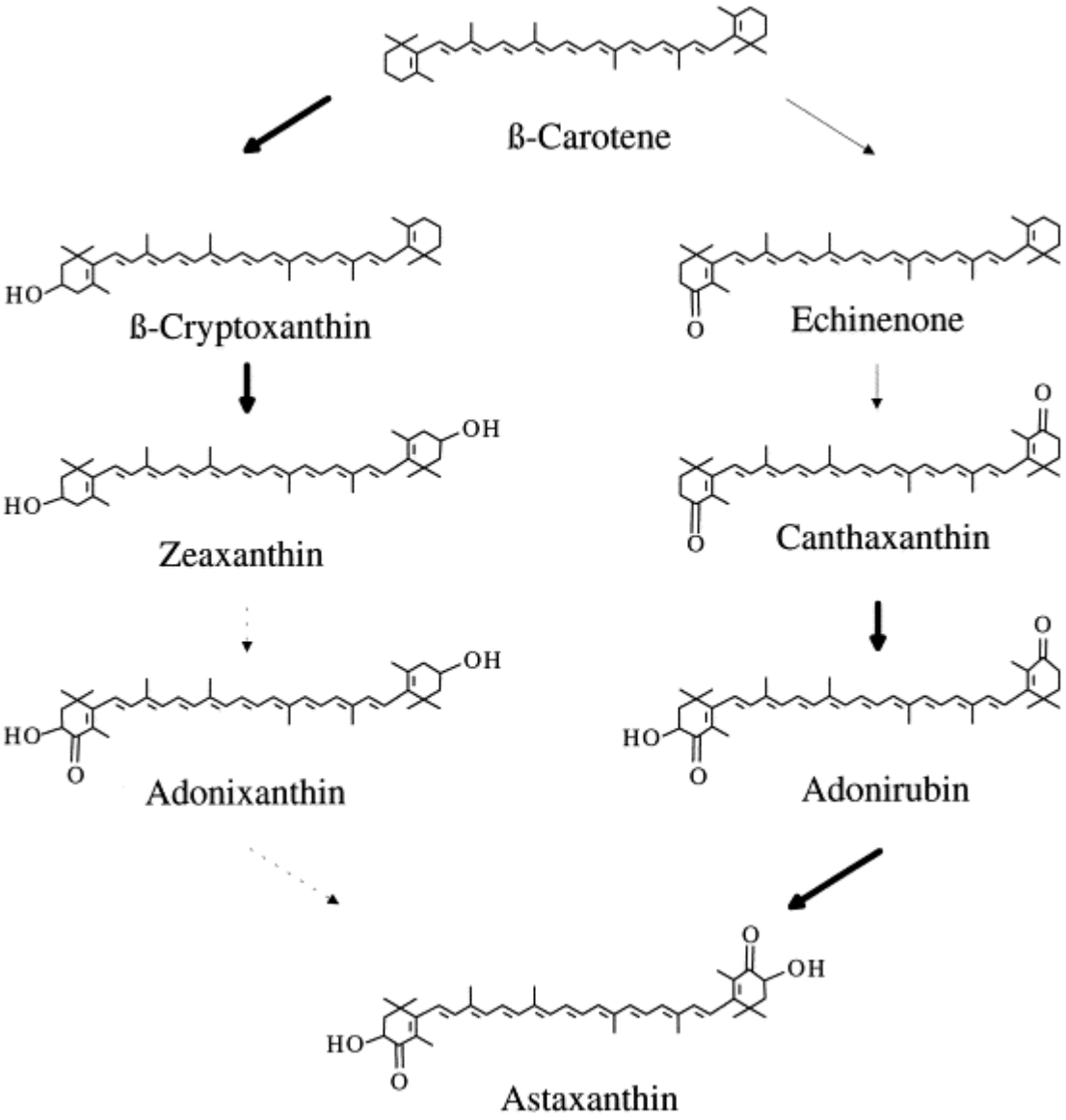

Figure 3.2 Pathway for astaxanthin biosynthesis on *H. pluvialis* (Misawa and Shimada, 1998)

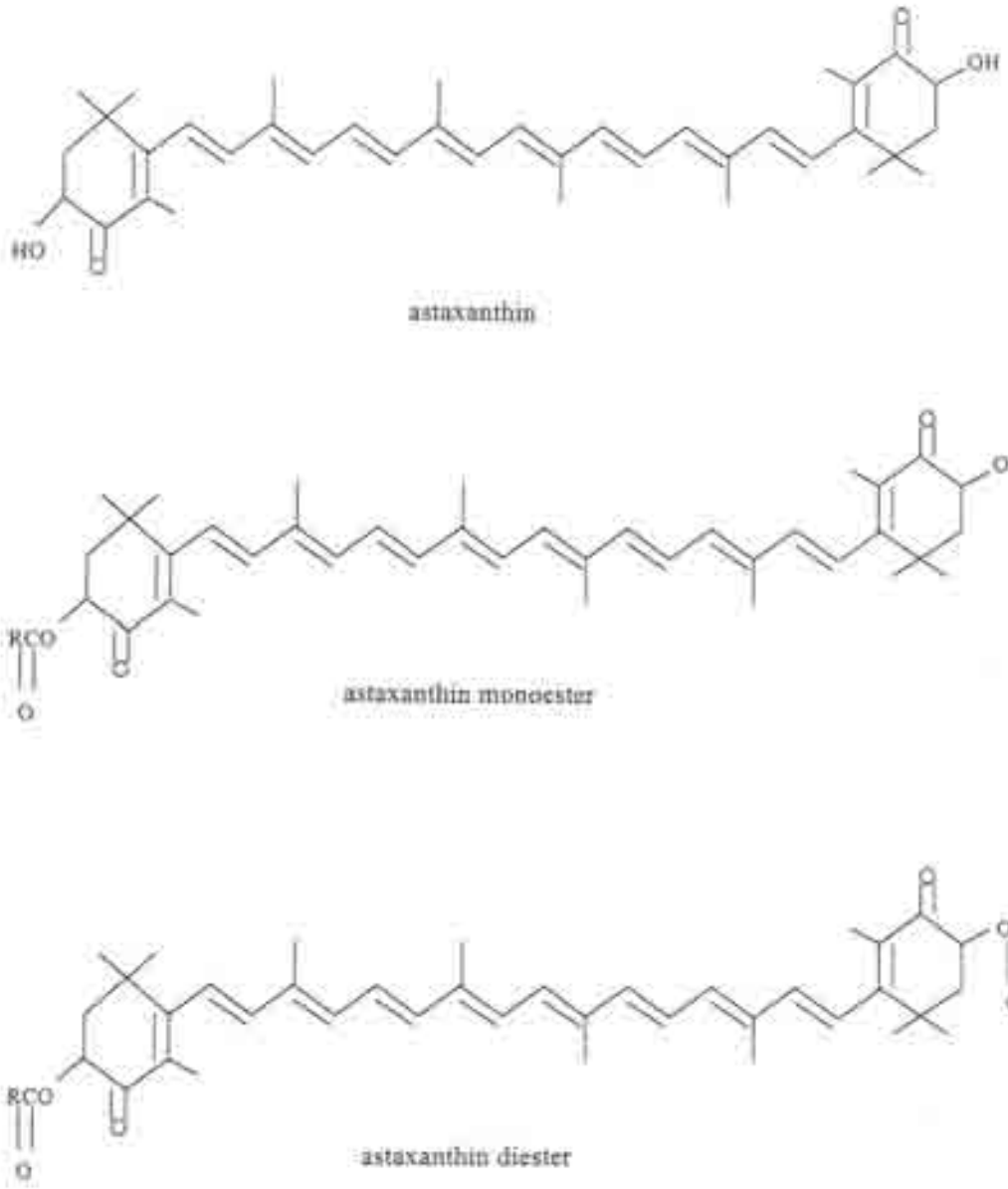

Figure 3.3 Molecular structure of astaxanthin

3.2.2 Activity of astaxanthin

Astaxanthin is known for its antioxidant activity 10 times more capable than other carotenoids and about 100 folds greater activity than vitamin E (Miki, 1991). Moreover, it also showed higher antioxidant activity than hydrocarbon carotenoids lycopene, α-carotene, β-carotene and the hydroxyl carotenoid lutein. Besides, Palozza and Krinsky (1992) reported that astaxanthin was as effective as α-tocopherol (vitamin E) and higher than β-carotene in habiting radical initiated in lipid oxidation. Additionally, it also has protected against UV light effect by quenching $^1O_2$ generated by photooxidation (Kobayashi and Sakamoto, 1999; Lorenz and Cysewski, 2000).

3.2.3 Sources of astaxanthin

There are two major sources of astaxanthin; chemical (synthetic) and biological (natural) sources.

3.2.3.1 Synthetic source

Synthetic astaxanthin is presently the principle source in aquaculture; more than 95% of this market consumes synthetically astaxanthin used in feed to produce coloration (Lorenz and Cysewski, 2000). However, this synthetic astaxanthin is expensive, unnaturally configurational and is considered lower quality when compared with that obtained from natural sources (Parker, 1992).

3.2.3.2 Natural sources

A. Crustaceans byproduct

Astaxanthin is isolated from shell on the back of a crustacean which has been used as natural pigment sources for trout and salmon. This process is very expensive, and the final product contains relatively low contents of astaxanthin and high levels of

water, ash and other nutrients, which cause several practical problems in feed formation that limit their usefulness in animal feed (Bubrick, 1991).

B. Yeast

The yeast *Xanthophyllomyces dendrorhous* (formerly *Phaffia rhodozyma*) is one of the best microbial sources of astaxanthin (Johnson and An, 1991). It contents of astaxanthin with an amount of 200 to 300 μg/g yeast (0.02-0.03%). The content of this compound depends on strain and a method of culture (John and An, 1991). However, the use of the yeast as a source of astaxanthin for aquaculture is limited since the cell wall is difficult to be digested by some microorganisms (Van Nieuwerburgh et al., 2005). Only free astaxanthin is found in the yeast which has lower antioxidant activity than the esterified forms (Choi et al., 2003).

C. Algae

Astaxanthin can be produced from other strains of algae such as *Ankistrodesmus brauii*, *Chlorella sp.*. For all that, the quantity of astaxanthin generated from these microorganisms is relatively low and not suitable for mass production. Unlike the other microorganisms, the green alga, *Haematococcus pluvialis* can generate and accumulate large quantity of astaxanthin and therefore is so far the only strain that has been used in commercial production of astaxanthin.

D. Other microorganisms

Some bacteria such as *Brevibacterium sp.* and *Mycobacterium lacticola* and fungi *Peniophora (Hymenomycetes)* are also reported to be able to accumulate astaxanthin (Borowitzka et al., 1989). However, it can only accumulate low level of carotenoid, not to mention its relatively slow growth (Droop, 1995). Copepods, which are tiny, shrimp-like crustaceans that swim in seas, lakes, and ponds, and are the main component of the natural diet of fish larvae, is one of the main sources of natural astaxanthin in the marine web chain. Copepods can synthesize astaxanthin

(Andersson et al., 2003) and the amount of astaxanthin presented in the copepods (data was withheld) is not dependent on the phytoplankton ingested (Van Nieuwerburgh et al., 2005). Some examples of sources of astaxanthin produced by microorganisms are shown in Table 3.1.

3.3 Cultivation systems for *H. pluvialis*

The production of astaxanthin from *H.pluvialis* often involves a two stage cultivation, i.e. (i) vegetative cell culture (algal mass production), and (ii) cyst culture (astaxantin stimulation). These two subsequent production stages are orderly displayed in below.

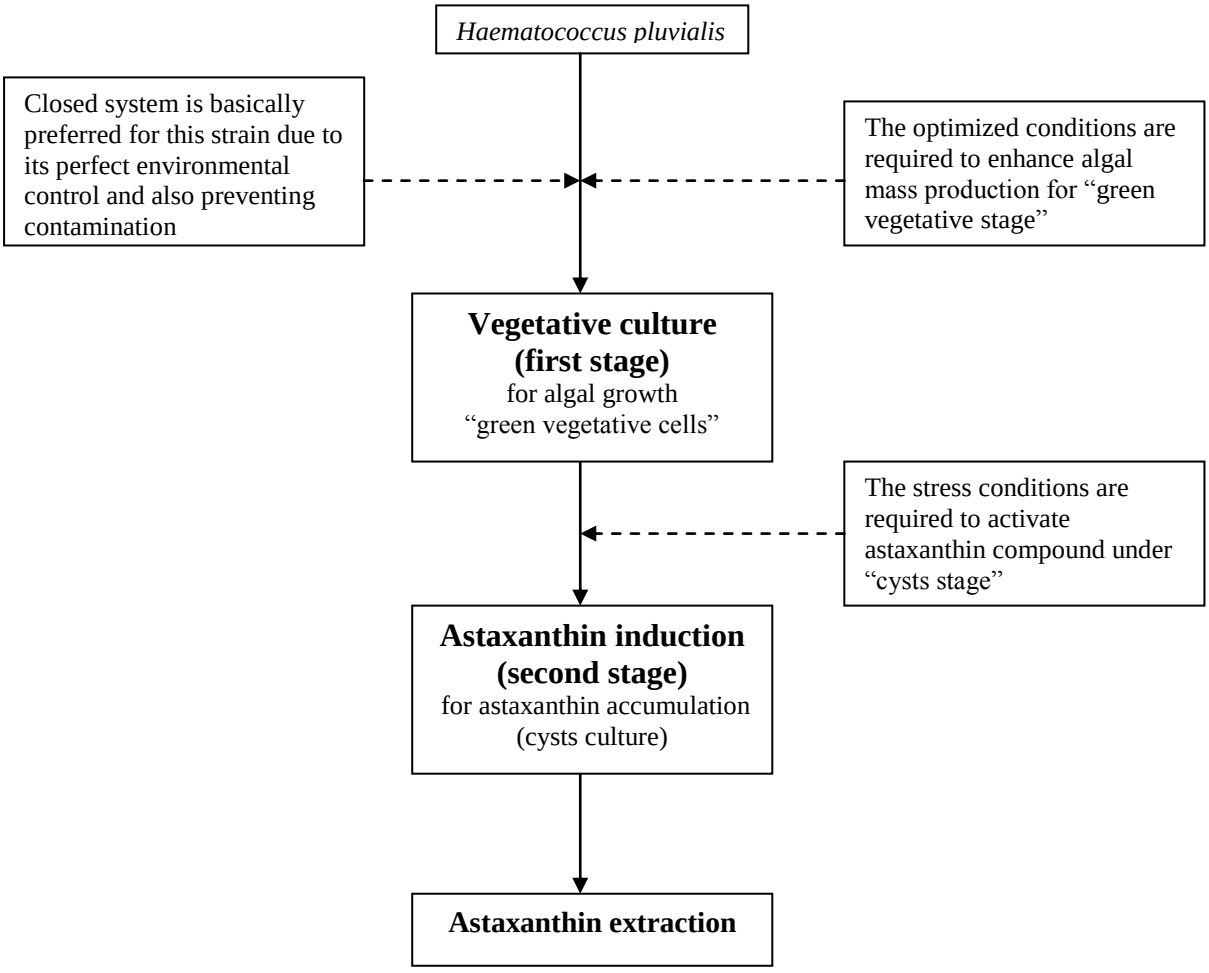

Figure 3.4 Hierarchical culture of *H.pluvialis* for the production of astaxanthin

The enhancement of algal mass production of *H. pluvialis* in the vegetative culture or the first stage could be operated both in open and closed systems. Special precaution of contamination with other fresh water algal species is to be aware of with open cultivation systems (tanks, shallow ponds, circular ponds and raceway ponds), and also a relatively lower reliability than the closed system cultivation is anticipated. A summary of advantages and disadvantages of open versus closed systems are demonstrated in Table 3.2.

Up to this time, *H. pluvialis* cultivation has been achieved widely deploying closed systems which totally aims to achieve high cell growth rate and high cell productivity in vegetative form, for example, stirred tanks, bubble columns and airlift bioreactors (Tredici and Materassi, 1992; Chaumont, 1993 and Borowitzka, 1996). A summary of characteristic properties of various manners of bioreactors is given in Table 3.3. Algal growth conditions (Table 3.5), such as temperature, light, and nutrient operated under closed system could be easily manipulated to attain the maximum cell productivity (Richmond, 1996; Vonshak, 1997; Lee and Richmond, 1998 and Lee, 2001). Literature review on algal production, prospects and limitations of different culture systems for versatile algal cultivation are summarized as shown in Table 3.4.

Similarly, the second stage (cysts) for astaxanthin generation could be also operated both in open and closed systems. However, the activation conditions (Table 3.6) for astaxanthin generation are totally different from the first stage where mild conditions are most favored. More deliberate details are about to discuss in Section 3.5.

Table 3.5 Environmental growth factors for green vegetative cells of *H. pluvialis*

Factor	Range
Light	2-24 Klux
Temperature	15-28 ^{0}C
pH	6 - 8
Nutrients	
(1) Macronutrients	
• Carbon	high quantities
• Nitrogen	
• Phosphorous	
(2) Micronutrients	
• Iron	low quantities (µg/L)
• Boron	
• Manganese	
• Copper	
• Vitamins	

Table 3.6 Suitable environmental factors for astaxanthin accumulation in *H. pluvialis*

Factor	Range
Light	2 - 360 Klux
Temperature	18 - 30 ^{0}C
pH	6.5 - 8
Salt stress	0.2 - 1% Sodium chloride

Remark; Summary of the operation conditions for the production of vegetative cells is given in Tables 3.7-3.9.

3.4 Photobioreactors for cultivation of vegetative cells of *H. pluvialis*

Key factors affecting the efficiency of the cultivation process of *H.pluvialis* are the continuous production of green vegetative cells and the application of a separate induction process under mild conditions that could avoid cell death. An airlift bioreactor has been employed in several studies for the production of astaxanthin from *H. pluvialis* (Harker et al., 1996b; Chen et al., 1997; Zhang et al., 1999 and Fabregas et al., 2001). However, their studies did not focus on the aspect of achieving high cell density of *H. pluvialis*, and most of the works could only achieve a low level cell density (small scale cultivation) in range of 0.7 x 10^5 to 10 x 10^5 cell mL^{-1}, and the productivity of cell was shown in range of 0.09x10^5 to 1.5x10^5cell mL^{-1} d^{-1}. Our recent works include the work of Kaewpintong et al. (2006) who successfully achieved the cultivation of vegetative cells of *H. pluvialis*, but still only in the small scale autotrophic 3L airlift bioreactor with a maximum cell density of 7.7 x 10^5 cells mL^{-1} and with the maximum specific growth rate of 0.45 d^{-1}. A few achievements were reported for a large scale system, such as the autotropic 30L airlift bioreactor investigated by Harker et al. (1996a) who obtained only a low cell concentration of 2.5 x 10^5 cells mL^{-1} with the specific growth rate of 0.13 d^{-1}. Moreover, Garcia et al. (2006) who accomplished a high cell density at 45 x 10^5 cells mL^{-1}. This system was operated in an outdoor 55L airlift tubular photobioreactor, nevertheless, the specific growth rate did not seem high (0.3 d^{-1}). Up to this time, the highest cell density ever reported was available from Ranjbar et al. (2007) and (2008) who reported the achievement of the cultivation with the highest cell density of above 50 x 10^5 and 70 x 10^5 cell mL^{-1} from an autotrophic 1.6L bubble column photobioreactor and 1L airlift photobioreactor, respectively. Notwithstanding, the attained specific growth rate from this work was only 0.22 and 0.2 d^{-1} respectively. The highest specific growth rate reported was by Katsuda et al. (2004) which is around 0.67 d^{-1}, but the culture was a mixotroph in a small 55 mL glass vessel. Issarapayup et al. (2009) reported the optimized growth conditions for the cultivation of *H. pluvialis* in a 17L developed photobioreactor defined as flat panel airlift photobioreactors (FP-ALPBRs) where the

maximum growth rate and cell density accomplished were 0.52 d^{-1} and 4.1 x 10^5 cell mL^{-1}, respectively.

3.5 Induction of astaxanthin in *H. pluvialis*

To be more understanding on the entire process of algal cultivation, some literature reviews on the induction of astaxanthin in *H. pluvialis* are described in this section. The culture requirements for astaxanthin accumulation are different from those for cell growth. Hence, the commercial processes for astaxanthin production is separated from the cultivation step, and the overall production of astaxanthin from *H. pluvialis* is often called a two-stage process (Boussiba et al., 2000; Lorenz and Cysewski, 2000 and Olaizola, 2000). The first stage is conducted in photobioreactor by maintaining proper environmental conditions to achieve high *H. pluvialis* growth rates in vegetative form. The cells at the stationary growth phase are transferred to the second reddening stage and the astaxanthin accumulation in the cells is then induced by environmental stresses, including light intensity, nutrient levels, metal ions, oxidative stress, salt stress, temperature, and pH (Zhang et al., 1999). Similar to the first stage, this step should be conducted in the closed system to protect the cells from alien species which was reported to be able to deduct cell biomass as fast as in 72 h (Spencer, 1989). Recently, del Rio et al. (2005, 2008) and Garcia-Malea et al. (2009) attempted to apply a simpler one-step strategy for the production of astaxanthin from *H. pluvialis*, in which cultures were operated in a fully continuous mode under limitation of nitrogen. Notwithstandingly, productivity and efficiency of the one step system versus the two stage counterpart have presently been rivaled, on the ground that "there is no real biotechnological advantage to vigorously growing cells for the production of the secondary carotenoid astaxanthin".

Most work reported the productivity of astaxanthin in a range of 0.12 to 20.8 mg L^{-1} d^{-1}. However, the highest productivities of astaxanthin were obtained from the work of del Rio et al. (2008) and Ranjbar et al. (2008) who could achieve by far 20.8 and 20 mg L^{-1} d^{-1}, respectively. Note that these systems were performed in an

autotrophic 2L bubble column as one-step strategy by del Rio et al. (2008) and an autotrophic 1L airlift photobioreactor as two-step strategy by Ranjbar et al. (2008). The highest productivity of astaxanthin in the large scale production was accomplished by Garcia-Malea et al. (2009) (8 mg L^{-1} d^{-1}) where the system was operated in an outdoor autotrophic 50L tubular photobioreactor.

Table 3.1 Biological sources of astaxanthin (Simpson et al., 1981; Borowitzka, 1989; Harker et al., 1996)

Sources	Astaxanthin ($\mu g\ g^{-1}$ of cell)	Astaxanthin (% dry cell)	References
Bacteria			
Brevibacterium sp.	30		Simpson et al., 1981
Mycobacterium lacticola	30		Simpson et al., 1981
Holobacterium salinarium	265		Simpson et al., 1981
Yeast			
Phaffia rhodozyma	200-300	0.02 - 0.03	Borowizka et al., 1989
Mold			
Peniophora (Hymenomycetes)	< 50		Borowizka et al., 1989
Algae			
Ankistrodesmus brauii	< 50		Harker et al., 1996a,b
Euglena sp.			
Chlorella sp.			
Chlamydomonas nivalis			
Neospongiococcum sp.			
Neochloris wimmeri			
Spongiochloris typica			
Dunaliella salina			
Haematococcus pluvialis	7,000-55,000	1.5 - 3	Lorenz and Cysewski, 2000

Table 3.2 Comparison between open and closed systems (Borowitzka, 1996)

Open system	Closed system
▪ Poor mixing	▪ Uniform mixing
▪ Poor light utilization	▪ Excellent light utilization
▪ Unable for temperature control	▪ Excellent temperature control
▪ Low gas transfer	▪ High gas transfer
▪ Low hydrodynamic stress on algal cell	▪ Low-high hydrodynamic stress on algal cell
▪ Difficult contamination control	▪ Easy contamination control
▪ Unable to operate in continuous mode	▪ Able to operate in continuous mode

Table 3.3 Comparison of properties of different scale of algal culture systems (Borowitzka, 1996)

Reactor type	Mixing	Light utilization efficiency	Temperature control	Gas transfer	Hydrodynamic stess on algae	Species control	Scale up
Unstirred shallow ponds	very poor	poor	none	poor	very low	difficult	very difficult
Tank	poor	very poor	none	poor	very low	difficult	very difficult
Circular stirred ponds	fair	fair good	none	poor	low	difficult	very difficult
Stirred tank reactor	largely uniform	fair good	excellent	low - high	high	easy	difficult
Airlift reactor	generally uniform	good	excellent	high	low	easy	difficult
Tubular reactor	uniform	excellent	excellent	low - high	low - high	easy	easy
Flat plate reactor	uniform	excellent	excellent	high	low - high	easy	difficult

Table 3.4 Prospects and limitations of various culture systems for algae

Culture system	Prospects	Limitations	References
Open ponds (ponds, lagoons, lakes)	Relatively economical, easy to clean up after cultivation, good for mass cultivation of algae	Little control of culture conditions, difficulty in growing algal cultures for long periods, poor productivity, occupy large land mass, limited to few strains of algae, culture are easily contaminated	Boussiba et al., 1988 Tredici and Materassi, 1992 Hase et al., 2000
Vertical column photobioreactor (bubble column, airlift photobioreactor, narrow tubular photobioreactor)	High mass transfer, good mixing with low shear stress, low energy consumption, high potential for scalability, easy to sterilize, readily tempered, good for immobilization of algae, reduce photoinhibition and photo-oxidation	Small illumination surface area, their construction require sophisticated materials, shear stress to algal cultures, decrease of illumination surface area upon scale-up	Sanchez et al., 2002 Choi et al., 2003 Vega-Estrada et al., 2005 Garcia et al., 2006 Kaewpintong et al., 2006 Ranjbar et al., 2007,2008
Flat plate photobioreactor	Large illumination surface area, suitable for outdoor cultures, good for immobization of algae, good light path, good biomass productivities, relatively cheap, easy to clean up, reasily tempered, low oxygen build up	Scale up require many compartments and support materials, difficulty in controlling culture temperature, some degree of wall growth, possibility of hydrodynamic stress to some algal strains	Tredici and Materassi, 1992 Hu et al., 1996 Zhang et al., 2002 Hoekema et al., 2002
Tubular photobioreactors	Large illumination surface area, suitable for outdoor cultures, fairly good biomass productivities, relatively cheap	Gradients of pH, dissolved oxygen and CO_2 along the tube, fouling, some degree of wall growth, requires large land space	Camacho Rubio et al., 1999 Ugwu et al., 2003 Vonshak and Torzillo, 2004 Garcia et al., 2006

Table 3.7 Summary of the operation conditions (autotrophic) for production of vegetative cells

References	Reactor	Volume	Medium	Condition	Modes of operation						Maximum cells density ($x10^5$cell mL^{-1})	Productivity of cells ($x10^5$ cell mL^{-1} day^{-1})	Specific growth rate (d^{-1})
					Light intensity (KLux)	Light source	pH	Temp. (^oC)	Aeration rate (cm s^{-1})	Agitation rate (rpm)			
Ranjbar et al., 2008	Airlift photobio reactor (A_d/A_r = 1.1) * Keep nitrate conc. at 8 mM (300 mL)	1 L	Standard inorganic medium	Autotrophic (batch) CO_2	1-2.4	fluorescent lamps	7.5	20	0.072-0.125		70	7.20	0.20
Ranjbar et al., 2007	Bubble column photobio reactor	1.6 L	Standard inorganic medium	Autotrophic CO_2	1 - 2.4	fluorescent lamps	8	20	0.067 - 0.1		50 - 60	4.80	0.22
Kaewpintong et al., 2006	Airlift photobio reactor	3 L	Modified F 1 (Added Vit. B12)	Autotrophic 1%CO_2	1	fluorescent lamps	7	27	0.4		7.7	0.55	0.45

Table 3.7 (cont.) Summary of the operation conditions (autotrophic) for production of vegetative cells

References	Reactor	Volume	Medium	Condition	Modes of operation						Maximum cells density ($x10^5$ cell mL^{-1})	Productivity of cells ($x10^5$ cell mL^{-1} day^{-1})	Specific growth rate (d^{-1})
					Light intensity (KLux)	Light source	pH	Temp. (^oC)	Aeration rate (mL min^{-1})	Agitation rate (rpm)			
Suh et al., 2006	A novel double-layered photobio reactor	11 L	Bold's Basal medium (BBM)	Autotrophic 5%CO_2	2 - 3	white fluorescent lamps	6.5	25	100		5.5	0.62	0.30
Garcia et al., 2006	Airlift tubular photobio-reactor	55 L	Inorganic medium free acetate	Autotrophic (batch) CO_2 (Outdoor)	50-2000 $\mu Em^{-2}s^{-1}$		8	20	500		45	7.00	0.30
	Bubble column photobio reactor	55 L	Inorganic medium free acetate	Autotrophic (batch) CO_2 (Outdoor)	50-2000 $\mu Em^{-2}s^{-1}$		8	20	500		25	4.00	0.22
Kang et al., 2006	Flask	250 mL	Primary treated piggery wastewater (PTP) *Diluted 4 fold	Autotrophic (batch) 5%CO_2	2.5	white fluorescent lamps	7.5	23	65		11	1.33	0.25

Table 3.7 (cont.) Summary of the operation conditions (autotrophic) for production of vegetative cells

References	Reactor	Volume	Medium	Condition	Modes of operation						Maximum cells density ($x10^5$ cell mL^{-1})	Productivity of cells ($x10^5$ cell mL^{-1} day^{-1})	Specific growth rate (d^{-1})
					Light intensity (KLux)	Light source	pH	Temp. (^oC)	Aeration rate (mL min^{-1})	Agitation rate (rpm)			
Lee et al., 2006	Bubble column photobio reactor	2.5 L	Modified Bold's Basal medium (MBBM)	Autotrophic (batch) 5%CO_2	35 $\mu Em^{-2}s^{-1}$	white fluorescent lamps	7	25	100		6.5	0.92	0.31
Vega-Estrada et al., 2005	Airlift photobio reactor (split plate) (A_d/A_r = 0.376)	2 L	Bold's Basal medium (BBM)	Autotrophic (batch)	8.5	white fluorescent lamps		26-28	250		11	1.00	0.26
Del Rio et al., 2005	Bubble column photobio reactor	2 L	Basal medium } Sodium nitrate	autotrophic (continuous) CO_2	1220 $\mu Em^{-2}s^{-1}$	white fluorescent lamps	7	25			20	0.30	0.28
Dominguez - Bocanegra et al., 2004	Flask	1000 mL	Bold's Basal medium (BBM)	Autotrophic 1.5%CO_2	9	white fluorescent lamps		28	100		3.5	0.48	0.36
Fabregas et al., 2001	Tube	70 mL	OHM medium	Autotrophic (batch) CO_2	2	white fluorescent lamps	7.2 - 7.8	25	250		6.25	0.45	0.13

Table 3.7 (cont.) Summary of the operation conditions (autotrophic) for production of vegetative cells

References	Reactor	Volume	Medium	Condition	Modes of operation						Maximum cells density ($x10^5$ cell mL^{-1})	Productivity of cells ($x10^5$ cell mL^{-1} day^{-1})	Specific growth rate (d^{-1})
					Light intensity (KLux)	Light source	pH	Temp. (^oC)	Aeration rate (mL min^{-1})	Agitation rate (rpm)			
Fabregas et al., 2000	Tube	70 mL	OHM medium	Autotrophic 5%CO_2	2	fluorescent lamps	< 8	25	250		3.8	0.76	0.27
Tripathi et al., 1999	Flask		Bold's Basal medium (BBM)	Autotrophic	1.5			25			1.5	0.15	0.04
Fabregas et al., 1998	Mini-reactor	70 mL	F1 medium	Autotrophic (batch) CO_2	2	fluorescent lamps	7.2 - 7.8	25	250		6	0.43	0.10
Grunewald et al., 1997	Flask	100 mL	Bold's Basal medium (BBM)	Autotrophic (batch)	7.5	white lights		20			2.9	0.85	0.49
Harker et al., 1996a	Airlift photobio reactor	30 L	Basal medium } Added NaCl	Autotrophic (batch)	2.5	fluorescent lamps			1500-3000		2.5	0.12	0.13

Table 3.8 Summary of the operation conditions (heterotrophic) for production of vegetative cells

References	Reactor	Volume	Medium	Condition	Modes of operation						Maximum cells density ($x10^5$ cell mL^{-1})	Productivity of cells ($x10^5$ cell mL^{-1} day^{-1})	Specific growth rate (d^{-1})
					Light intensity (KLux)	Light source	pH	Temp. (^oC)	Aeration rate (mL min^{-1})	Agitation rate (rpm)			
Hata et al., 2001	Flask	500 mL	Basal medium	Hetero-trophic (fed batch)			8	25		40	10	1.12	0.29
Tripathi et al., 1999	Flask		KM1 medium	Hetero-trophic	1.5			25			4.35	0.87	0.29
Chen et al., 1997	Stirred tank	3.7 L		Hetero-trophic (batch)			7	25	1666	400	0.7	0.09	0.32

Table 3.9 Summary of the operation conditions (mixotrophic) for production of vegetative cells

References	Reactor	Volume	Medium	Condition	Modes of operation						Maximum cells density ($x10^5$ cell mL^{-1})	Productivity of cells ($x10^5$ cell mL^{-1} day^{-1})	Specific growth rate (d^{-1})
					Light intensity (KLux)	Light source	pH	Temp. (^oC)	Aeration rate (mL min^{-1})	Agitation rate (rpm)			
Katsuda et al., 2004	Glass vessels	55 mL	Kobayashi's basal medium	Mixotrophic	0.1-0.6	fluorescent lamps or Blue flashing light LED (100 Hz)	6.8	20			4.3	1.50	0.67
Kobayashi et al., 1997	Flask	200 mL	Basal medium	Mixotrophic	1.5	fluorescent lamps	6.8	20			7	1.50	0.57
Chen et al., 1997	Stirred tank	3.7 L		Mixotrophic (batch)	8.5	fluorescent lamps	7	25	1666	400	1.45	0.23	0.44
Chumpolkulwong et al., 1997			Basal medium } Added sodium acetate	Mixotrophic	7			20			5.5	1.17	0.34
Tjahjono et al., 1994	Flask	200 mL	Basal medium Added 45 mM MSA + 450mM Fe^{2+}	Mixotrophic	8.6	white fluorescent lamps	6.8	20			5.22	1.40	0.55

CHAPTER IV
Materials and Methods

4.1 Experimental setup

4.1.1 Setup of the flat panel airlift phorobioreactor (FP-ALPBR)

Table 4.1 shows an overall of geometric details for FP-ALPBR. The ratio between the downcomer and riser cross-section area (A_d/A_r) was varied at 0.4, 1.5, and 3.0 by altering the vertical plate position. The column and draft tube were made of clear acrylic plastic with the thickness of 5 and 2 mm, respectively. The 17L bioreactor had a dimension of 20 cm wide (W_R), 50 cm high (H_R) and 20 cm long (L_R). FP-ALPBRs with a volume of 50, 90 and 200L were also constructed by extending the length of the column (L_R) to 50, 100, 200 cm, respectively, whilst maintaining the width (W_R) and the height (H_R) of the column constant at 20 and 50 cm, respectively. A schematic diagram of FP-ALPBRs is demonstrated in Figure 4.1.

The liquid circulation in the FP-ALPBR was agitated by supplying air bubbles through equipped spargers at the bottom of the airlift column. Spargers were installed along the length of the airlift, with an interval of 5 cm, which helped distribute gas bubbles within the contactor. Air from air compressor passed through two air filters before metered through a flow-meter. The first filter was a rough type following by the second, fine filter (0.22 μm Gelman filter). Similarly, the CO_2 enriched air was also sterilized by two filters and then mixed with cleaned air before entering the system at the bottom side of the reactor. The schematic diagram of experimental setup in FP-ALPBR is shown in Figure 4.2. The concentration of CO_2 was adjusted to 1% by volume (Issarapayup et al., 2009). The algal temperature was maintained at 27±3 ^oC in the evaporative room. Figure 4.3 illustrates various sections of the evaporative room used in this work.

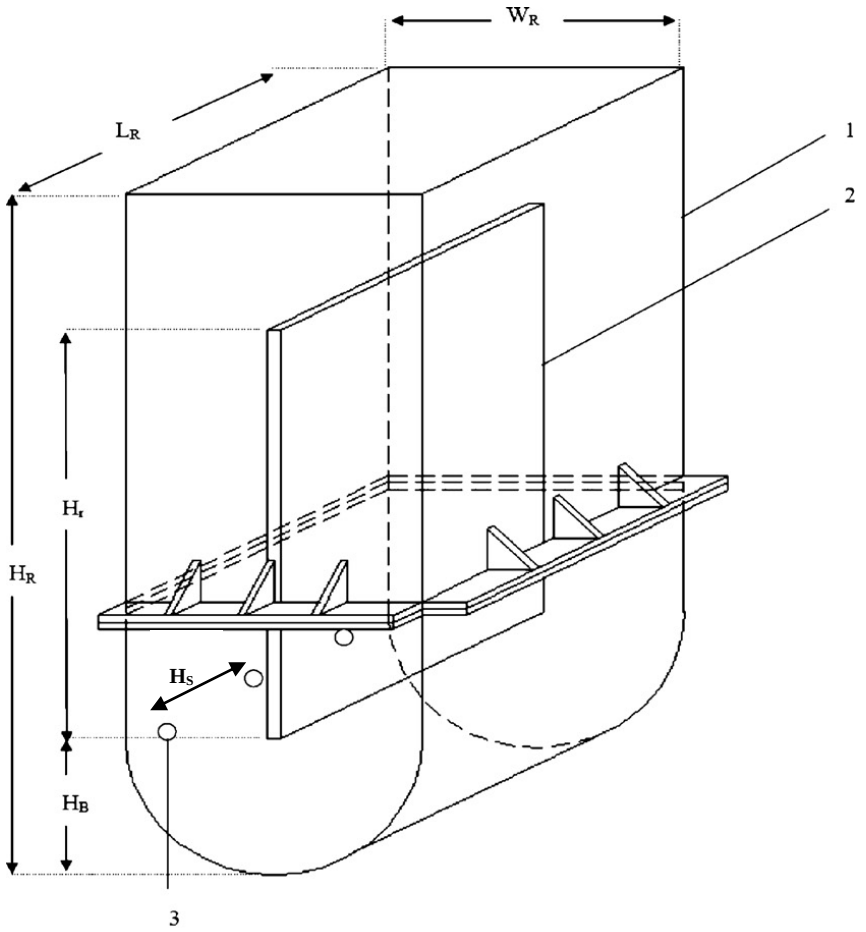

	Symbol	17 L FP-ALPBR	50 L FP-ALPBR	90 L FP-ALPBR	200 L FP-ALPBR
Total volume (L)		19	60	95	210
Working volume (L)		17	50	90	200
Column height (cm)	H_R	50	50	50	50
Column length (cm)	L_R	20	50	100	200
Column width (cm)	W_R	20	20	20	20
Draft tube height (cm)	H_r	30	30	30	30
Bottom clearance (cm)	H_B	10	10	10	10
Number of gas sparger		3	10	19	32
Space for each sparger (cm)	H_S	5	5	5	5

Figure 4.1 Geometric details of flat panel airlift photobioreactors (FP-ALPBRs) Symbol, 1 = reactor column; 2 = vertical plate; 3 = sparger

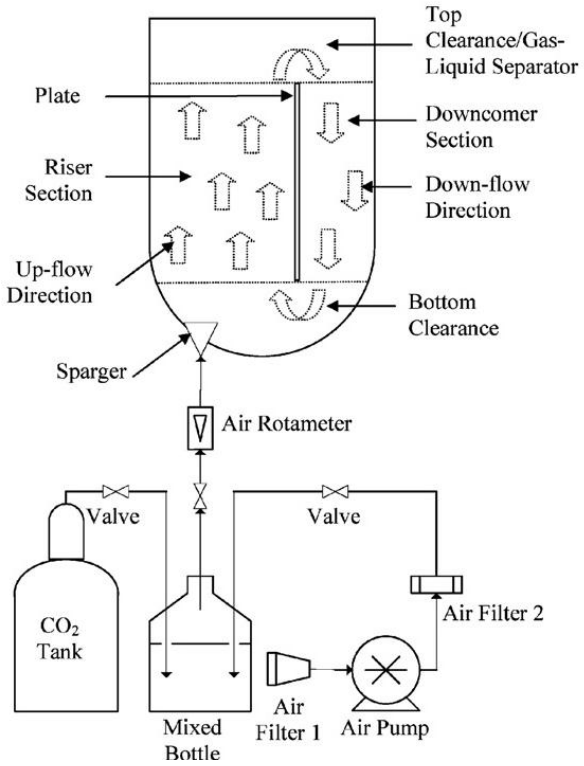

(A)

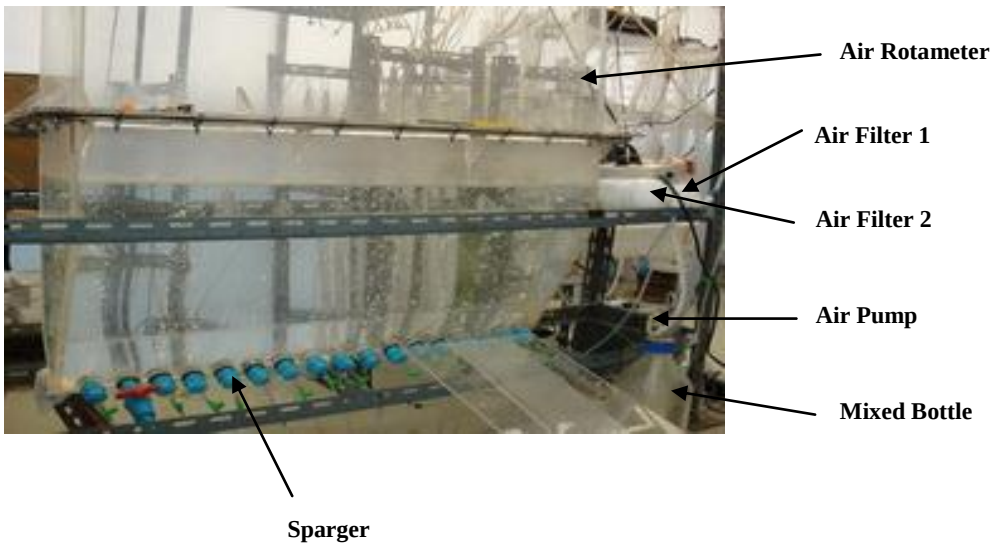

(B)

Figure 4.2 Experimental setup for flat panel airlift photobioreactor (A) Sketch view; (B) Actual view

Evaporative room (Outside view)


Fan


Controller Box


Temperature Sensor Probe

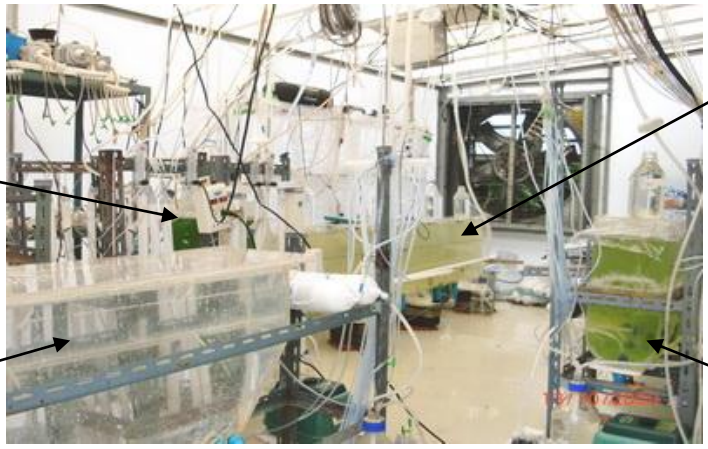

Evaporative room (Inside view)

Figure 4.3 Evaporative room used to control temperature

Light for the FP-ALPBRs was supplied from the vertical cool white fluorescent lamps installed on both sides of the column. The distance of each lamp from the outer surface of the column could be altered from 1-10 cm to manipulate the light intensity. The illumination intensity incident to airlift bioreactor outer surface was measured with a digital LX-5 Lux meter, where Photon flux density and irradiance are readily interconverted from (Thimijan et al., 1982):

$$1\ \mu mol\ (m^{-2}s^{-1}) = 1\ \mu E\ m^{-2}s^{-1} = \frac{119.7}{\lambda}\ W\ m^{-2} = 74\ Lux \qquad (4.1)$$

where λ is the wave length of the light in nanometer.

4.1.2 Preparation of the bioreactor

1) setup the bioreactor as described in Section 4.1.1
2) sterilize the whole system using hot steam for 10-15 min
3) fill the tap water into the bioreactor depending on the volume requirement
4) add chlorine (as sodium hypochloride) to remove contaminant species in the tab water
5) use a small amount of potassium iodide to check the remaining chlorine solution (By dropping a little amount of potassium iodide to the solution, if the color of the mixture turns to yellow, there is still chlorine remaining in the solution which is not ready to use)

4.2 Experiments

4.2.1 Determination of hydrodynamic and mass transfer behavior

4.2.1.1 Gas holdup

The overall gas holdup was determined using a volume expansion technique. The U-tube manometer was used to measure the pressure difference between the two defined levels, which enabled the determination of downcomer gas holdup. The

experimental steps follow:

1) add water into the reactor until liquid level is 7 cm above the draft tubes
2) measure the liquid level (h_L)
3) open air valve
4) adjust superficial velocity
5) measure the liquid level again (h_D)
6) measure pressure drop
7) calculate overall gas holdup used Equation 4.6
8) repeat Steps 2 to 7 by varying gas superficial velocity from 0.2 to 3.0 cms^{-1}

4.2.1.2 Liquid velocity

The measurement of liquid velocity in the airlift system was achieved by employing the tracer injection method as described below:

1) add water into the reactor until liquid level is 7 cm above the draft tubes
2) define two vertical distances for the dye tracer to travel
3) open air valve
4) adjust superficial velocity
5) inject the color tracer and measure the time for the tracer to travel between the two defined points
6) calculate liquid velocity used Equation 4.7
7) repeat Steps 2 to 6 by varying gas superficial velocity from 0.2 to 3.0 cms^{-1}

4.2.1.3 Mass transfer coefficient

The overall volumetric mass transfer coefficient can be determined by the dynamic method. The dissolved oxygen (DO) meter was used to measure oxygen concentration in the system. The steps are:

1) add water into the reactor until liquid level is 7 cm above the draft tubes
2) open nitrogen valve until DO reaches zero % air saturation
3) close nitrogen valve and open air valve
4) adjust superficial velocity
5) record the dissolved oxygen concentration with respect to time from the point where air was distributed into the system until the water was saturated with oxygen
6) calculate k_La (Equation 4.9)
7) repeat Steps 2 to 6 by varying gas flow rate from 0.2 to 3.0 cm s^{-1}.

4.2.2 Determination of growth

4.2.2.1 Preparation of inoculum

1) obtain a green alga, *H. pluvialis* strain NIES-144 from Center of Excellence for Marine Biotechnology, Faculty of science, Chulalongkorn University, Thailand. The original strain was from the National Institute of Environmental Studies, Japan.
2) prepare F1 medium with chemical composition as indicated in Table 4.1
3) sterilize the medium in autoclave at 121 ^{0}C for 20 min
4) inoculate 10% by volume of cell into 500 mL sterilized fresh F1 medium in 1,000 mL Erlenmeyer flask
5) incubate the flask at 22 ^{0}C and supply continuous light intensity of 20 µmol photon.m^{-2}.s^{-1} to the surface of the culture vessel
6) manually shake the flask daily
7) harvest the active green motile cells under exponential phase and use as inoculum for other experiments

Table 4.1 Composition of F1 medium (Fabregas et al., 1998)

Substances	Amount (mg per liter)
$CaCl_2.2H_2O$	9.87
KNO_3	410
Na_2HPO_4	300
$C_6H_5FeO_7.5H_2O$	2.22
$MgSO_4.7H_2O$	16.41
$CuSO_4.5H_2O$	0.008
$Na_2MoO_4.2H_2O$	0.08
MoO_3	0.66
Cr_2O_3	0.05
SeO_2	0.036
$CoCl_2.6H_2O$	0.0078
$NH_4Fe(C_6H_5O_7)$	6

4.2.2.2 Batch culture system

1) set the airlift system according to the description in Section 4.1 above. A_d/A_r was firstly fixed at 0.4 (Issarapayup et al., 2009)
2) fill the bioreactor with 10% by volume of starter innoculum. The exact quantity of the starter medium depended on the required initial concentration in the ALPBP. An initial density of *H. pluvialis* for all experiments was fixed around 0.2 x 10^5 cell mL^{-1}.
3) sparge a mixture of air and CO_2 (from the preset concentration) through the reactor bottom at superficial gas velocity of 0.4 cm s^{-1} (Issarapayup et al., 2009)
4) in case of using the artificial light (fluorescent lamps) for algal growth, the supplement of artificial light for algal growth was contributed light intensity of constantly 30 µmol photon.m^{-2}.s^{-1} for 24 h through the end of cultivation.
5) in case of using the natural light (sun light) for algal growth, the supplement of natural light for algal growth was contributed light intensity of approximately 100 to 500 µmol photon.m^{-2}.s^{-1} where light was

manipulated by ratio of light and dark cycle (12 h:12 h).

6) the algal temperature was controlled using evaporative room in the range of 27±3 ^{0}C
7) measure cell properties as described in Section 4.3

4.2.2.3 Semi-batch culture system

1) set the airlift system according to the description in Section 4.1. A_d/A_r was firstly fixed at 0.4 (Issarapayup et al., 2009)
2) fill the bioreactor with 10% by volume of starter innoculum. The exact quantity of the starter medium depended on the required initial concentration in the ALPBP. An initial density of *H. pluvialis* for all experiments was fixed around 0.2 x 10^5 cell mL^{-1}
3) sparge a mixture of air and CO_2 (from the preset concentration) through a bottom of the reactor at superficial gas velocity of 0.4 cm s^{-1} (Issarapayup et al., 2009)
4) take samples and count for the cell density using Haemacytometer until the stationary growth was observed
5) subculture the cells and adjusted its concentration to 1.0 x 10^5 cell mL^{-1} and replace with the fresh F1 medium
6) measure cell properties as described in Section 4.3

All experiments were carried out in duplicate. In the batch operation, the culture was grown in the bioreactor until the stationary phase was reached, whereas in the semi-continuous mode, the cultivation was started off as a batch culture, and once the cell concentration reached a required value, 50% volume of culture broth was harvested. This harvested portion was replaced with a fresh medium.

4.3 Analyses and calculations

4.3.1 Overall gas holdup

The overall gas holdup was determined using a volume expansion technique, where the difference between liquid levels before and after gas dispersion. The definition of gas holdup is

$$\varepsilon = \frac{V_G}{V_G + V_L} \tag{4.2}$$

Because the volume of gas could not be measured directly, we defined V_D (dispersed volume) as the total volume of gas phase plus volume of liquid phase. Then

$$\varepsilon_o = \frac{V_D - V_L}{V_D} \tag{4.3}$$

$$\varepsilon_o = 1 - \frac{V_L}{V_D} \tag{4.4}$$

$$\varepsilon_o = 1 - \frac{h_L A}{h_D A} \tag{4.5}$$

finally,

$$\varepsilon_o = 1 - \frac{h_L}{h_D} \tag{4.6}$$

where ε_o is overall gas holdup (-)

h_D is dispersed liquid height (cm)

h_L is unaerated liquid height (cm)

4.3.2 Liquid circulation velocity

The tracer injection method was used to measure the liquid velocity in riser only. In downcomer the tracer injection method could not be used because color had a high distribution. The time that tracer traveled between two fixed positions is used to calculate liquid velocity in riser from:

$$v_{Lr} = \frac{x}{t} \tag{4.7}$$

where v_{Lr} is riser liquid velocity (cm s^{-1})

x is distance of tracer travel (cm)

t is tracer travel time (s)

4.3.3 Mass transfer coefficient

The volumetric mass transfer coefficient was determined by the dynamic method. Dissolve oxygen concentration was measured by DO meter. The oxygen balance in bioreactor gives:

$$\frac{dC_L}{dt} = k_L a(C_L^* - C_L) \tag{4.8}$$

Integrating both sides of Equation 4.8 from $C_L = 0$ to $C_L = C_L$ leads to

$$\ln \frac{(C_L^* - C_o)}{(C_L^* - C_L)} = k_L a t \tag{4.9}$$

where C_L^* is saturation dissolved oxygen concentration. (% air saturation)

C_o is initial oxygen concentration in liquid phase (% air saturation)

C_L is dissolved oxygen concentration in liquid phases (% air saturation)

$k_L a$ is overall volumetric mass transfer coefficient (s^{-1})

t is time (s)

4.3.4 Cell density

Cell density was measured by microscope and the counting of cells was performed using an improved Neubauer haemacytometer (Figure 4.3).

1) take 125 µL of culture and place them on a clean haemacytometer
2) place clean cover slip on the drop so that the drop was evenly dispersed under the cover slip

3) count cells under a microscope (objective 10x) (see Figure 4.4)
4) calculate the number of cells as follows :

$$N = \frac{n_1 + n_2}{8} \times 10^4 \quad (4.10)$$

where N is cell number (cell mL^{-1})
n_1 and n_2 are number of cells count in upper and lower grid (cells)

4.3.5 Specific growth rate

The specific growth rate is calculated from:

$$\mu = \frac{\ln(N_2) - \ln(N_1)}{t_2 - t_1} \quad (4.11)$$

where μ is specific growth rate (μ; d^{-1})
N_1 and N_2 are cells density at t_1 and t_2 (cell mL^{-1})
t is time (d)

4.3.6 Cell dry weight

Cell dry weight was done when the cell almost reached maturation stage.

1) count the cells by haemacytometer by fix volume at 200 ml
2) filter the cells by membrane filter (diameter of 10 μm), which was dried by oven for 24 h
3) dry the membrane filter and cells in oven for 24 h
4) bring it into the dessiccator until it cools down
5) weigh it by four position digital balance
6) calculate by following equation

$$\%\ Dry\ weight = \frac{C \times V}{G} \times 100 \quad (4.12)$$

where	C	is	cells density (cell mL^{-1})
	V	is	volume (mL)
	G	is	mass of membrane filter and cells – mass of membrane filter

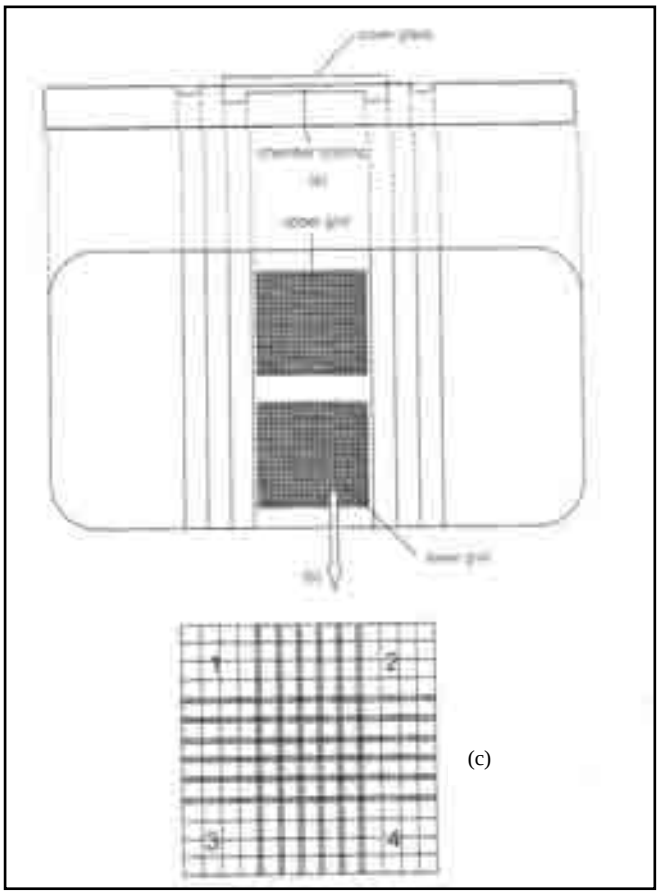

Figure 4.4 (a) Side view of the cell counting chamber showing the cover glass and the space beneath it that holds a microalgae suspension. (b) Top view of the chamber. The chamber has two grids located in the center of the slide. (c) An enlarged view of the grid. The microalgae in the squares 1, 2, 3 and 4 are used for cell count.

Count the cells in the square and those who touch the top and left borders (●)

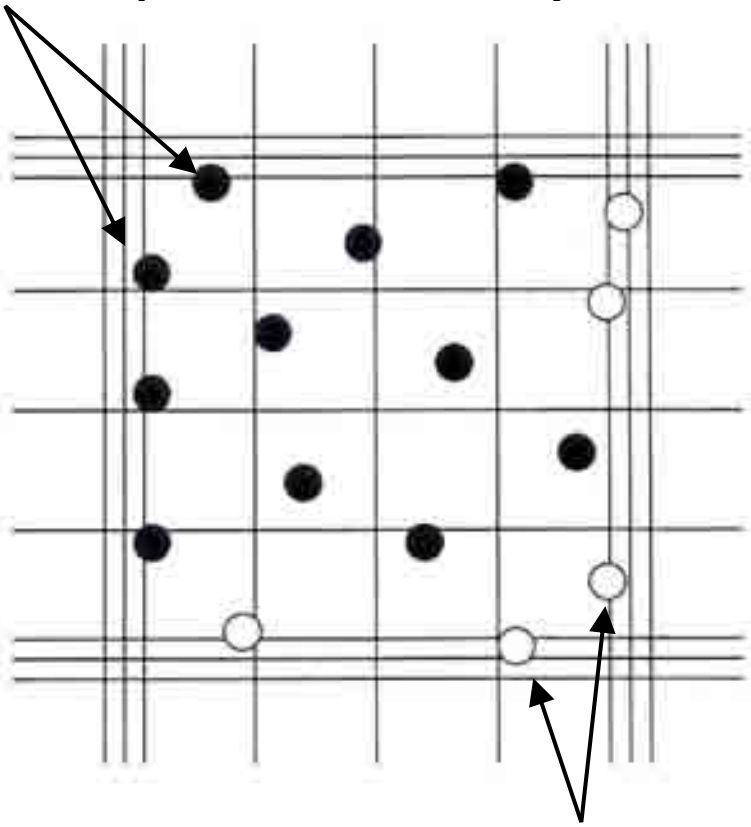

Do not count the ones touching the right and lower borders (O)

Figure 4.5 Counting cell density

4.3.7 Logistic law as a model to describe cell growth

In this work, the logistic function (Bellgardt, 1991) was employed to represent the growth kinetics of *H. pluvialis*. The algal cell density (X) was measured daily by microscope with an improved Neubauer hemacytometer (BOECO Germany). The growth equation in the batch mode cultivation, and the corresponding productivity (g dry cell day^{-1}) can then be calculated from:

$$\frac{dX}{dt} = kX\left(1-\frac{X}{X_{\max}}\right) \qquad (4.13)$$

when X = initial cell density, X_0, at $t = 0$

$$X = \frac{X_0 \exp(kt)}{\left(1 - \frac{X_0(1-\exp(kt))}{X_{max}}\right)} \quad (4.14)$$

where X_0 and X_{max} (cell mL^{-1}) are initial cell density and maximum cell density at time t (day), and k (day^{-1}) is the Logistic law coefficient (or equivalent to specific growth rate). Note that the initial cell density was kept constant for all experimental runs at $1x10^5$ cell mL^{-1}.

The harvest of cell was performed when cell density reached its maximum and the harvesting volume was calculated such that the remaining culture when mixed with the replenishing nutrient would give the initial cell concentration of $1x10^5$ cell mL^{-1}. With this operation, the productivity could be calculated from

$$J = \frac{G \times I \times 1000}{H} \quad (4.15)$$

where	J	is	productivity (g dry cell day^{-1})
	G	is	dry weight (g L^{-1})
	I	is	harvesting volume (m^3)
	H	is	harvesting period (day)

4.3.8 Nitrate (NO_3^- - N) concentration

Nitrate concentration (mg-N L^{-1}) was analyzed by the UV screening method. Water sample was filtered through GF/C filter and measured directly by UV-visible spectrophotometer at 220 and 275 nm (AOAC, 1980). Calculation of nitrate concentration of nitrate concentration was as following:

$$Nitrate(mg - N\,L^{-1}) = \frac{(Abs_{220nm} - Abs_{275nm}) \times A}{B} \quad (4.16)$$

where A is concentration of nitrate in standard curve (mg-N L^{-1})
B is absorbance (220 nm - 275 nm) of standard nitrate

The standard nitrate solution was prepared using 1-10 mg-N L^{-1} of sodium nitrate. It had to be note that, this method must be strictly used with nitrate concentration between 1-10 mg-NO_3^-- N L^{-1}. Water sample containing high nitrate concentration (over 10 mg-N L^{-1}) could be diluted with de-ionized water prior to analysis but water containing low nitrate concentration (below 1 mg-N L^{-1}) was not acceptable with this method. Moreover, high nitrate concentration could interfere with nitrate measurement hence concentration of nitrate must be subtracted with nitrite concentration.

1) take the sample and separate the cells from the culture medium by centrifuge at 3,000 rpm with 30 min
2) take the clear solution about 3 mL for the measurement of nitrate
3) measure the sample mixture solution by Spectrophotometer with nitrate operation mode based on the absorption at the wavelength 220 and 275 nm
4) prepare nitrite solutions at 0.05, 0.5, 1.0, 3.0 and 5.0 mg N L^{-1} as standard curve
5) calculate amount of nitrate (mg-NO_3^-- N L^{-1}) with standard curve

4.3.9 Phosphate (PO_4^{2-} - P) concentration

Phosphate analysis (mg- P L^{-1}) follows the method suggested by Strickland and Parsons (1972). Mixed reagent was the mixture of four solutions i.e. ammonium molybdate solution (dissolve 15g of $(NH_4)_6Mo_7O_{25}.4H_2O$ in 500 mL dH_2O), sulfuric acid solution (add 140 mL of conc. H_2SO_4 in 900 mL of dH_2O), ascorbic solution (dissolved 27 g of ascorbic acid in 500 mL of dH_2O) and potassium antimonyl-tartrate

solution (dissolved 0.34 g of potassium antimonyl-tartrate in 250 mL of dH_2O), at the mixing ratio of 2:5:2:1. One milliliter of water sample was added with 100 µL of the mixed reagent, homogenized and left for 2 hours reaction time. Thereafter, the sample was measured by spectrophotometer at 885 nm wavelength. Standard phosphate solution was 0.1-2.0 mg- P L^{-1} of KH_2PO_4.

1) take the sample and separate the cells from the culture medium by centrifuge at 3,000 rpm with 30 min
2) take the clear solution about 1 mL for the measurement of phosphate
3) add 0.1 mL of mix reagent into the sample solution and shake
4) measure the sample mixture solution by spectrophotometer with phosphate operation mode based on the absorption at the wavelength 885 nm
5) prepare the phosphate solution at 0.05, 0.5, 1.0, 3.0 and 5.0 (mg- P L^{-1}) as standard curve
6) calculate amount of phosphate (mg- P L^{-1}) with standard curve

4.3.10 Nutritional value

The analysis of the sample was conducted by the Food and Testing Laboratory, Faculty of Science, Chulalongkorn University. The samples were analyzed for their protein, carbohydrate and total fat contents following.

- Protein

The crude protein content was obtained by multiplying the amount of nitrogen content by the factor of 6.25. The nitrogen content was calculated from the amount of ammonia produced and was expressed as the percentage by mass or in grams per kilogram. The crude protein content, w_p, was calculated as a percentage by mass, using the following equation: (Reference: Thai Industrial Standard, Part 2: Block digestion/steam distillation method)

$$w_p = w_n \times F \tag{4.17}$$

where

w_N	is	the nitrogen content of the sample, expressed as a percentage by mass to four decimal places
F	is	the factor to convert Kjeldahl nitrogen to protein; for feedstuffs, F = 6.25

- Total fat

The total fat content was obtained the method as follows: (Reference: AOAC, Official methods of analysis, Method 920.39)

1) extract 2 g test portion on small paper in funnel with five 20 mL portion H_2O prior to drying for ether extraction
2) use thimble with porosity permitting rapid passage of ether
3) extract period may vary from 4 h at condensation rate of 5-6 drop s^{-1} to 16 h at 2-3 drop s^{-1}
4) dry extract 30 min at 100 ^oC
5) cool and weigh

- Carbohydrate

Calculate protein, fat, ash, and moisture contented in the cell dry weight, then calculate the percentage of total carbohydrate in cell dry weight by subtracting the sum of percentages of protein, fat, moisture and ash from 100, according to the following equation:

% Total carbohydrates = 100 - (% protein + % fat + % moisture + % ash) (4.18)

4.3.11 CHN/O content

The analysis of the sample was conducted by the Food and Testing Laboratory, Faculty of Pharmaceutical Science, Chulalongkorn University. The analysis required at least 5 g of cell dry weight and the analysis was conducted in CHNS/O analyzer (Perkin Elmer PE2400 Series II), using gaseous products fed by pyrolysis in high purify oxygen and were chromatographically detected with a thermal conductivity detector.

4.3.12 Trace elements content

The analysis of trace elements in algal medium was conducted by the Food and Testing Laboratory, Faculty of Pharmaceutical Science, Chulalongkorn University. Those elements were measured using ICP atomic emission spectrometry (Inductively coupled plasma atomic emission spectrometer; Perkin Elmer Model PLASMA-1000). The liquid sample is introduced to the inductively coupled plasma to produce excited atoms and ions that emit electromagnetic radiation at wavelengths characteristic of a particular element. The intensity of this emission is indicative of the concentration of the element within the sample.

CHAPTER V

Behavior of Flat Panel Airlift Photobioreactors for the scalable cultivation of vegetative cells of *H. pluvialis*

This chapter will be divided into two parts. The first part discusses the behavior of the FP-ALPBRs while the second part examines the use of such reactor in the cultivation of *H. pluvialis*. Note that the airlift employed in this work is designed as a flat panel to facilitate the changing in the size which can be achieved simply by varying the length of the reactor. Such simplicity in the size manipulation is therefore called "scalable" cultivation in this chapter.

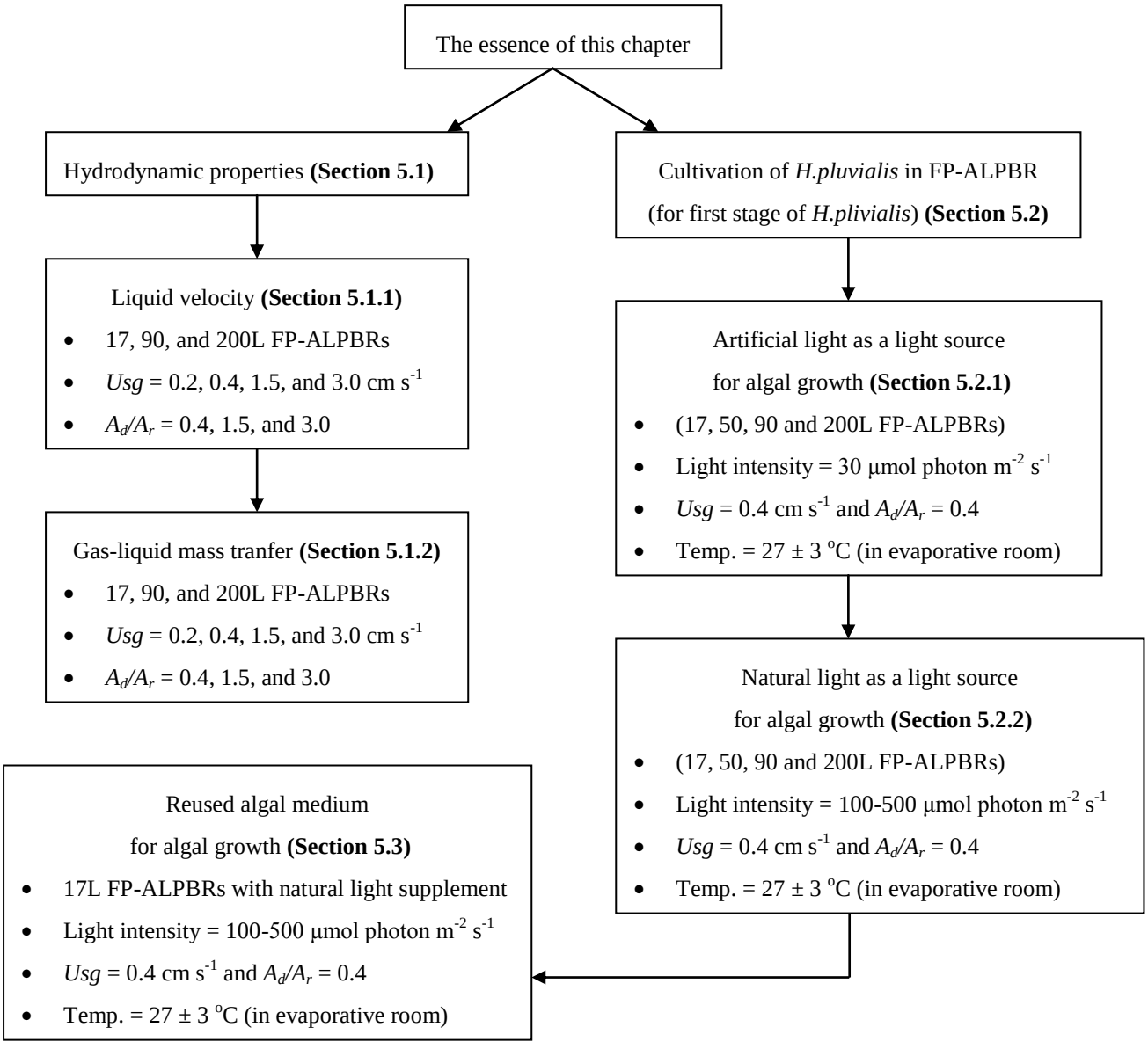

5.1 Hydrodynamic properties of FP-ALPBRs

Certain designs of photobioreactors suit one particular algal strain than the others. This is due primarily to the different nature of microorganisms, e.g. some grow well in moving nutrient, some like to move by themselves in still environment. However, one certain flow pattern that algae would need particularly for the vertical type photobioreactors is the vertical circulation. This is to make sure that most cells are circulated to the high light intensity zone where they can photosynthesize. This first part of this chapter provides information on hydrodynamic characteristics of the flat panel airlift photobioreactors (FP-ALPBRs) which could be useful in explaining some certain phenomena during algal growth. Hydrodynamic properties of interest in this chapter include: liquid velocity and overall volumetric gas-liquid mass transfer.

It is noted here that the hydrodynamic study was only performed with the flat panel airlift (FP-ALPBR) with the sizes of 17, 90 and 200L as they set the boundary of the investigation in this work. The properties of 50L are not examined as some intrapolation might be applied if necessary.

17L FP-ALPBR

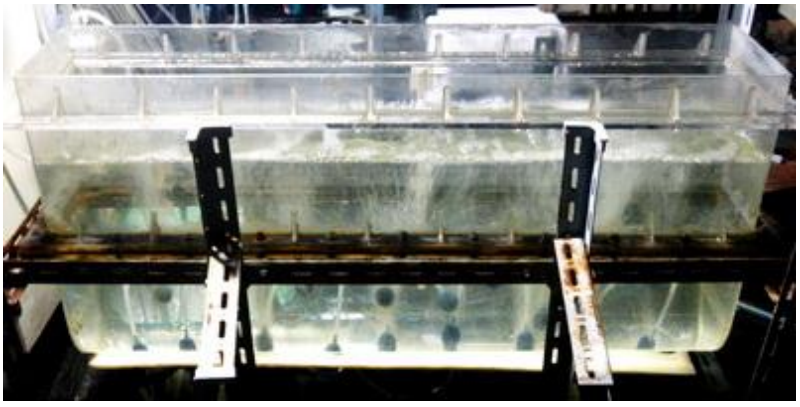

90L FP-ALPBR

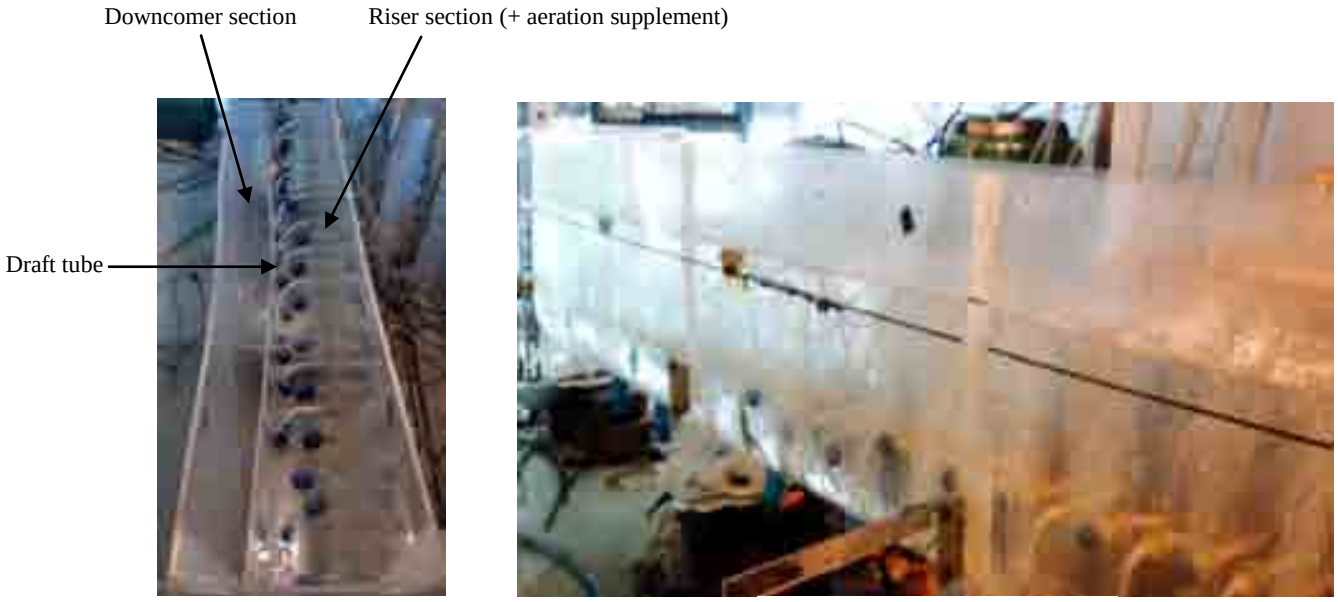

200L FP-ALPBR (Top view) 200L FP-ALPBR (Side view)

Figure 5.1 The FP-ALPBRs system used for hydrodynamic study

5.1.1 Liquid velocity

The measurement of liquid velocity was conducted in riser of 17, 90, and 200L FP-ALPBRs as shown in Fig. 5.1 which were subject to the supply of superficial velocity (U_{sg}) in range of 0.2 to 3.0 cm s^{-1} and three cross sectional area ratios between downcomer and riser (A_d/A_r of 0.4, 1.5 and 3.0).

To briefly recall the procedure of conducting this experiment (Section 4. 2.1.2), the measurement of liquid velocity in the airlift system was achieved by employing the tracer injection method (soluble blue ink) where a vertical distance for the dye tracer to travel was defined. Then, the blue color tracer was injected to the system and the time for the tracer to travel between the two defined points was counted. Finally, equation 4.7 (Chapter IV) was used to calculate the liquid velocity.

Figure 5.2 illustrates that, for the 17L FP-ALPBR, an increase in superficial velocity led to an increase in riser liquid velocity (U_l), and the fastest velocity (in the range of 5.9-11.1 cm s^{-1}) was obtained from the system with the largest A_d/A_r (= 3). At A_d/A_r of 1.5, U_l was in the range of 3.2 - 6.7 cm s^{-1} and at A_d/A_r of 0.4, U_l ranged from 1.2 - 6.3 cm s^{-1}. Considering the large scale 90 and 200L FP-ALPBRs employed in

this work, the results exhibited a similar trend to that of the small scale, 17L FP-ALPBR, which means that an increase in superficial gas velocity could cause a faster movement of liquid in the riser section.

When compared the performance of liquid velocity achieved by 17, 90 and 200L reactors at the same ratio of downcomer and riser cross-sectional area (at A_d/A_r of 0.4, for example), the larger reactor (200L) clearly exhibited greater liquid velocity with a range of 3 - 10 cm s^{-1} than that of the smaller counterpart (in 90L ranged of 2 - 9 cm s^{-1} and 17L ranged of 1.2 - 6.3 cm s^{-1}, respectively) as demonstrated in Fig. 5.3. To clarify this further, an analysis of bubble size was carried out in the 17 and 200L systems and the results indicate that, although the two were operated at the same superficial velocity and the same gas sparger, bubble coalescence seemed to occur more significantly in the large scale 200L airlift than in the smaller scale reactors (as illustrated in Fig. 5.4). Visual observation demonstrates clearly that there was more local liquid circulation within the large scale airlift and this increased the colliding incidences among the bubbles. And since the system worked in the bubbly flow regime, bubble collision often leads to the coalescence of bubbles rather than the breaking up. It should be noted that the collision of bubbles can result in bubble coalescence or bubble breakup depending on the flow regime and bubble size. Usually at low gas flow rate, bubbles seem to combine when they hit each other.

17L ALPBR 200L ALPBR

Figure 5.4 Bubble distributions in 17 and 200L FP-ALPBRs

For ellipsoidal bubbles, the major and minor axes of bubble images were measured. The equivalent size of the bubble (d_B), representing the diameter of a sphere whose volume was equal to that of the bubble, is calculated from;

$$d_B = (p^2 q)^{1/3}$$

where p is major axes of bubble images

q is minor axes of bubble images

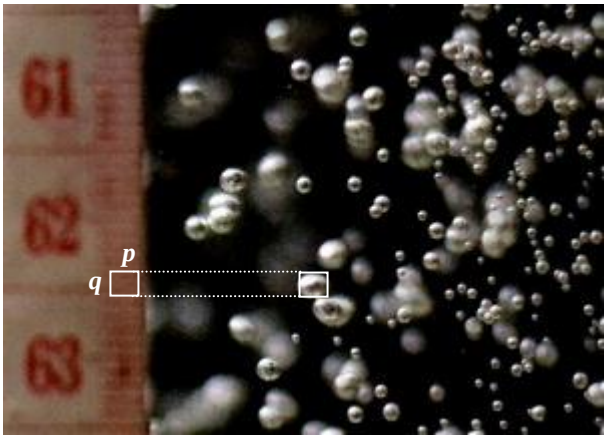

17L ALPBR (Enlarged view)

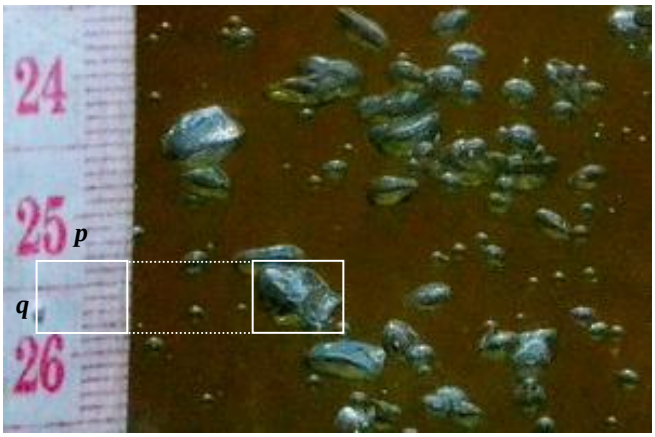

200L ALPBR (Enlarged view)

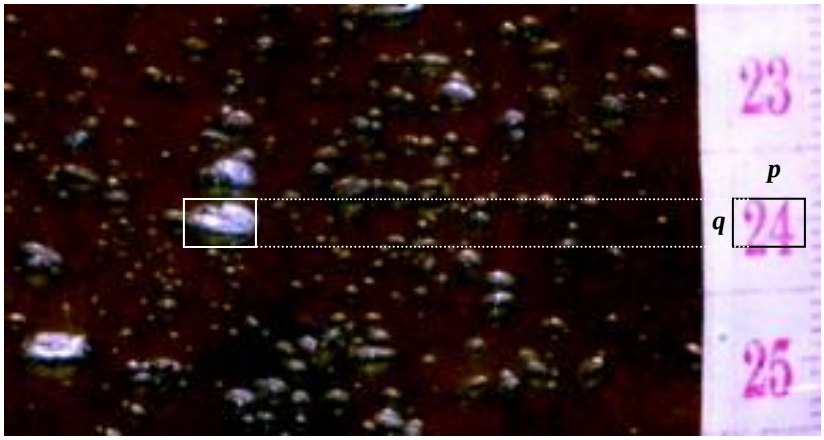

90L ALPBR (Enlarged view)

FP-ALPBR system	Averaged bubble size (dB)
17L	0.1 ± 0.04 cm
90L	0.31 ± 0.10 cm
200L	0.4 ± 0.11 cm

In the 200L reactor (averaged d_B = 0.4 ± 0.11 cm), as the bubbles combined and became larger in size, they moved at a faster speed than the small bubbles in the smaller scale reactors. Thus the 200L system was mostly governed by chubby air bubbles which had more energy to transfer to liquid leading to a faster liquid velocity when compared to the 17L system (averaged d_B = 0.1 ± 0.04 cm), where fine air particles were mostly occupied.

5.1.2 Gas-liquid mass transfer

The gas-liquid mass transfer in the airlift photobioreactor is typically measured in terms of the overall volumetric mass transfer coefficient (K_La) where could be determined by the dynamic method. The dissolved oxygen (DO) meter was used to measure oxygen concentration in the system (Section 4.2.1.3). Finally, Equation 4.9 (Chapter IV) was used to calculate the overall volumetric mass transfer coefficient (K_La).

The effect of superficial velocity (U_{sg}) on K_La as illustrated in Fig. 5.5 was examined in photobioreactors with various A_d/A_r and aeration conditions (0.2 - 3.0 cm s^{-1}). From the experiments with 17L FP-ALPBR, the results revealed that K_La rose with an increase in U_{sg}. However, increasing ratio of downcomer to riser cross-sectional area (A_d/A_r) significantly diminished K_La, e.g. A_d/A_r of 0.4 exhibited K_La ranged of 0.000358 to 0.0066 s^{-1}, whereas A_d/A_r of 1.5 would see K_La in the range of only 0.00051 to 0.0027 s^{-1}. However, a further increase in A_d/A_r above 1.5, i.e. at A_d/A_r of 3.0, K_La did not seem to decrease and was found to have a value from 0.000588 to 0.0021 s^{-1} along the range of U_{sg} employed in this work.

When compared the performance of the overall volumetric mass transfer coefficient (K_La) achieved by 17, 90 and 200L reactors at the same ratio of downcomer and riser cross-sectional area (at A_d/A_r of 0.4, for example). The 200L FP-ALPBR exhibited similar gas-liquid mass transfer results of similar nature to that of the smaller reactors, where an increase in superficial velocity enhanced K_La in the system. Fig. 5.6 indicates that, at the same A_d/A_r of 0.4, the enlarged system (200L)

provided almost the same value (very slightly higher) of K_La (0.001716 to 0.0068 s^{-1}), compared to smaller systems (K_La of 0.001152 to 0.0065 s^{-1} for 90L) and (K_La of 0.000358 to 0.0066 s^{-1} for 17L), respectively.

This finding might be further clarified by separately considering the overall mass transfer coefficient *(K_L)* and the specific mass transfer area *(a)* as shown in Table 5.1. The overall mass transfer coefficient *(K_L)* is adversely proportional to the film resistance between gas and liquid interface where the higher liquid velocity could result in decreasing gas-liquid film resistance, thus increasing the rate at which oxygen transfers between bubble and bulk liquid. The later factor, the specific mass transfer area *(a)* was significantly related to bubble size where the small bubbles (with the same volume) could give a much higher mass transfer area, and facilitate the mass transfer rate.

Table 5.1 Comparison of K_La in 17, 90 and 200L FP-ALPBRs

System	Overall mass transfer coefficient *(K_L)*	Specific mass transfer area *(a)*	Overall volumetric mass transfer coefficient (K_La)
17L	**Low value of K_L** (Low value of U_l = 1.2 - 6.3 cm s^{-1})	**High value of *a*** (Majority of fine bubbles with averaged d_B = 0.1 ± 0.04 cm)	0.000358 to 0.0066 s^{-1}
90L	**High value of K_L** (High value of U_l = 2 - 9 cm s^{-1})	**Low value of *a*** (Majority of chubby bubbles with averaged d_B = 0.31 ± 0.10 cm)	0.001152 to 0.0065 s^{-1}
200L	**High value of KL** (High value of U_l = 3 - 10 cm s^{-1})	**Low value of *a*** (Majority of chubby bubbles with averaged d_B = 0.4 ± 0.11 cm)	0.001716 to 0.0068 s^{-1}

Remark: based on the assumption that 17 and 200L systems (operated at the same ratio of downcomer and riser cross-sectional area, at A_d/A_r of 0.4, for this case, and at the same aeration rate) should have a potential to equally produce air bubbles.

It is important to remark that the study of gas hold up as described in Chapter IV (Section 4.3.1) could not be achieved in the reactor employed here. The unaerated water level was not significantly different from the aerated level within the range of aeration employed in this work, which did not allow the measurement of the overall gas holdup. In addition, the column height was too small and not adequate to give the differences in the manometer for the measure of riser gas holdup. Nevertheless, based on literature, gas holdup would take the value around 10% with aeration rate as employed in this experiment.

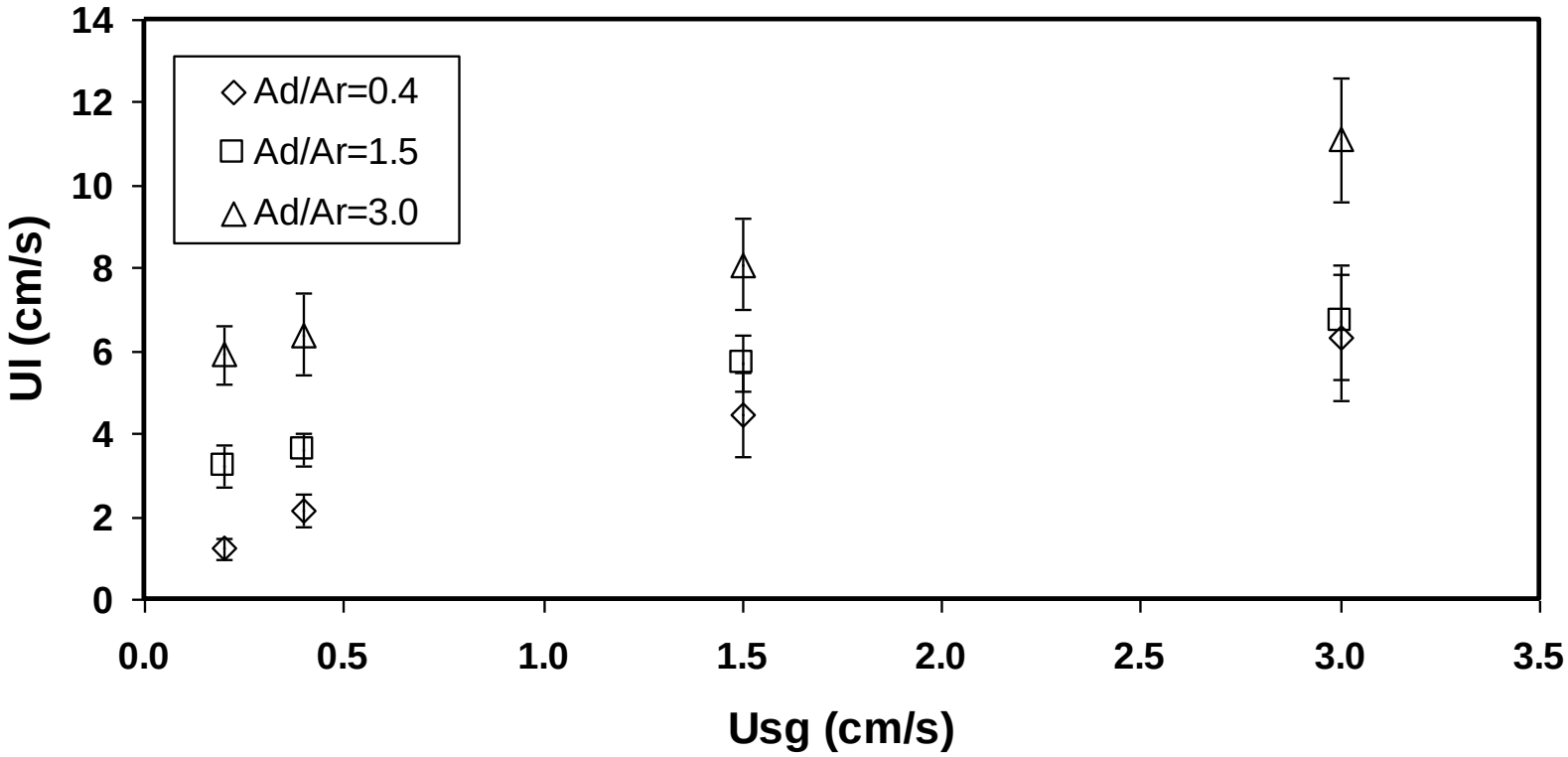

Figure 5.2 Effect of superficial velocity (U_{sg} = 0.2, 0.4, 1.5 and 3.0 cm s^{-1}) on liquid velocity (U_l) operated in 17L FP-ALPBR at different ratio of downcomer and riser cross sectional area (A_d/A_r = 0.4, 1.5 and 3.0)

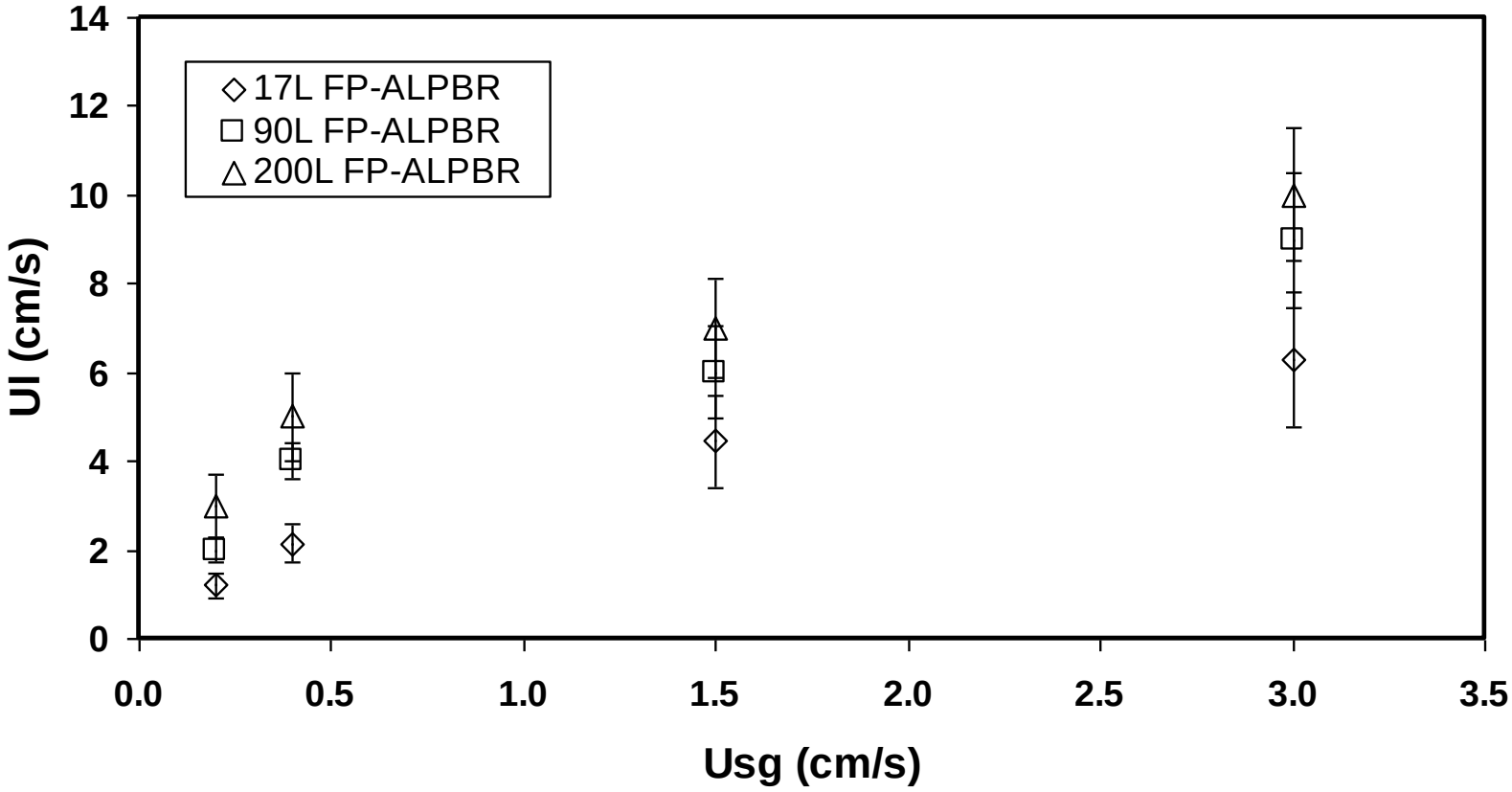

Figure 5.3 Effect of superficial velocity (U_{sg} = 0.2, 0.4, 1.5 and 3.0 cm s^{-1}) on liquid velocity (U_l) operated in 17, 90 and 200L FP-ALPBRs at the same ration of downcomer and riser cross sectional area (A_d/A_r =0.4)

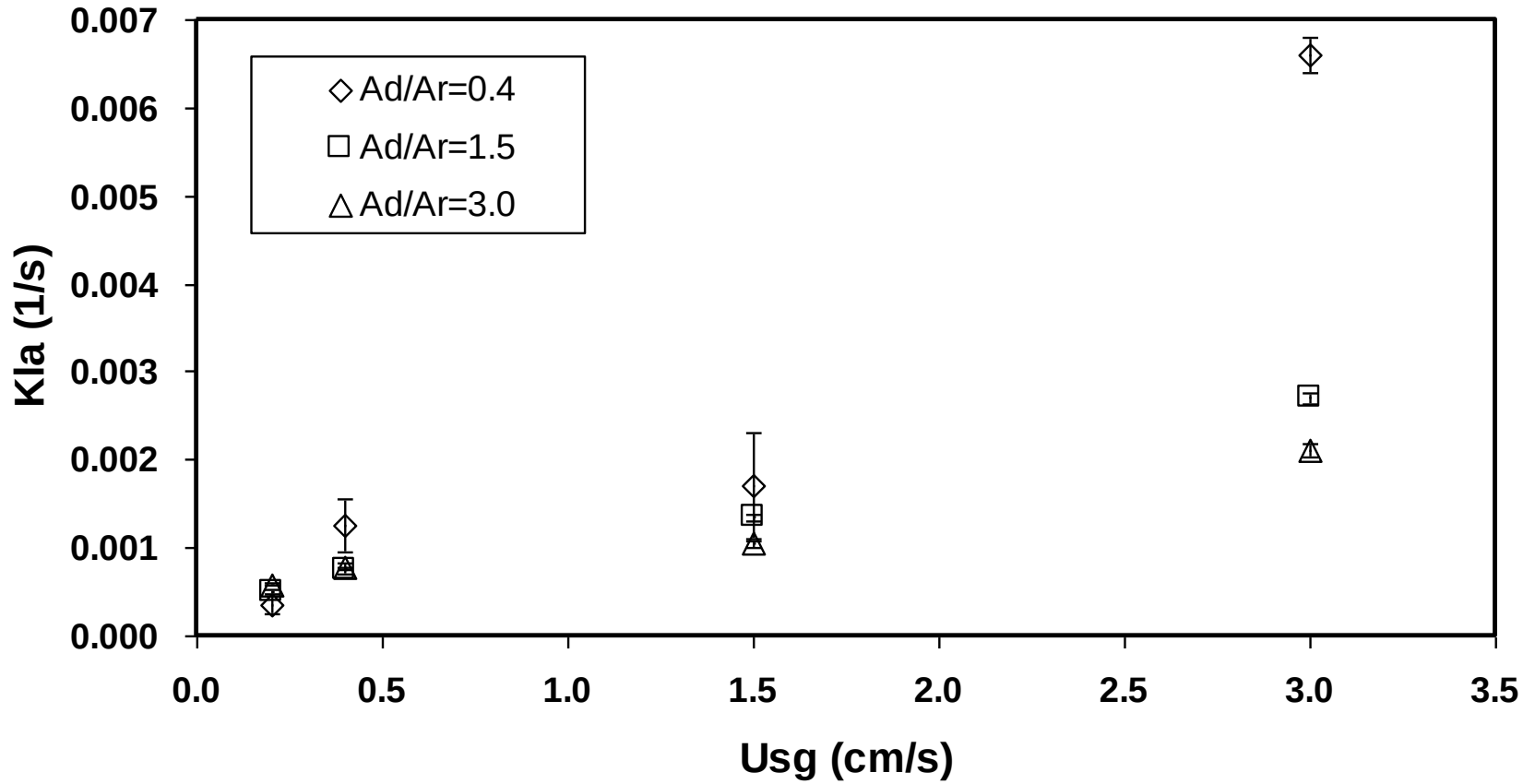

Figure 5.5 Effect of superficial velocity (U_{sg} = 0.2, 0.4, 1.5 and 3.0 cm s^{-1}) on overall volumetric gas-liquid mass transfer operated in 17L FP-ALPBR at different ratio of downcomer and riser cross sectional area (A_d/A_r = 0.4, 1.5 and 3.0)

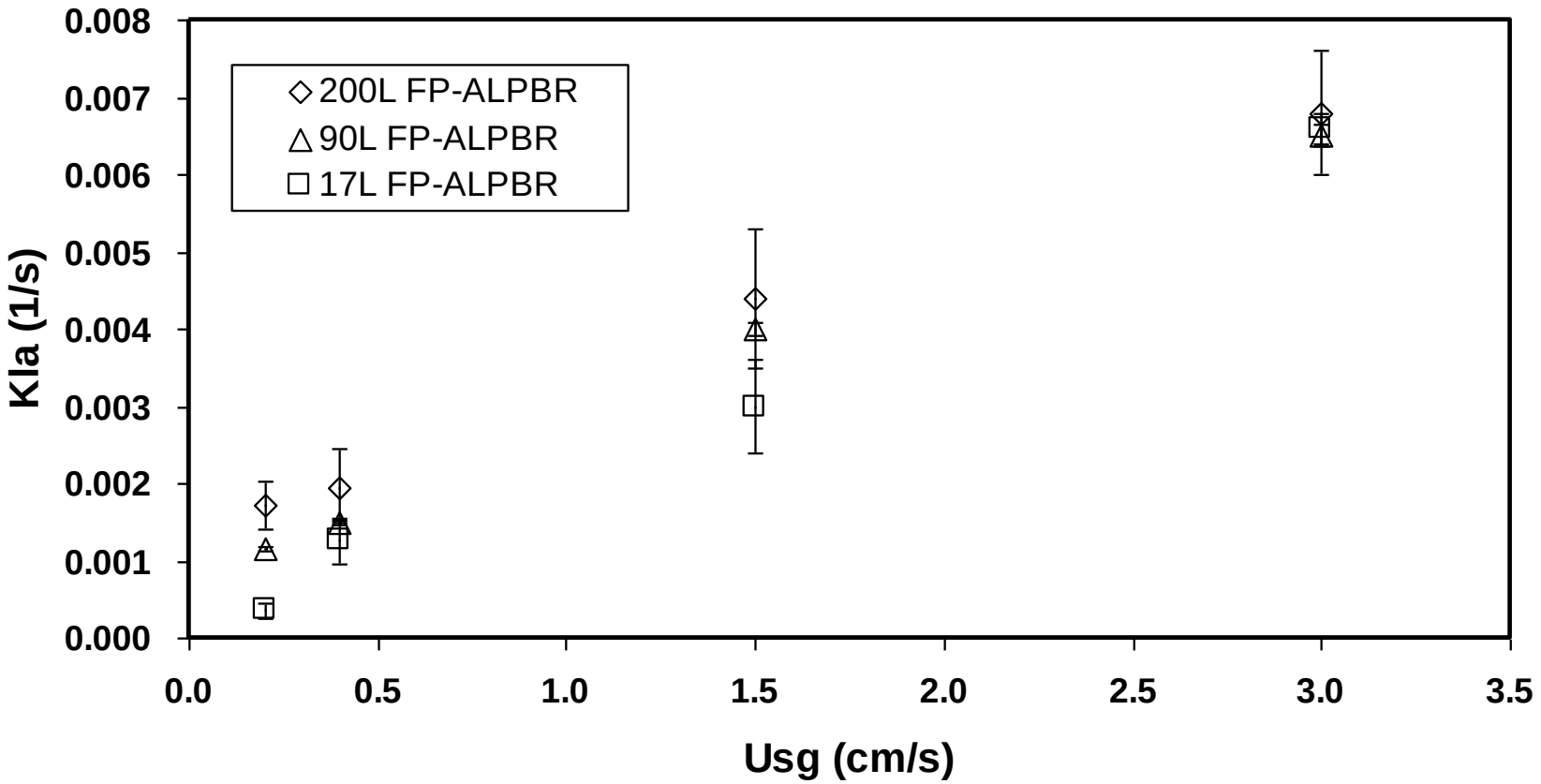

Figure 5.6 Effect of superficial velocity (U_{sg} = 0.2, 0.4, 1.5 and 3.0 cm s^{-1}) on overall volumetric gas-liquid mass transfer operated in 17, 90 and 200L FP-ALPBRs at the same ration of downcomer and riser cross sectional area (A_d/A_r =0.4)

5.2 Scale up of FP-ALPBRs for the cultivation of *H. pluvialis*

This section examines the feasible strategies of cultivating *H. pluvialis* with a variety of light supplements where fluorescence lamps as an artificial light source and sun light as a natural light source are investigated. Moreover, the study of the reused medium (natural light is conducted) is also given to evaluate the effectiveness of the culture system running with reused medium. It must be mentioned that all experiments were carried out in the evaporative room to ensure a proper temperature control ($27 \pm 3\ ^{o}C$).

5.2.1 Artificial light for *H. pluvialis* cultivation

The cultivation of *H. pluvialis* with the use of artificial light as a light source for algal growth was examined. All systems were performed in a confined evaporative room. Providing this consistent artificial light intensity, a rapid growth of green vegetative cells was anticipated. A bunch of successful studies on growing vegetative cells of *H. pluvialis* was available but mostly only operated in small volume, under a well controlled environmental and this was already stated in the literature review section. To compare this system performance (FP-ALPBRs) to those past reports, a preliminary test on enlarging scale (17 and 50L ALPBRs) for the cultivation of *H. pluvialis* had been performed using artificial light. It was reported in the previous work that the optimal airlift design for the cultivation of such vegetative cells was with the ratio of downcomer/riser cross-sectional area of 0.4 and the aeration rate of 0.4 ($cm\ s^{-1}$) (Issarapayup et al., 2009). It was also evident (from Section 5.1) why such design must have given the best cultivation performance achieved by past experience as they provided the lowest liquid velocity which corresponds to the condition with the mildest shear force (to the cells). As *H.pluvialis* is not a shear tolerant alga, they would rather grow best in the system with low shear. Therefore, this design parameter became the starting point of this work as will be discussed from here onwards.

The experiments were conducted in 17 and 50L flat panel airlift bioreactors

(FP-ALPBRs) where the cultivation process was subject to the preceding optimized growth conditions (The experiment display is pictured in Fig. 5.7).

- The ratio of downcomer/riser cross-sectional area of 0.4 and the aeration rate of 0.4 (cm s^{-1}) were employed.
- The CO_2 enriched air was mixed with air before entering into the system where concentration of CO_2 was 1% by volume.
- The system was illuminated at a constant light intensity of around 30 µmol photon m^{-2} s^{-1} by fluorescence lamps.
- The artificial light was subject to the system for 24 h through the end of cultivation.
- The temperature of the culture was maintained at 27 ± 3 ^{o}C during the whole course of growth cultivation in evaporative room.

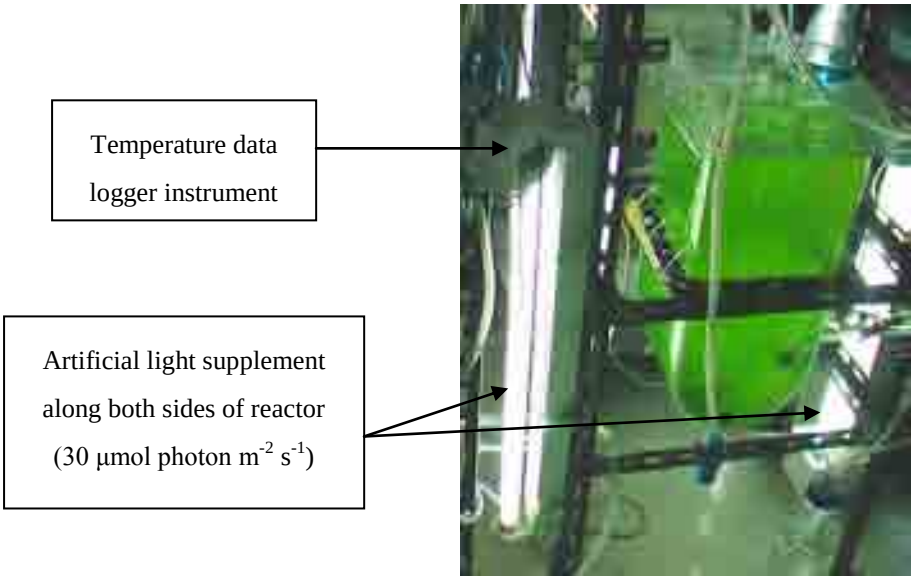

Figure 5.7 Culture system with artificial light supplement

The results show that the 17L FP-ALPBR could achieve a reasonably high cell density of 3.2 x 10^6 cells mL^{-1} with a specific growth rate of 0.64 day^{-1}. For the 50L ALPBR, a high cell density of 3.87 x 10^6 cells mL^{-1} with a specific growth rate of 0.63 day^{-1} could well be accomplished. This clearly shows that with this flat panel design configuration, the system could be up-scaled without losing growth capacity.

5.2.2 Natural light for *H. pluvialis* cultivation

The cultivation of *H. pluvialis* with natural light (sun light) penetrated through the translucent evaporative room was applied for the large scale cultivation (17, 50, 90, and 200L FP-ALPBRs) of *H. pluvialis*. Instead of using artificial light supplement, an energy-saved operation using the natural light was introduced where the light distribution was randomly monitored through a variety period of time (sunny day at day time, rainy day at day time, and at night time). The light and temperature distribution profile are shown in Fig. 5.8.

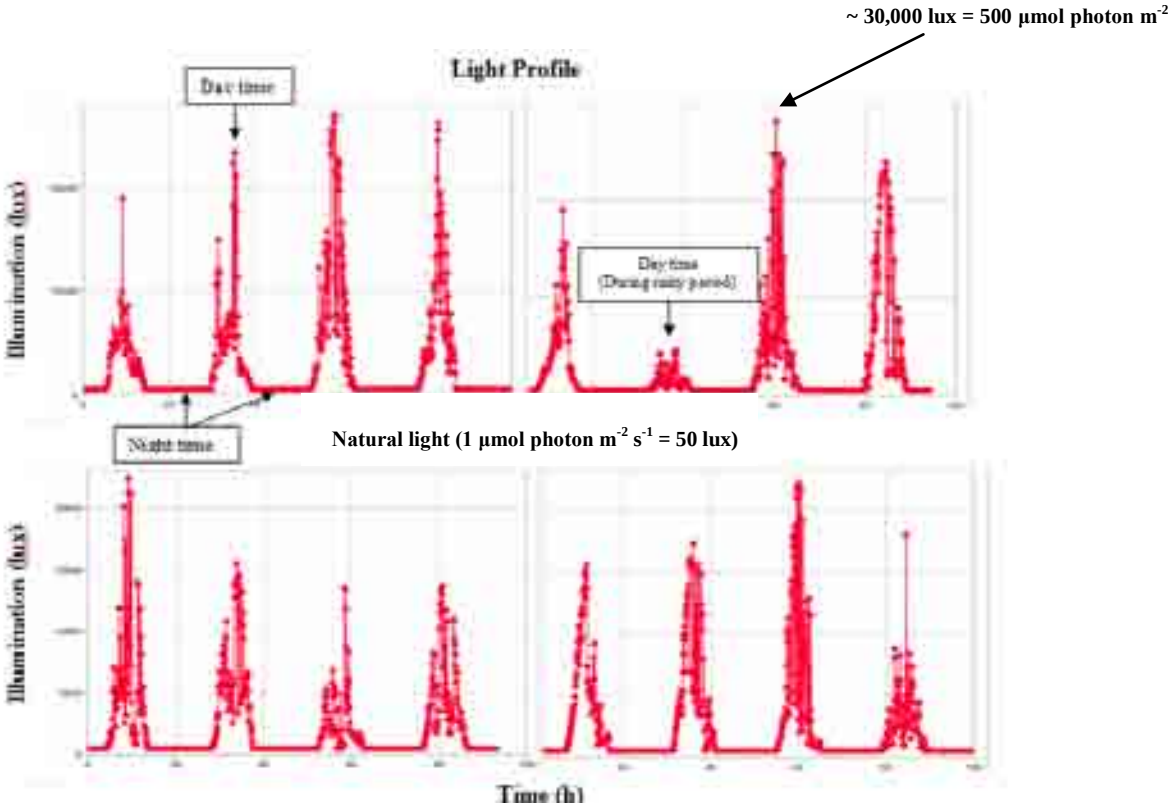

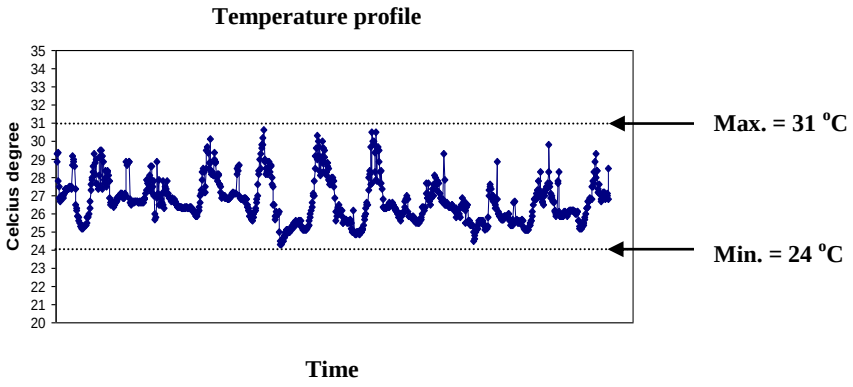

Figure 5.8 Light intensity profile and temperature profile under evaporative room operation

The experiments were conducted in 17, 50, 90, 200L flat panel airlift bioreactors (FP-ALPBRs) where the cultivation process was subject to the preceding optimized growth conditions.

- The ratio of downcomer/riser cross-sectional area of 0.4 and the aeration rate of 0.4 (cm s^{-1}) were employed.
- The CO_2 enriched air was mixed with air before entering into the system where concentration of CO_2 was 1% by volume.
- The system was illuminated at light intensity of around 100 - 500 µmol photon m^{-2} s^{-1} by sun light.
- The contribution of natural light was naturally controlled by ratio of light and dark cycle (12h : 12 h).
- The temperature of the culture was maintained at 27 ± 3 ^{o}C during the whole course of growth cultivation in evaporative room.

Unfortunately, the achieved result with natural light supplement was evidently proved that the absence of constant lighting (artificial light) significantly resulted in a recession of algal growth. Fig. 5.9 demonstrates that the 17L FP-ALPBR provided the best performance for the natural light cultivation of such alga in terms of cell density (290 x 10^4 cell mL^{-1}) and specific growth rate (0.49 day^{-1}). The other three FP-ALPBRs exhibited similar growth performance with the 50L FP-ALPBR providing a

slightly better growth at the maximum cell density of 140 x 10^4 cell mL^{-1} and the growth rate of 0.53 day^{-1}, followed by the 200L FP-ALPBR (147 x 10^4 cell mL^{-1} and 0.47 day^{-1}) and 90L FP-ALPBR (110 x 10^4 cell mL^{-1} and 0.45 day^{-1}), respectively. This was only one-half of the maximum cell density obtained by 17L FP-ALPBR. It is interesting to observe that, for all systems, the specific growth rate took the values in the range of 0.45 – 0.53 day^{-1} (see Fig. 5.9), which was still quite high when compared with the airlift operated by artificial light supplement (Section 5.2.1). This means that the cells still could grow at a reasonably high rate but could not increase in its number which could primarily be due to the inadequate light supply.

Although the drop in the growth performance in the large scale system was relatively small which could in fact be neglected, this discrepancy of algal growth could occur due to the differences in the system behavior as revealed in Section 5.1. It was observed that the smaller size airlift (17L FP-ALPBR) exhibited lower liquid circulation velocity compared with the larger scale system (200L) and this inherited a small shear stress for the cells. In addition, the inevitable non-uniformity of fluid flow in the large scale system might also give some negative impact to the growth of such alga.

Moreover, although this effect is not substantial, the 17L FP-ALPBR (259 cm^2 L^{-1}) seems to have a higher area per volume than those of the other three reactors (160, 156, 130 cm^2 L^{-1} for 50, 90 and 200L FP-ALPBRs, respectively). This character might be allowed a better light penetration for the growth of the alga.

5.3 Reused medium strategy for *H. pluvialis* cultivation

The natural light supplement for *H. pluvialis* cultivation was conducted again in this section with the reuse of spent algal medium. This was mainly proposed to cut down the algal nutrient cost (F1) and the water usage supplied to the system, thus minimizing an algal production cost. During the algal growth period, the fresh F1 medium was utilized for cell growth and therefore some essential elements (in F1

formula) were expected to reduce due to algal consumption. To inspect for those consumed elements, nitrate and phosphate were analyzed with the spectrophotometric method whereas ICP atomic emission spectrometry was used to analyze the remaining trace elements. For this study, it should be mentioned that this evaluation was conducted using the small sizes 10L glass bottle and 17L FP-ALPBR to mainly minimize the use of medium, and the cultivation was performed in the evaporative room with natural light supplement. This examination was done in two different experiments, i.e. one without the nutrient replenishment and the other with replenishment of nutrients and some trace elements in consecutive reusing cycles. An overall of this study is orderly shown below:

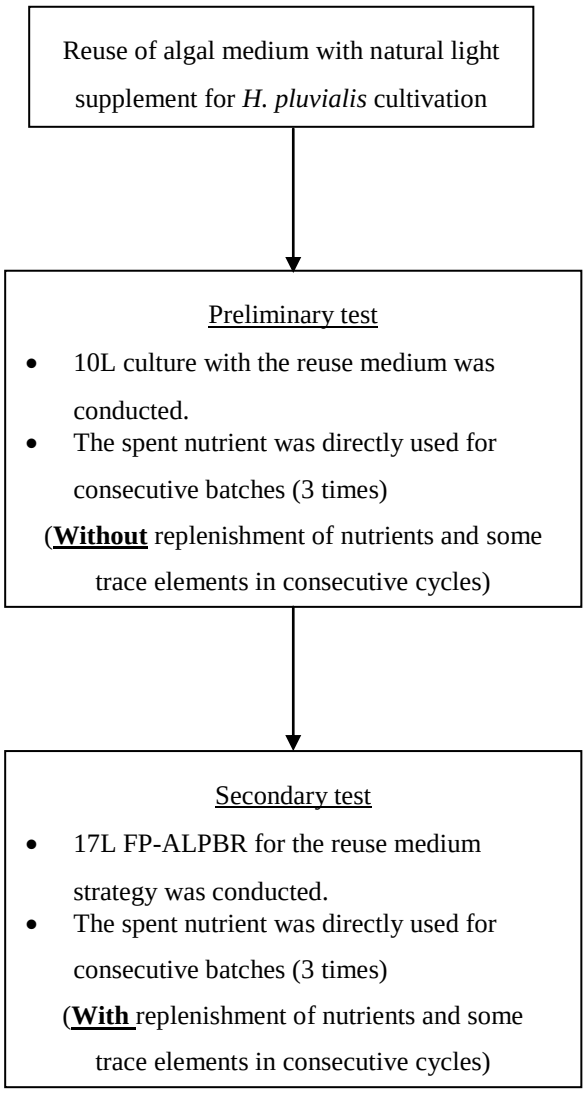

In the preliminary experiment, *H. pluvialis* was firstly cultured in the F1 medium, and the spent nutrient was directly used for consecutive batches (3 times). Note that the spent medium was collected after the cell harvest (by centrifuge) and was autoclaved before being reused, and this was performed in the 10L glass bottles under an evaporative room with natural light supplement (The experiment feature for a preliminary test is illustrated in Figure 5.10).

- The system was illuminated at light intensity of around 100 - 500 µmol photon m^{-2} s^{-1} by sun light.
- The contribution of natural light was naturally controlled by ratio of light and dark cycle (12h : 12 h).
- The temperature of the culture was maintained at 27 ± 3 ^{o}C during the whole course of growth cultivation in evaporative room.

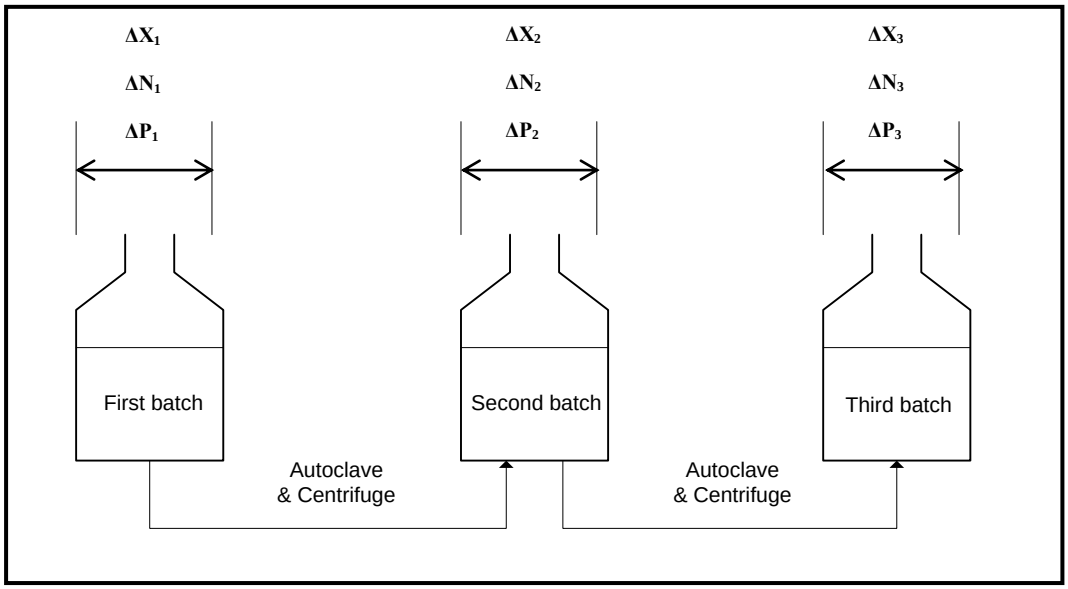

Figure 5.10 Experimental set up for the reuse medium experiment (Preliminary test)

From the fresh nutrient (first batch), the maximum achievable cell density and specific growth rate were 15 x 10^4 cell mL^{-1} and 0.4 day^{-1}. As the cells were removed, the spent medium was directly used in the next batch and it was found that the system

could still maintain similar growth characteristics with a satisfied maximum cell density and specific growth rate of 13 x 10^4 cell mL^{-1} and 0.38 day^{-1}, respectively. However, a drastic drop in growth performance became obvious in the third batch (the reused medium was used for the second time) where the maximum cell density and specific growth rate achievable were only 9 x 10^4 cell mL^{-1} and 0.23 day^{-1}. This lower performance with the reused medium might be resulted from a stressful environmental condition where algal cell probably generated some extracellular compounds which could inhibit the growth.

Table 5.2 illustrates the growth yield based on the available nutrients. From the results of the first batch, the ratio of the generated biomass, ΔX, and the nitrate consumed, ΔN, ($\Delta X/\Delta N$) and the ratio of the generated biomass and phosphate consumed ($\Delta X/\Delta P$) were 13.05 and 182.3, respectively. These values are quite close to the amount of the two compounds resided in the alga and therefore are considered as preferable yields for algal growth. However, these ratios became out of range during the second and third runs, $\Delta X/\Delta N = 262$, $\Delta X/\Delta P = 5$ for the second batch, and $\Delta X/\Delta N = 39$, $\Delta X/\Delta P = 11.55$ for the third run. This meant cells accumulated quite low level of nitrogen but very high level of phosphorus. This could indicate that cells must have been grown in environmental conditions which might not be so good for algal growth. In addition, those obtained results were rechecked using CHONS/O analyzer (Section 4.3.11) for measurement of the nutritional value actually contained in green vegetative cell (i.e., C = 32.43 %, N = 4.69 %, Carbohydrate = 19.64 %, and Protein = 29.20 %) as shown in Table 5.3.

Based on the disclosed information, nitrogen content in the green vegetative dry cell was 4.69 % and this value could compute back to obtain an actual nitrate composition in the cell and also simulate a value of the generated biomass and nitrate consumed ($\Delta X/\Delta N$). As a stimulated result, the actual $\Delta X/\Delta N$ was approximately of 21.32. With respect to $\Delta X/\Delta N$ achieved by Table 5.2, it was clearer that in the second run might have been unfavorable condition for algal growth since it was shown an unusual value of $\Delta X/\Delta N$ (= 262).

Table 5.2 Growth yield based on available nutrients (Preliminary test)

System	Growth yield for substrate ($Y_{X/S}$)	
	$\Delta X/\Delta N$	$\Delta X/\Delta P$
First batch	13.05	182.3
Second batch	262	5
Third batch	39	11.55

Remark;

- The first batch uses fresh medium.
- The second batch uses reused medium from the previous batch.
- The third batch uses reused nutrients from the second batch.
- Table 5.2 illustrates the analyses results for nitrate (ΔN) and phosphate (ΔP).

Table 5.3 Nutrient characteristic of green vegetative cell

element	% content
C	32.43
H	5.57
N	4.69
O	57.31

Nutritional value	% content
Moisture	12.17
Protein	29.20
Total fat	0.66
Ash	38.33
Carbohydrate	19.64

The results from the nutritional analyses illustrate that there was a serious shortage of essential elements, especially phosphorus for the second recycling batch as about 71 % reduction was found during the second batch with reused medium (as shown in Table 5.4). This drop in phosphorus could be responsible for the drop in the growth performance as observed. This finding was quite comparable to Tocquin et al. (2011) who reported that a drought of phosphate (P) appeared to be a critical

parameter that maintained actively dividing cells at macrozoid stage (green vegetative cells). Note that this drop in phosphate might not be resulted from cellular growth, but it could be also from precipitation at high pH.

Table 5.4 Reduction (%) of elements in reused algal medium (Preliminary test)

elements	**First batch**			**Second batch**			**Third batch**		
	Concentration (mg L^{-1})		% Reduction (Δ1)	Concentration (mg L^{-1})		% Reduction (Δ2)	Concentration (mg L^{-1})		% Reduction (Δ3)
	Initial day	Final day		Initial day	Final day		Initial day	Final day	
N	**13.82315**	**13.15275**	**4.85**	**13.15275**	**13.12435**	**0.21**	**13.12435**	**13**	**0.95**
P	**2.158632**	**2.110508**	**2.23**	**2.110508**	**0.61796**	**70.72**	**0.61796**	**0.2**	**67.64**
Cr	0.0544	0.0184	66.18	0.0184	0.01	45.65	0.01	0.007	30
Cu	0.0246	0.0079	67.89	0.0079	0.006	24.05	0.006	0.004	33.33
Se	0.0424	0.0214	49.53	0.0214	0.021	1.87	0.021	0.018	14.28

In the secondary experiment, *H. pluvialis* was firstly cultured in the F1 medium, and the spent medium was replenished with the nutrients before that medium was used in the consecutive batches. Note that the spent medium was autoclaved before being reused. However, the harvesting by centrifuge was not applied for this secondary experiment in order not to cause the nutrient precipitation. A gravitational precipitation method was instead implemented (when shut down the air pump, green algal cells suspended in the liquid culture were gradually fell down to a bottom of the reactor) and this study was performed in the 17L FP-ALPBR under an evaporative room with natural light supplement (The experiment feature for a secondary test is illustrated in Figure 5.11).

- The ratio of downcomer/riser cross-sectional area of 0.4 and the aeration rate of 0.4 (cm s^{-1}) were employed.
- The CO_2 enriched air was mixed with air before entering into the system where concentration of CO_2 was 1% by volume.
- The system was illuminated at light intensity of around 100 - 500 µmol

photon m^{-2} s^{-1} by sun light.

- The contribution of natural light was naturally controlled by ratio of light and dark cycle (12h : 12 h).
- The temperature of the culture was maintained at 27 ± 3 ^{o}C during the whole course of growth cultivation in evaporative room.

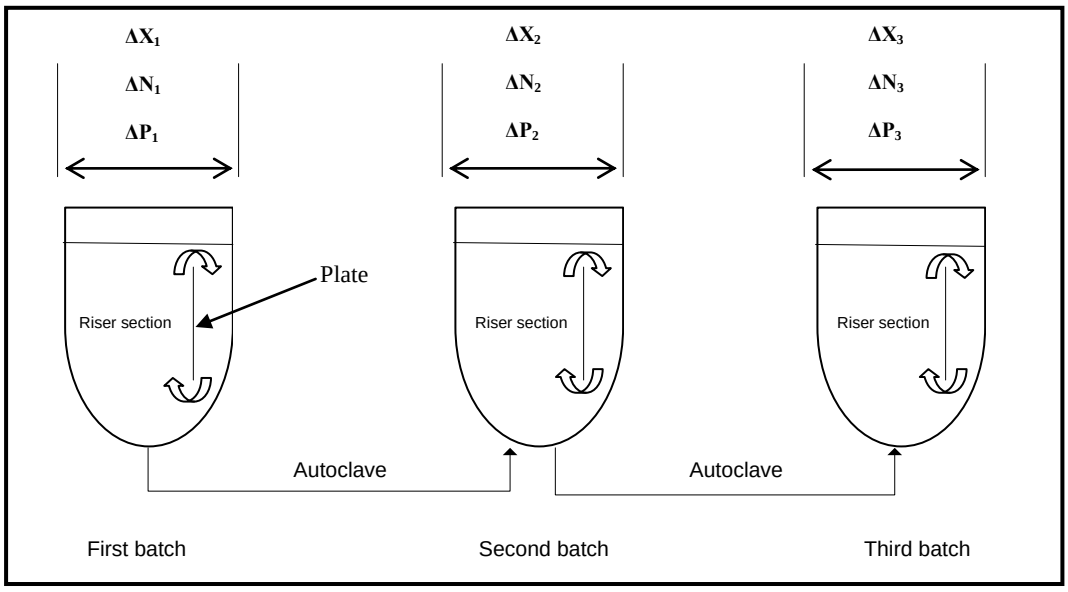

Figure 5.11 Experimental set up for reuse medium experiments (Secondary test)

The assessment shows that there were shorts of some important nutrients/trace elements after cell growth, i.e. nitrate (19% reduction), phosphate (36% reduction), chromium (82% reduction), and copper (45% reduction). These compounds were mostly consumed during cell growth (Table 5.5). Therefore the nutrients were then replenished with these elements in proper amounts before being reused as a medium for the next cultivation batch.

The results from the cultivations with the reused nutrients (as demonstrated in Fig. 5.12) illustrates that the performances of such reused nutrients (2 consecutive harvesting cycles) were slightly inferior to that with fresh nutrient. The maximum cell density and specific growth rate were 200 x 10^4 cell mL^{-1} and 0.47 day^{-1} (the second

batch) and 198 x 10^4 cell mL^{-1} and 0.46 day^{-1} (the third batch), when compared with 290 x 10^4 cell mL^{-1} and 0.49 day^{-1} obtained from the fresh medium as shown in Fig. 5.13.

Table 5.5 Reduction (%) of elements in reused algal medium (Secondary test)

Elements	**First batch**			**Second batch**			**Third batch**		
	Concentration (mg L^{-1})		% Reduction (Δ1)	Concentration (mg L^{-1})		% Reduction (Δ2)	Concentration (mg L^{-1})		% Reduction (Δ3)
	Initial day	Final day		Initial day	Final day		Initial day	Final day	
N	**70.06**	**56.81**	**18.91**	**70.06**	**8.06**	**11.5**	**70.06**	**64**	**8.65**
P	**0.703**	**0.453**	**35.56**	**0.703**	**0.103**	**14.65**	**0.703**	**0.483**	**31.29**
Cr	0.038	0.007	81.58	0.038	0.028	73.68	0.038	0.01	72.12
Cu	0.021	0.0115	45.24	0.021	0.003	14.28	0.021	0.018	16.24
Se	0.24	0.18	25	0.24	0.05	20.83	0.24	0.19	22

Based on the first batch, the yields of cell based on the two major nutrients, i.e., $\Delta X/\Delta N$, and $\Delta X/\Delta P$ were 10.83 and 574, respectively. These values were considered as a preferable condition for algal growth. Yields for the second and third batches were: $\Delta X/\Delta N$ = 15.32, $\Delta X/\Delta P$ = 686 and $\Delta X/\Delta N$ = 17.08, $\Delta X/\Delta P$ = 470, respectively (see Table 5.6). This indicates that, supplying necessary nutrients could bring back the favorable growth condition for *H. pluvialis* which indicates the potential of reusing nutrients for consecutive cultivations

As the nitrate concentration consisted in the green vegetative cell biomass was found with up to 4.69 % (Table 5.3). Therefore, the generated biomass and nitrate consumed ($\Delta X/\Delta N$) were calculated based on the algal growth condition under the secondary experiment as described above. This simulated $\Delta X/\Delta N$ was used as a reference value in order to predict how much of nitrate concentration might be uptake by this alga (this value was about to compare with $\Delta X/\Delta N$ obtained by Table 5.6). As a stimulated result, the actual $\Delta X/\Delta N$ was approximately of 21.32, comparable to $\Delta X/\Delta N$ achieved by Table 5.6 ($\Delta X/\Delta N$ = 10.83 for first batch, $\Delta X/\Delta N$ = 15.32 for

second batch, and $\Delta X/\Delta N$ = 17.08 for third batch). These values are quite close to that amount of the actual $\Delta X/\Delta N$ resided in the alga ($\Delta X/\Delta N$ = 21.32) and therefore are considered as preferable yields for algal growth. In conclusion, it was shown that it was possible to apply the use of the spent medium as a new medium as long as some of the depleted nutrients are replenished. However, there might occur some other unwanted compounds generated or released from the cells into the growth medium during the growth which retarded subsequent growth.

Table 5.6 Growth yield based on available nutrients (Secondary test)

System	Growth yield for substrate ($Y_{X/S}$)	
	$\Delta X/\Delta N$	$\Delta X/\Delta P$
First batch	10.83	574
Second batch	15.32	686
Third batch	17.08	470

Remark;

- For table 5.2, the analyses for nitrate (ΔN) and phosphate (ΔP) were measured with the spectrophotometric method.

By discussing that, it is worth noticing that a standard requirement of nitrate (as potassium nitrate) in the F1 medium is as much as 410 mg L^{-1}. The possibility of reusing the spent nutrients should be further explored as this could pose a serious operating cost for the growth of the alga.

5.4 Concluding remarks

This chapter summarizes the hydrodynamic and mass transfer behaviors of the airlift photobioreactors used for the cultivation of *H. pluvialis*. The results seemed to

support the results on cell growth as the conditions for the highest growth were those with potentially the lowest shear stress, i.e. low gas throughputs and large riser which slowed down the bubble entrance velocity and induced liquid movement at the lowest speed.

The investigation also reveals that the use of artificial light under evaporative room could enhance cell growth. Although this seemed to give positive impact to the final cell productivity, the economic assessment of the cultivation process of *H. pluvialis* is to promisingly evaluate. Options for maintaining low operating costs are therefore further examined and this is the subject of the next chapter.

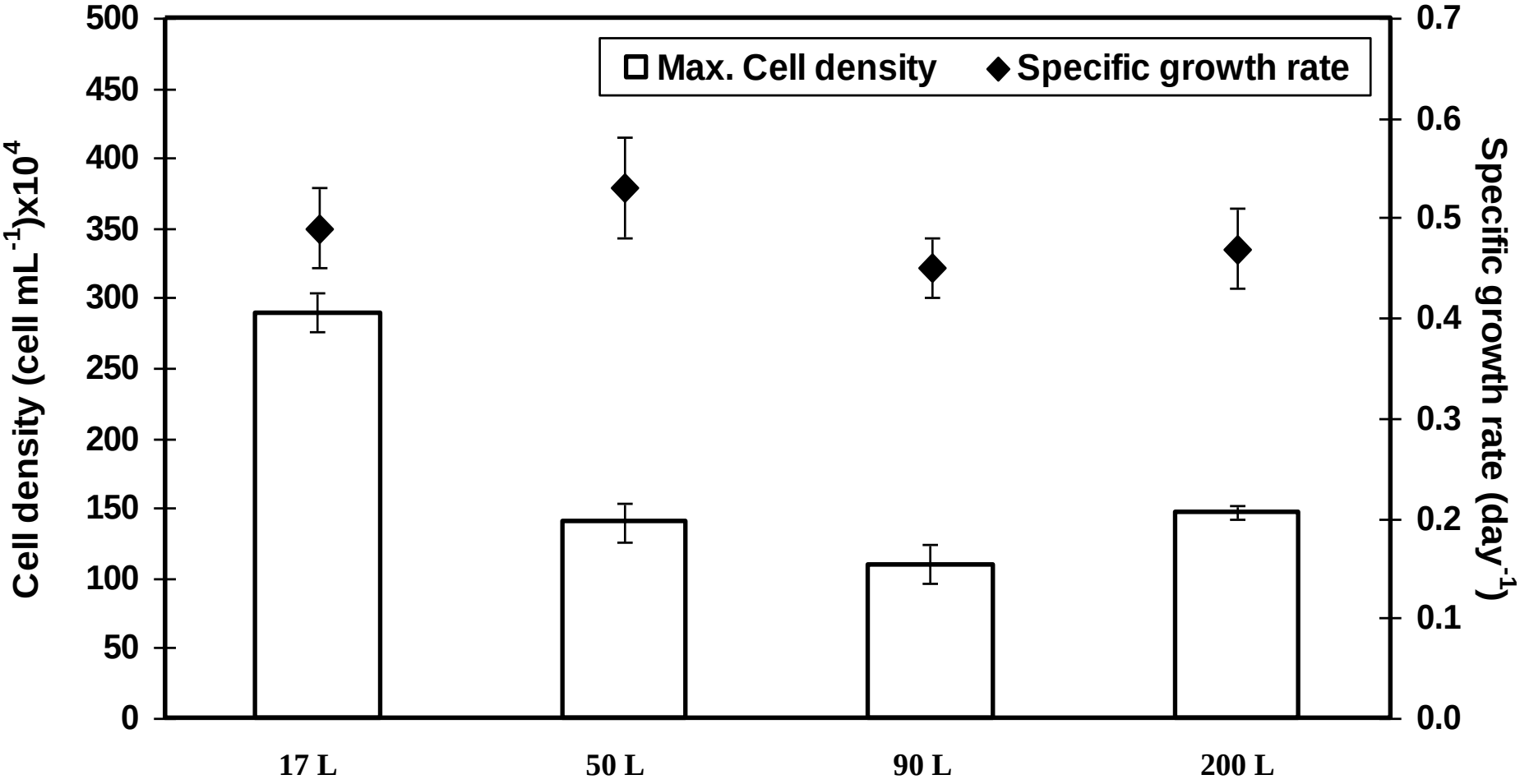

Figure 5.9 Maximum cell density and specific growth rate of *H. pluvialis* in 17, 50, 90 and 200L FP-ALPBRs operated in evaporative room with natural light supplement (100-500 μmol photon m^{-2} s^{-1}); A_d/A_r = 0.4 and U_{sg} = 0.4 cm s^{-1}

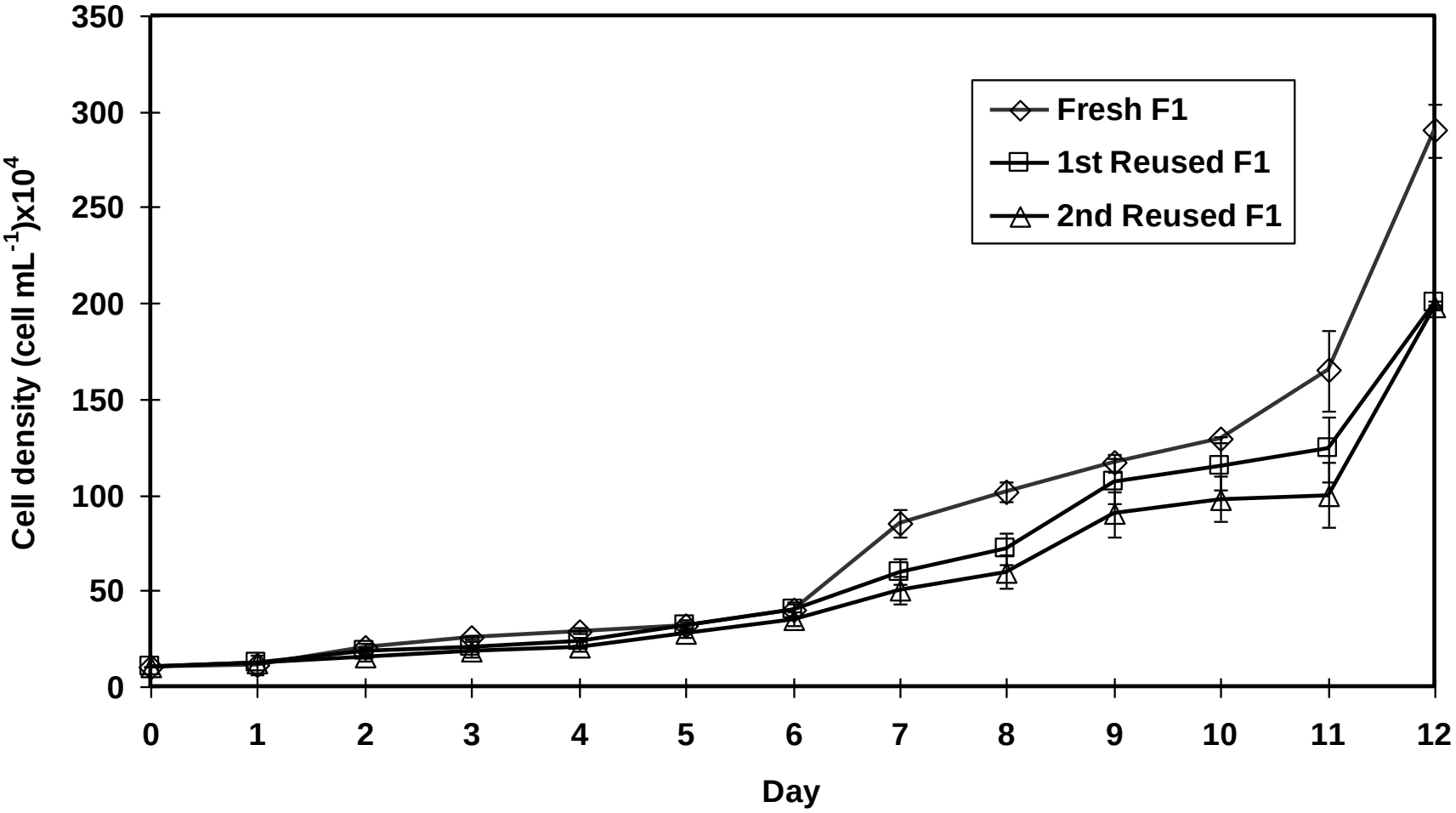

Figure 5.12 Growth rate of *H. pluvialis* (in 17L FP-ALPBR) operated with reused algal medium in evaporative room with natural light supplement (100 -300 μmol photon m^{-2} s^{-1}); A_d/A_r = 0.4 and U_{sg} = 0.4 cm s^{-1}

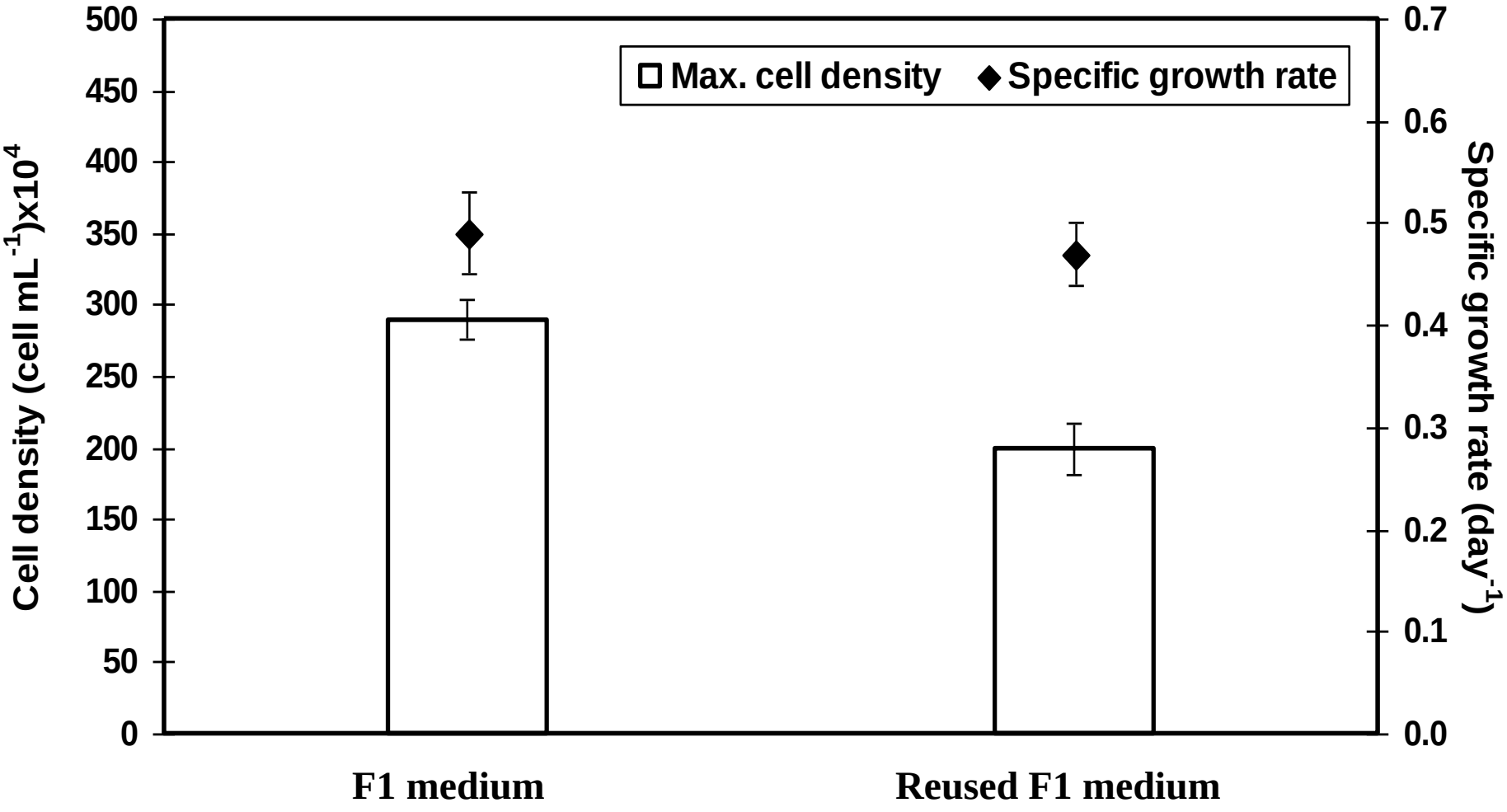

Figure 5.13 Maximum cell density and specific growth rate of *H. pluvialis* in 17 L FP-ALPBR operated with reused algal medium in evaporative room with natural light supplement (100 -300 μmol photon m^{-2} s^{-1}); A_d/A_r = 0.4 and U_{sg} = 0.4 cm s^{-1}

CHAPTER VI

Economical review of *Haematococcus pluvialis* culture in Flat-panel airlift photobioreactors

6.1 Economical assessment of FP-ALPBRs for the cultivation of *H. pluvialis*

Based on the study of the cultivation of green vegetative cell, *H. pluvialis*, the rigorous attempts to economically minimize the operating costs were put into our serious consideration described in this chapter. Viable information regarding the commercially economical production of such alga has rarely been disclosed, thus drawing the authors an attraction to explore this discrepancy. It must be denoted that, related to attained results in this chapter, the logistic law was employed to simulate the growth of the cells which would allow the estimates of several other designing parameters such as harvesting period (day), harvesting volume (m^3) and productivity (g dry cell $year^{-1}$). The use of this equation is based on an assumption of self-limiting growth or self-contained biological population (described in Chapter IV). In other words, an excess of cell density could cause growth inhibition (Bellgardt, 1991).

For *H. pluvialis* culture, it was unlikely that the culture will exhibit self inhibition effect at the beginning of growth stage (lag phase) as light could still easily pass through the culture. However, during the late exponential phase, the dense algal culture would block the light passage and inhibit the growth. Along with the depletion of major nutrients, the growth dropped. This kind of growth behavior can be mimicked with the logistic law which can then be used to simulate the harvesting period (day) and harvesting volume (m^3).

The logistic law as mentioned in Chapter IV is as follows:

$$\frac{dX}{dt} = kX\left(1-\frac{X}{X_{\max}}\right) \quad (4.13)$$

and

$$X = \frac{X_0 \exp(kt)}{\left(1-\frac{X_0(1-\exp(kt))}{X_{\max}}\right)} \quad (4.14)$$

The time profile of cell density (X) is needed to be plotted to obtain logistic law coefficient where:

Parameter	Definition	Value
X	cell density (cell mL^{-1}) at time t (day)	cell density obtained from the algal cultivation at time t (day)
X_0	initial cell density (cell mL^{-1})	X_0 = 10 x 10^4 cell mL^{-1}, as an initial cell density for all simulations
X_{max}	maximum cell density (cell mL^{-1})	maximum cell density obtained from the algal cultivation in each individual batch
K	logistic law coefficient (d^{-1})	K is a slope obtained from Equations (4.13) and (4.14)

Assumptions and constraints were established and installed as a part of economical evaluation. The operating and investment expenses were calculated using local utility costs in Thailand in 2010 so that they were integrated into the overall total investment for an entire process of cultivation of green vegetative cell, *H. pluvialis.*

The assumptions employed for this evaluation are listed below:

- The basis of calculation was based on the maximum capacity of 500 g dry vegetative cells. Fig. 6.1 shows that this quantity of cell could be obtained from the operation of 200L FP-ALPBR at its maximum capacity for the period of one year.

- 300 operating days per annum was applied.
- Commercially price for dry green vegetative cell was approximately at 250 US$ per kg. This was calculated based on the price of a commercially available dry cysts cell of 500 US$ per kiligram (quoted in 2010). Besides, all green vegetative cells cultivated by this system was assumed to completely be converted to cysts without cell loss, and no extraction was necessary.
- Life-spans of reactor and pumps were evaluated at 10 and 5 years, respectively
- Life-span of evaporating room was 20 years.
- Artificial light operation was available 24 h (300 days).
- Fan (allocated in evaporative room) was available 12 h per day (300 days).
- The controlling system (allocated in evaporative room) was available 24 h (300 days).
- Electric charge was computed at 0.1 $US per kWh.
- Water charge was estimated at 0.31 $US per cubic meter
- The operating and investment expenses were calculated using local utility costs in Thailand in 2010.

The economical evaluation of *H. pluvialis* culture neglected the following factors:

- Land acquisition and improvements
- Laboratory equipment (flask, pipette, silicone tube, etc.) and some instruments (centrifuge, autoclave, etc.)
- CO_2 gas and CO_2 storage tank
- Valves, piping and air controller (air rotameter)
- Engineering (labor) and supervisor
- Maintenance system

6.2 Economical consideration based on the availability of light source for the cultivation of *H. pluvialis*

The cultivation systems for *H. pluvialis* conducted with and without artificial

light supplement were compared in a view of economical potential. The performance of the 50L FP-ALPBR with artificial supplement (387 x 10^4 cell mL^{-1} and 0.63 d^{-1}) clearly outperformed the cultivation with only natural light supplement (140 x 10^4 cell mL^{-1} and 0.53 d^{-1}) both in terms of maximum cell density and specific growth rate (as shown in Fig. 6.2). The operating conditions for both experiments were shown below;

1) Artficial light for *H. pluvialis* cultivation (Section 5.2.1)

- 50L FP-ALPBR was the system size.
- The ratio of downcomer/riser cross-sectional area of 0.4 and the aeration rate of 0.4 cm s^{-1} were employed.
- The CO_2 enriched air was mixed with air before entering into the system where concentration of CO_2 was 1% by volume.
- The system was illuminated at a constant light intensity of around 30 µmol photon m^{-2} s^{-1} by fluorescence lamps.
- The artificial light was subject to the system for 24 h through the end of cultivation.
- The temperature of the culture was maintained at 27 ± 3 ^oC during the whole course of growth cultivation in evaporative room.

2) Natural light for *H. pluvialis* cultivation (Section 5.2.2)

- 50L FP-ALPBR was the system size.
- The ratio of downcomer/riser cross-sectional area of 0.4 and the aeration rate of 0.4 cm s^{-1} were employed.
- The CO_2 enriched air was mixed with air before entering into the system where concentration of CO_2 was 1% by volume.
- The system was naturally illuminated at the light intensity range of around 100 - 500 µmol photon m^{-2} s^{-1}.
- The system was exposed to light at the natural light and dark cycle of around 12h : 12 h.

- The temperature of the culture was maintained at 27 ± 3 ^{o}C during the whole course of growth cultivation in the evaporative room.

This results reveal that the use of natural light was not adequate to yield high cell biomass, and almost 16% lower growth rate was obtained when compared to the system with well controlled light supply. Several inhibited factors could be responsible for this phenomenon such as the fluctuation in light intensity during the day time. The very high light intensity during the day time could negatively impact on the growth of such alga, thus resulting in a lower growth in the natural light system. Additionally, seasonal changes which significantly affected the sun light intensity might also have great influence on the cell growth, but this matter was not investigated in this work.

However, the system with artificial supplement during the whole course of cultivation with the resulting high growth rate demonstrated that an extra additional electricity cost was required. Practically, one of the major costs for the cultivation of *H. pluvialis* was the lighting electricity cost which contributed almost 40% of the total operating costs as portrayed in Fig. 6.3 (extracted from Fig. 6.1). Among the total investment charges for algal cultivation, electricity charge was a major expense which contributed 81.9% of the total expenses for artificial light operation and 46.5% for natural light operation.

In this experiment, the natural light supplement (100 to 500 µmol photon m^{-2} s^{-1}) for algal cultivation was carried out, and the performance was compared to the system using artificial light supplement (30 µmol photon m^{-2} s^{-1}). The algal growth performance is illustrated in Fig. 6.2. This experiment was conducted in the same volume of bioreactor, 50L FP-ALPBR to evaluate whether the supply of artificial lighting or natural light supplement could enhance the profit.

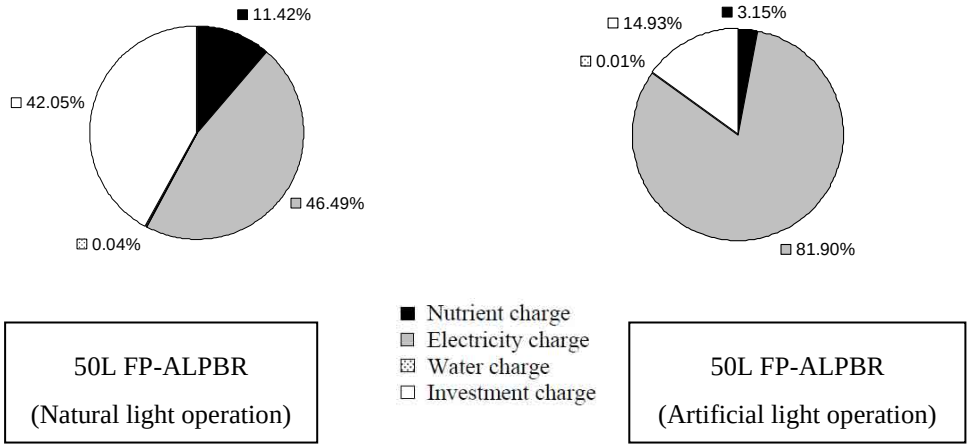

Figure 6.3 (%) distribution of the total investment charges for algal cultivation in 50L system (natural light and artificial light operation)

The economical evaluations of reactor systems were determined and the results are illustrated in Fig. 6.4. The same assumptions and logistic law model as indicated above were applied here. It was clearly observed that the system with natural light supplement exhibited a lower growth performance than the system with artificial light supplement, e.g. in the 50L FP-ALPBR, algal growth with natural light supplement yielded the optimal cell density of 104 x 10^4 cell mL^{-1}, harvesting period of 7 days, and the productivity of 0.57 g dry cell day^{-1}, on the other hand, using artificial light supplement with a constant light intensity could potentially raise the growth rate to 0.63 day^{-1} with the productivity of 0.71 g dry cell day^{-1}. However, by supplying artificial light supplement, the electricity cost became a significant serious issue, and the total cost increased magnificently from 169 to 476 US$ annually (for 0.5 kg of dry cells). In this case, the presence of high operating cost with artificial lighting had adverse effect on the overall profitability of the system where 351 US$ per year deficit was resulted. This option (artificial supplement) undoubtedly became unattractive as there was further no realizable annual profit as demonstrated in Fig. 6.4 compared to the system with natural light supplement (which was already 44 US$ per year deficit).

As the natural supplement for algal cultivation was evidently proved to cut down the electricity operating cost, in particular, the economical evaluation for *H.*

pluvialis in various sizes of FP-ALPBRs operated by evaporative room with natural light supplement was investigated further.

- 17, 50, 90 and 200L FP-ALPBRs were carried out.
- The ratio of downcomer/riser cross-sectional area of 0.4 and the aeration rate of 0.4 cm s^{-1} were employed.
- The CO_2 enriched air was mixed with air before entering into the system where concentration of CO_2 was 1% by volume.
- The system was illuminated at light intensity of around 100 - 500 µmol photon m^{-2} s^{-1} by sun light.
- The operation was subject to the natural dark-light cycle if approximately 12h : 12 h.
- The temperature of the culture was maintained at 27 ± 3 ^{o}C during the whole course of growth cultivation in evaporative room.

The results (Fig. 6.5) reveal that the cultivation of green vegetative cell, *H. pluvialis* deployed in 17, 50 and 90 FP-ALPBRs was rather unattractive as algal production by showing 77, 44, and 10 US$ deficits per year, respectively, while a slightly in profit was introduced to 200L FP-ALPBRs at 4 US$ per year. In other words, although the small scale 17L FP-ALPBR exhibited the best performance for the cultivation of such alga (harvesting cell density of 250 x 10^4 cell mL^{-1} at 10.5 days), its system was operated with the highest total operating cost (197 US$ per year). The largest system, 200L FP-ALPBER, on the other hand, required significantly lower costs per unit production (121 US$ per year) at the harvesting cell density of 120 x 10^4 cell mL^{-1} at harvesting period of 9 days. In fact, it was demonstrated that the unit cost of production was inversely proportional to the scale of production, and the profit started to be clearly realized when the reactor size reached 200L (4 US$ per year).

6.3 Economical consideration based on the possibility of reusing growth medium

In this evaluation the reuse of spent growth medium with proper replenishment of nutrients, the 17L FP-ALPBR working under evaporative room with natural light supplement was used as it required less labor and resources and the results were proven not to be significantly different from the other larger reactors.

- 17L FP-ALPBR was carried out.
- The ratio of downcomer/riser cross-sectional area of 0.4 and the aeration rate of 0.4 cm s^{-1} were employed.
- The CO_2 enriched air was mixed with air before entering into the system where concentration of CO_2 was 1% by volume.
- The system was illuminated at light intensity of around 100 - 500 µmol photon m^{-2} s^{-1} by sun light.
- The operation was subject to the natural dark-light cycle if approximately 12h : 12 h.
- The temperature of the culture was maintained at 27 ± 3 ^{o}C during the whole course of growth cultivation in evaporative room.

Based on the summarized in Fig. 6.6 (extracted from Fig. 6.1), the algal medium costs approximately 6.38% of the total investment charges for algal cultivation. The reused medium strategy could only cut down the total investment charges by 3.69%. In other words, it was saved by a relative small (8 US$ a year) compared to the system without reused medium (as shown in Fig. 6.7). However, it should be mentioned that the evaluation in case of reuse of spent growth medium without replenishment of the absent nutrients, the 10L glass bottle working under natural light operation was used, might not be given an attraction to significantly diminish the total investment charges for algal cultivation.

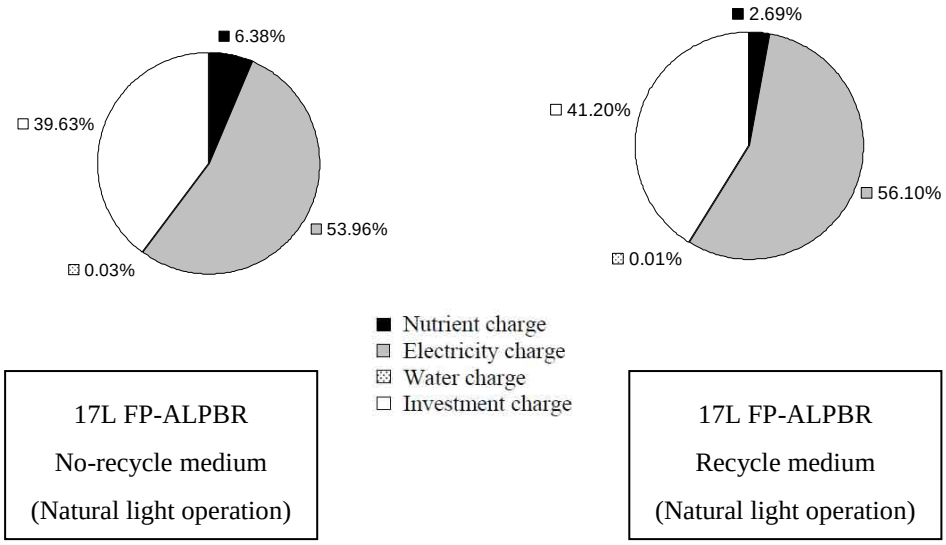

Figure 6.6 (%) distribution of the total investment charges for algal cultivation in 17L system a natural light operation (no-recycle and recycle medium)

Since the nutrient cost only contributed a small fraction to the overall expenses, the benefits obtained from the use of spent nutrient became quite invisible. Moreover, the growth tended to slightly drop with the use of spent nutrient and therefore this option was not further investigated here. It should be noted, however, that the spent nutrient, if not reused, might need to enter the wastewater treatment system which might incur some extra charge, but this is not in the scope of the study here.

Details	Symbol	Unit	17 L FP-ALPBR	50 L FP-ALPBR	90 L FP-ALPBR	200 L FP-ALPBR	50 L FP-ALPBR	17 L FP-ALPBR	17 L FP-ALPBR
Conditions			Natural light supplement	Natural light supplement	Natural light supplement	Natural light supplement	Artificial light supplement	Artificial light supplement	Natural light supplement (Reused medium)
Volume	A (Experiment)	m^3	0.017	0.05	0.09	0.2	0.05	0.017	0.017
Specific growth rate	B (Logistic coefficient = K= μ_1)	d^{-1}	0.49	0.53	0.45	0.47	0.63	0.64	0.47
Maximum cell density	C (Experiment = Xmax)	cell ml^{-1}	2.90E+06	1.40E+06	1.10E+06	1.47E+06	3.87E+06	3.20E+06	1.99E+06
Dry weight (at Maximum cell density)	D (Experiment)	g l^{-1}	0.15	0.12	0.12	0.12	0.16	0.16	0.13
Initial cell density	E (Experiment = X_0)	cell mL^{-1}	1.0E+05	1.0E+05	1.0E+05	1.0E+05	1.00E+05	1.0E+05	1.00E+05
Economical operation conditions (* Using Logistic Law as a model)									
Cell density	F (Logistic law)	cell ml^{-1}	2.50E+06	1.04E+06	7.90E+05	1.20E+06	3.20E+06	2.80E+06	1.50E+06
Dry weight	G (Logistic law)	g l^{-1}	0.129	0.088	0.087	0.099	0.132	0.14	0.099
Harvesting period (per crop)	H (Logistic law = t)	day	11	7	8	9	9	9	9
Harvesting volume (per crop)	I = A-(A*E/F)	m^3	0.016	0.045	0.079	0.183	0.048	0.016	0.016
Productivity (per reactor)	J = (G*I*1000)/H	g dry cell day^{-1}	0.19	0.57	0.85	2.02	0.71	0.26	0.17
	K = J*300	g dry cell $year^{-1}$	57	170	256	605	213	77	52
	L = K/(A*1000)	g dry cell $year^{-1}$ $volume^{-1}$	3.38	3.41	2.85	3.03	4.26	4.50	3.08
Target productivity	M	g dry cell $year^{-1}$	500	500	500	500	500	500	500
Reactor requirements	N = M/K		9	3	2	1	3	7	9
Maximum reactors in chamber room	O		18	9	6	3	9	18	18
Nutrient requirements									
Nutrient charge	P = (0.003*A*N*1000)*(300/H)	\$US $year^{-1}$	12.52	19.29	20.25	20.00	15.00	11.90	5.10
Electricity requirements									
1. lighting	Q	W	0	0	0	0	144	72	0
(* Based on 24 hours per day, 300 days per year operation)	R = (Q*300*24/1000)*N	kWh	0	0	0	0	3110	3629	0
2. Fan	S	W	350	350	350	350	350	350	350
(* Based on 12 hours per day, 300 days per year operation)	T = (S*300*12/1000)*(N/O)	kWh	630	420	420	420	420	490	630
3. Controlling system	U	W	20	20	20	20	20	20	20
(* Based on 24 hours per day, 300 days per year operation)	V = (U*300*24/1000)*(N/O)	kWh	72.0	48.0	48.0	48.0	48.0	56.0	72.0
4. Number of air pumps	W	Unit	5	2	1	1	2	3	5
5. Air pump	X	W	10	22	22	22	22	10	10
(* Based on 24 hours per day, 300 days per year operation)	Y = (X*300*24/1000)*W	kWh	360.0	316.8	158.4	158.4	316.8	216.0	360.0
Total electricity requirements	Z = R+T+V+Y	kWh	1062.0	784.8	626.4	626.4	3895.2	4390.8	1062.0
Electricity charge (Electricity charge = 0.1 \$US per kWh)	a = 0.1*Z	\$US $year^{-1}$	106.2	78.5	62.6	62.6	389.5	439.1	106.2
Water requirements									
1. Nutrient solution	b = A*N*1000	L	153	150	180	200	150	119	51
2. Washing activity	c	L	38.25	37.5	45	50	37.5	29.75	12.75
Total water consumption	d = b+c	L	191.25	187.5	225	250	187.5	148.75	64
Water charge (Water charge = 0.31 \$US per cum)	e = (d*0.31)/1000	\$US $year^{-1}$	0.06	0.06	0.07	0.08	0.06	0.05	0.02
Total operating charge	f = P+a+e	\$US $year^{-1}$	**119**	**98**	**83**	**83**	**405**	**451**	**111**
Other requirements (peripherals)									
1. Reactor cost	g	\$US	63	125	156	172	125	63	63
Reactor charge per unit (=Reactor cost/Life time) (Reactor life time = 10 years)	h = (g/10)*N	\$US $year^{-1}$	56.3	37.5	31.3	17.2	37.5	43.8	56.3
2. Air pump cost	i	\$US	9	62	62	62	62	9	9
Air pump charge per unit (=Reactor cost/Life time) (Air pump life time = 5 years)	j = (i/5)*W	\$US $year^{-1}$	9.3	24.8	12.4	12.4	24.8	5.6	9.3
3. Construction cost	k	\$US	500	500	500	500	500	500	500
Construction charge per unit (=Reactor cost/Life time) (Construction life time = 20 years)	l= (k/20)*(N/O)	\$US $year^{-1}$	13	8	8	8	8	10	13
Total investment charge	m= h+j+l	\$US $year^{-1}$	**78**	**71**	**52**	**38**	**71**	**59**	**78**

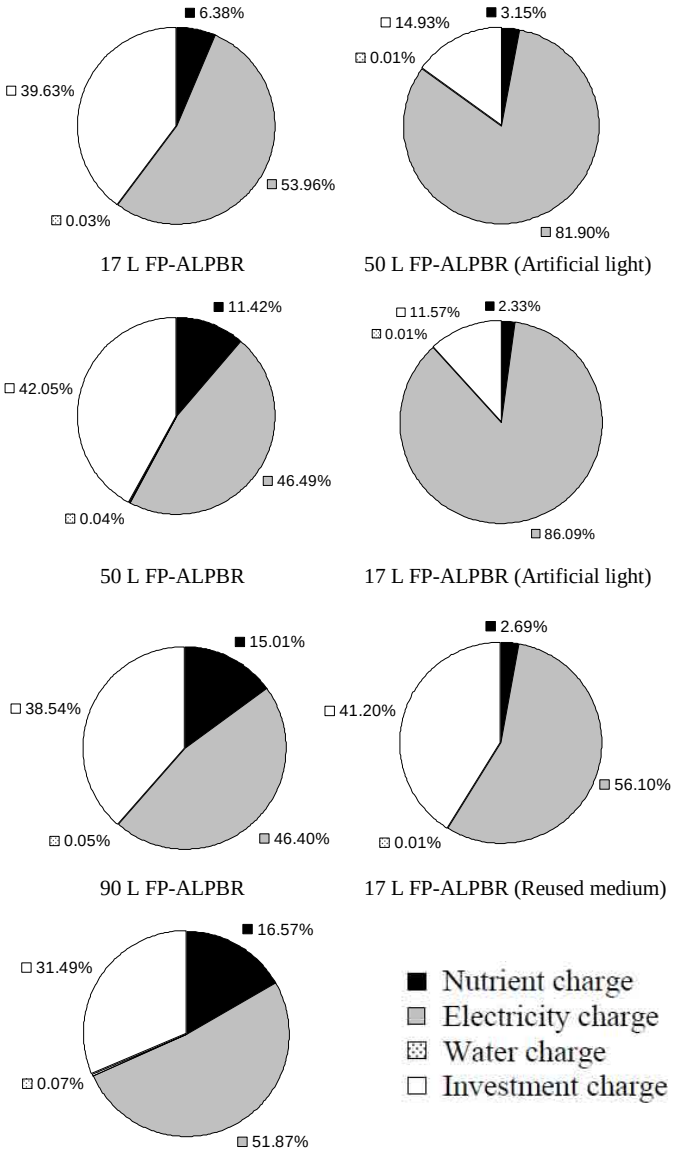

Figure 6.1 Economic break-down for *H. pluvialis* cultivation in various sizes of FP-ALPBRs operated in the evaporative room (temperature was controlled at 27±3 ^{o}C); A_d/A_r = 0.4 and U_{sg} = 0.4 cm s^{-1}

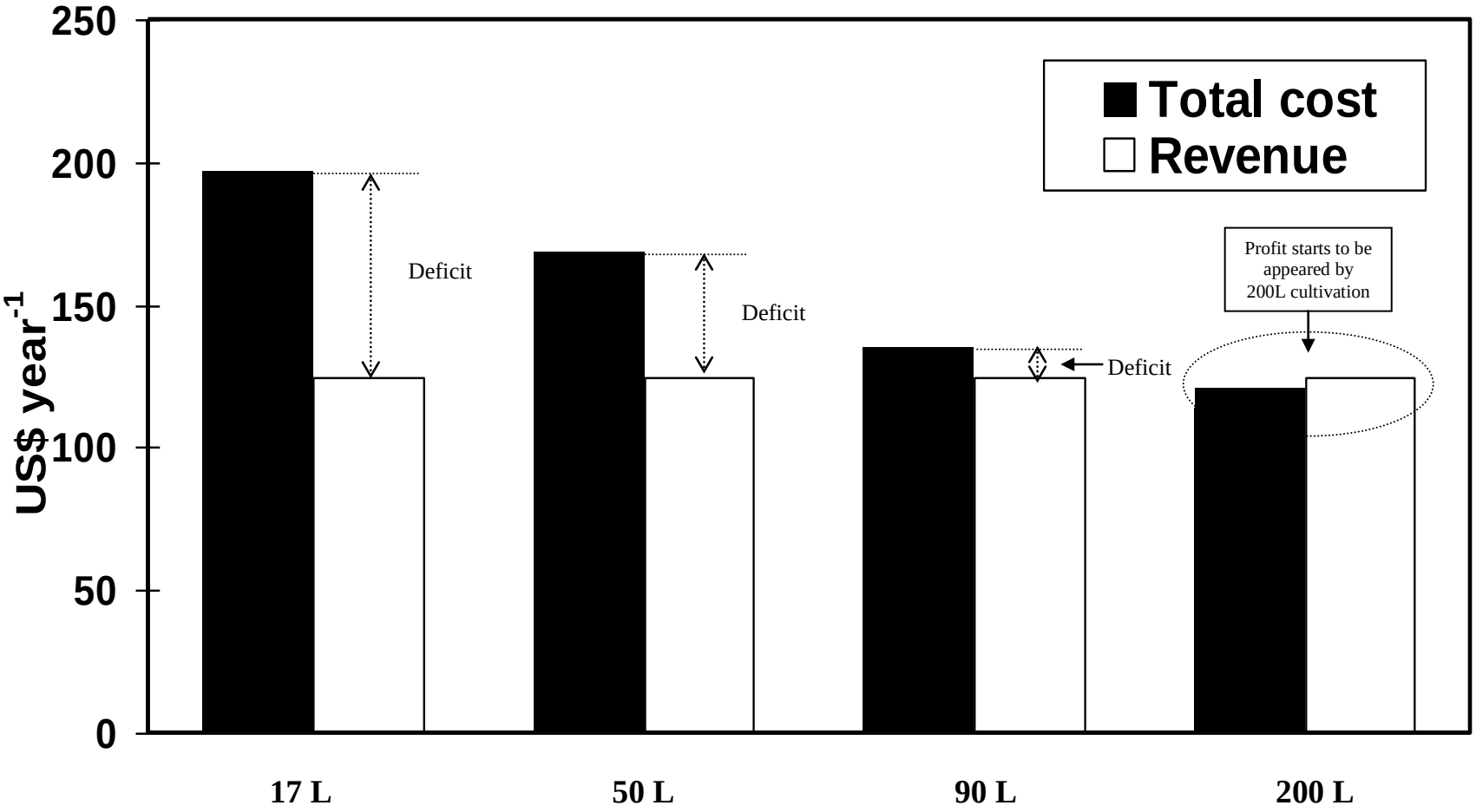

Figure 6.5 Economical evaluation of FP-ALPBRs (17, 50, 90 and 200L) for *H. pluvialis* mass cultivation operated in the evaporative room (temperature was controlled at 27±3 ^{o}C) with natural light supplement (100-500 μmol photon m^{-2} s^{-1}); A_d/A_r = 0.4 and U_{sg} = 0.4 cm s^{-1}

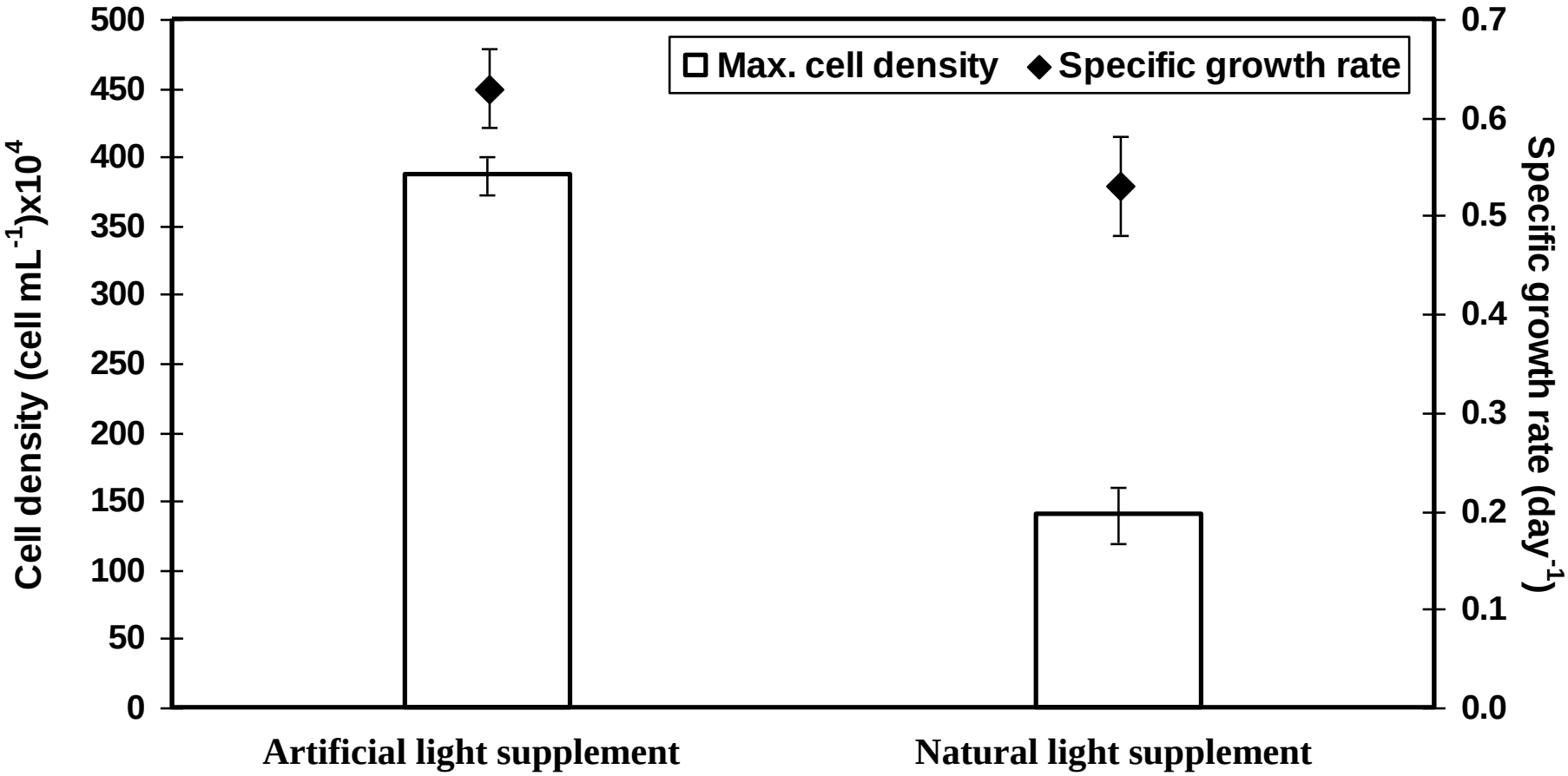

Figure 6.2 Maximum cell density and specific growth rate of *H. pluvialis* in 50L FP-ALPBR operated under different light sources [artificial light supplement (30 μmol photon m^{-2} s^{-1}) VS natural light supplement (100-500 μmol photon m^{-2} s^{-1})] were conducted in evaporative room (temperature was controlled at 27±3 ^{o}C); A_d/A_r = 0.4 and U_{sg} = 0.4 cm s^{-1}.

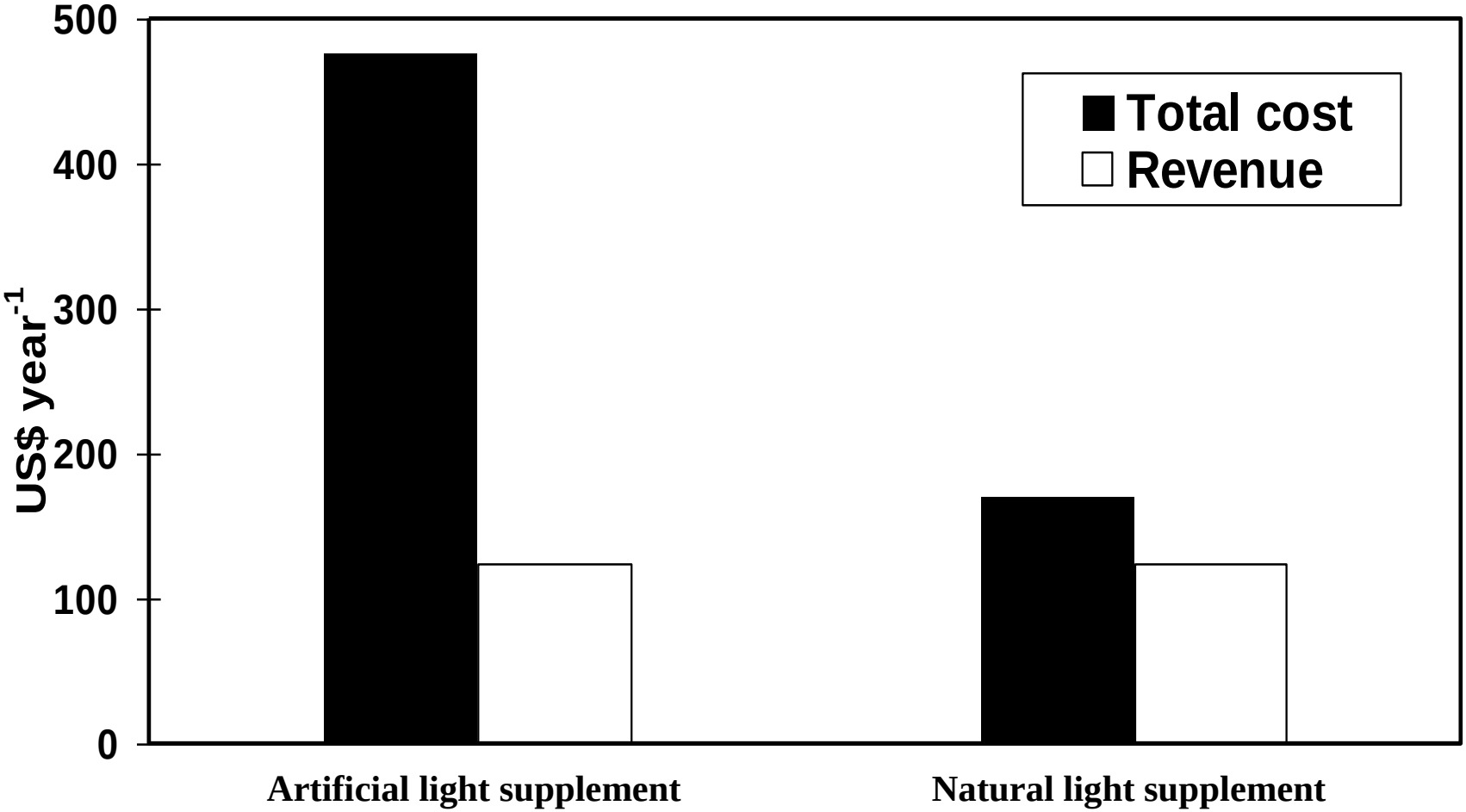

Figure 6.4 Economical evaluation of 50L FP-ALPBR for *H. pluvialis* mass cultivation operated under different light sources [artificial light supplement (30 μmol photon m^{-2} s^{-1}) VS natural light supplement (100-500 μmol photon m^{-2} s^{-1})] was conducted in evaporative room (temperature was controlled at 27±3 ^{o}C); A_d/A_r = 0.4 and U_{sg} = 0.4 cm s^{-1}.

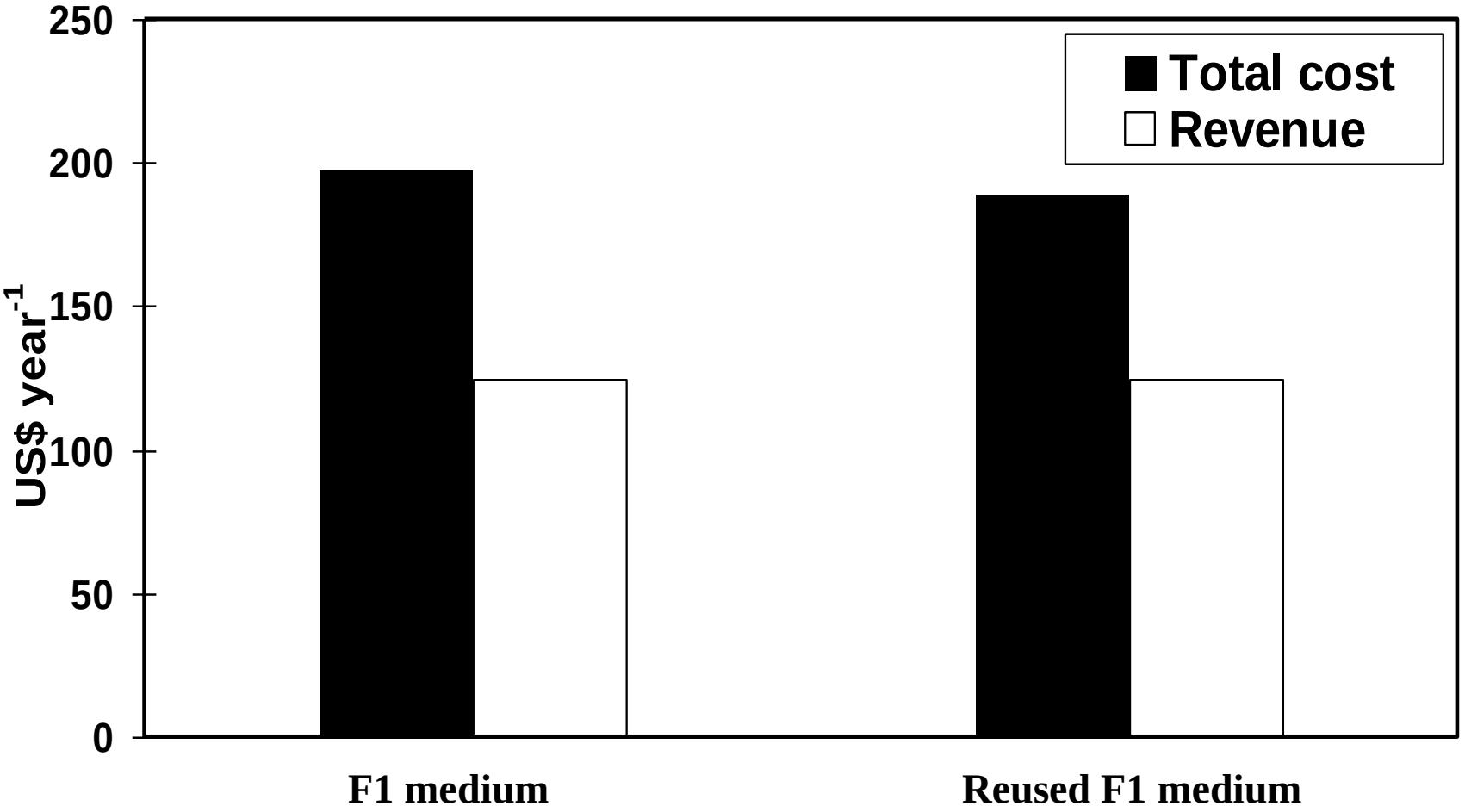

Figure 6.7 Economical evaluation of 17L FP-ALPBR for *H. pluvialis* mass cultivation operated with reused algal medium (the replenishment of nutrients and some trace elements in 2 consecutive cycles was required) was conducted in evaporative room (temperature was controlled at 27±3 ^{o}C) with natural light supplement (100-500 μmol photon m^{-2} s^{-1}); A_d/A_r = 0.4 and U_{sg} = 0.4 cm s^{-1}.

CHAPTER VII

Conclusions and Contributions

7.1 Conclusions

Major findings from this work can be summarized as follows:

1. The pilot scale for cultivation of *Haematococcus pluvialis* NIES-144 in flat panel airlift photobioreactors (FP-ALPBRs) was proven to have economical attraction. The flow chart of the sub-tasks in this study was orderly distributed below.

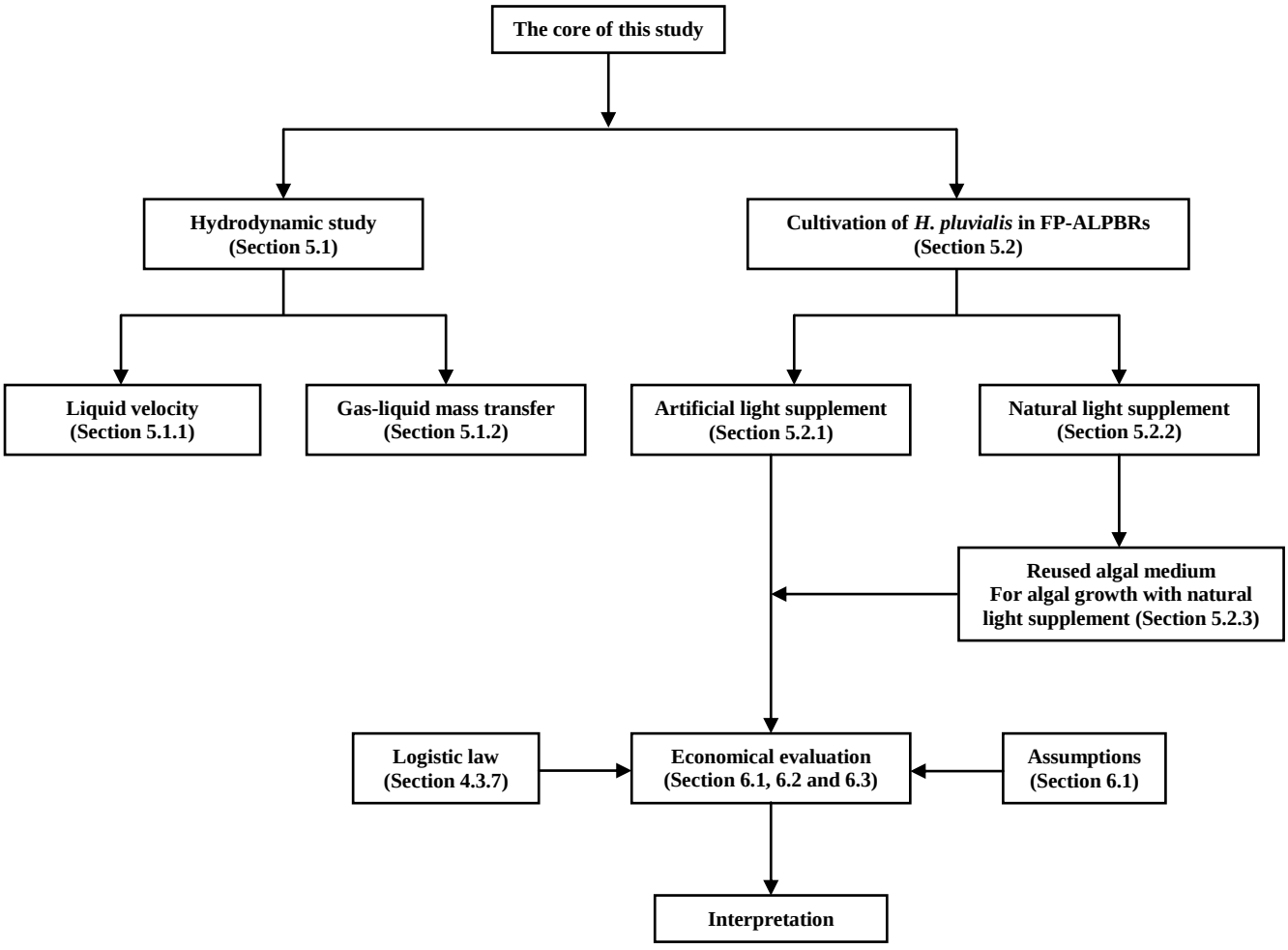

2. The hydrodynamic study reveals that the system with A_d/A_r of 0.4 provided the lowest liquid velocity for 17L ALPBR system (U_l ranged from 1.2-6.3 cm s^{-1}), and the greatest amount of overall volumetric mass transfer coefficient (K_La ranged from 0.000358 to 0.0066 s^{-1}). This condition provides the lowest shear stress which makes it suitable for the green vegetative stage of *H. pluvialis* (as concluded in Issarapayup et al., 2009).

3. Replacing artificial lighting (fluorescent lamp) with natural light supplement (sun light) was found to annually decrease the total production cost by as much as 307 US$ per 0.5 kg dry cell in the 50L FP-ALPBR. Nevertheless, the lack of control of diurnal light intensity sacrificed some growth performance with cell density decreasing from 387 x 10^4 to 140 x 10^4 cell mL^{-1}, and specific growth rate from 0.63 to 0.53 day^{-1}, respectively. Therefore, it can be concluded that the use of natural light supplement was proven to be a viable option for avoiding the high electricity cost but with a cost of biomass productivity lost.

4. The size of reactor appeared to be significant for the profitability of the system. To achieve 0.5 kg dry cell, enlarging the FP-ALPBR from 17 to 200L led to a noticeable reduction in the total cost of algal production (197 US$ for the 17L system, 169 US$ for the 50L, 135 US$ for the 90L, and 121 US$ for the 200L system). Unfortunately this had to be compensated by a drop in the growth performance with cell density decreasing from 290 to 147 cell mL^{-1} and specific growth rate from 0.49 to 0.47 day^{-1} accomplished with 17 and 200L systems, respectively.

5. The reuse of spent growth medium (under natural light operation) with proper replenishment of nutrients (nitrate, phosphate, chromium, selenium and copper) for the first and second reused rounds caused 31% and 31.4% drop in the cell growth. While, the reuse of spent growth medium without replenishment of those absent nutrients for the first and second reused rounds caused 13.3% and 40% drop in the cell growth. Thus far, this proposed

strategy did not seem to provide an attractive response as the overall deduction of total production cost achieved by this option was relatively small compared to the total cost.

7.2 Contributions

This work has achieved a steady and successful operation of *H.pluvialis* cultivation under Thailand climate conditions. Although the maximum size of the reactor employed in this work is limited at 200L, the results have positively shown that the upscale of such reactor should not pose serious concern to the level of efficiency the system might reach. Several productivity enhancement options were proposed including the selection of reactor size, the use of natural sunlight, and the reused of the spent medium. Economical evaluation, on the other hand, indicates that only a large scale working under natural sunlight is feasible if the green vegetative cells of *H. pluvialis* are the target product. The reused medium, although could deduct the total cost of the production, was proven not to be an appealing option as it did not seem to enhance the productivity of the system.

7.3 Recommendation

The enlarged scale FP-ALPBR systems, i.e., 200L for *H. Pluvialis* mass production, based on its hydrodynamic characteristic, is evidently allocated a non-uniformity of fluid flow due to an extension of its column length. Among of other factors (i.e., light availability) causing to algal cell death, this manner is one of those to draw an negative impact on a drop of *H. Pluvialis* growth compared to the small scale system i.e., 17L. Therefore, a feasible idea is launched to overcome this problem where the solution was come out with a small renovated infrastructure design of FP-ALPBR system. More sectional area in such system body is sub-divided into several parts in order to confine direction of up-warded liquid with disciplinal movement. Therefore, this could make its behavior manner similar to small scale design where high algal cell production was achieved.

REFERENCES

Al-Masry., W.A. 1999. Effect of antifoam and scale-up on operation of bioreactors. Chemical Engineering Process 38:197

Andersson, M., Van Nieuwerburgh, V. and Snoeijs, and V. 2003. Pigment transfer from phytoplankton to zooplankton with emphasis on astaxanthin production in the Baltic Sea food web. Marine Ecology Process Series 254: 213–224.

A.O.A.C, 1980. Official Methods of Analysis, 13th ed. Association of official Analytical Chemists. Washington D.C. 376-384**.**

Baten van, J.M., Ellenberger, J., and Krishna, R. 2003. Hydrodynamics of internal air-lift reactors: experiments versus CFD simulations. Chemical Engineering and Processing 42:733-742.

Bellgardt, K. H. 1991. Cell models. In: K. Schügerl, Editor, Biotechnology 4:267-298.

Blazej, M., Kisa, M., and Markos, J. 2004. Scale influence on the hydrodynamics of an internal loop airlift reactor. Chemical Engineering and Processing 43:1519-1527.

Borowitzka, M.A. 1989. Fat, oils and hydrocarbon. Cambridge: Cambridge university press, 27-58.

Borowitzka, M.A. 1996. Closed algal photobioreactor: design considerations for large-scale systems. Journal of Marine Biotechnology 4:185-191.

Boussiba, S. 2000. Carotenogenesis in the green alga *Haematococcus pluvialis*: Cellular physiology and stress reponse. Physiologia Plantarum 108: 111-117.

Boussiba, S., Sandbank, E., Shelef, G., Cohen, Z., Vonshak, A., Ben-Amotz, A., Arad, S., and Richmond, A. 1988. Outdoor cultivation of the marine microalga Isochrysis galbana in open reactors. Aquaculture 72:247–253.

Bubrick, P. 1991. Production of astaxanthin from *Haematococcus*. Bioresource Technology 38:327-329.

Camacho Rubio, F., Acien Fernandez, F.G., Sanchez Perez, J.A., Garcıa Camacho, F., and Molina Grima, E. 1999. Prediction of dissolved oxygen and carbon dioxide concentration profiles in tubular photobioreactors for microalgal culture. Biotechnology and Bioengineering 62:71–86.

Chaumont, D. 1993. Biotechnology of algal biomass production-A review of systems for outdoor mass culture. Journal of applied phycology 5:593-604.

Chen, F., Chen, H., and Gong, X. 1997. Mixotrophic and heterotrophic growth of *Haematococcus lacustris* and theological behavior of the cell suspension. Bioresouce Technology 62:19-24.

Choi. S.L., Suh, I.S., and Lee, C.G. 2003. Lumostatic operation of bubble column photobioreactor for *Haematococcus pluvialis* cultures using a specific light uptake rate as a control parameter. Enzyme and Microbial Technology 33:403-409.

Christiansen, R., and Torrissen, O.J. 1997. Effects of dietary astaxanthin supplementation on fertilization and egg survival in Atlantic salmon (suzmo sazar L.). Aquaculture 153:51-62

Chumpolkulwong, N., Kakizono, T., Handa, T., and Nishio, N. 1997. Isolation and characterization of compactin resistant mutants of an astaxanthin systhesizing green alga *Haematococcus pluvialis*. 1997. Biotechnology Letters 19(3):229-302.

Del Rio, E., Acien, F.G., Garcia-Melea, M.C., Rivas, J., Molina-Grima, and E., Guerrero, M.G. 2005. Efficient one-step production of astaxanthin by the micrpalga *Haematococcus pluvialis* in continuous culture. Biotechnology and Bioengineering 91:808-815.

Del Rio, E., Acien, F.G., Garcia-Melea, M.C., Rivas, J., Molina-Grima, and E., Guerrero, M.G. 2008. Efficient Assessment of the One-Step Production of Astaxanthin by the Microalga *Haematococcus pluvialis*. Biotechnology and Bioengineering 100(2):397-402.

Dominguez-Bocanegra, A.R., Guerrero Legarreta, I., Martinez Jeronimo, F. and Tomasini Campocosio, A. 2004. Influence of environmental and nutritional factors in the production of astaxanthin from *Haematococcus pluvialis*. Bioresource Technology 92:209-214.

Droop, M.R. 1954. Condition governing haematochrome formation and loss in the algae *Haematococcus pluvialis.* Microbiology 20:391-397.

Droop, M.R. 1995. Carotenogenesis in *Haematococcus pluvialis.* Nature 175:42

Fabregas, J., Domınguez, A., Garcıa-Alvarez, D., Lamela, T., and Otero, A., 1998. Induction of astaxanthin accumulation by nitrogen and magnesium deficiencies in *Haematococcus pluvialis*. Biotechnology Letters. 20: 623–626.

Fabregas, J., Domınguez, A., Regueiro, M., Maseda, A., and Otero, A. 2000. Optimization of culture medium for the continuous cultivation of the microalga *Haematococcus pluvialis*. Applied Microbiology Biotechnology 53:530-535.

Fabregas, J., Otero, A., and Dominguez, A. 2001. Two-stage culture for the production of astaxanthin from *Haematococcus pluvialis*. Journal of Biotechnology 89:65-57.

Garcıa-Malea, M.C., Acien, F.G., Fernandez, J.M., Ceron, M.C., and Molina, E. 2006. Continuous production of green cells of *Haematococcus pluvialis*: Modeling of the irradiance effect. Enzyme and Microbial Technology 38 : 981–989.

Garcıa-Malea, M.C., Acien, F.G., Rio, E.D., Fernandez, J.M., Ceron, M.C., Guerrero, M.G., and Molina-Grima, E. 2009. Production of Astaxanthin by *Haematococcus pluvialis*: Taking the One-Step System Outdoors. Biotechnology and Bioengineering 102(2):651-657.

Grunewald, K., Hagen, C., and Braune, W. 1997. Secondary carotenoid accumulation in flagellates of the green alga *Haematococcus lacustris.* European Journal of Phycology 32:387-392.

Gudin, C., and Chaumont, D. 1991. Cell fragility-The key problem of microalgae mass production in closed photobioreactor. Bioresource Technology 38:145-151.

Hagen, C., and Braune, S.S.W., 2002. Ultrastructural and chemical changes in the cell wall of *Haematococcus pluvialis* (Volvocales, Chlorophyta) during aplanospore formation. European Journal of Phycology 37:217–226.

Harker, M., Tsavalos, A.J., and Yong, A.J. 1996(a). Autotrophic growth and carotenoid production of in 30 liter air-lift photobioreactor. Journal of Fermentation and Bioengineering 82(2):113-118.

Harker, M., Tsavalos, A.J., and Yong, A.J. 1996(b). Factor responsible for astaxanthin formation in the Chlorophyte *Haematococcus pluvialis*. Bioresource Technology 55:207-214.

Hase, R., Oikawa, H., Sasao, C., Morita, M., and Watanabe, Y. 2000. Photosynthetic production of microalgal biomass in a raceway system under greenhouse conditions in Sendai City. Journal of Bioscience and Bioengineering. 89:157-163.

Hata, N., Ogbonna, J.C., Hasegawa, Y., Taroda, H., and Tanaka. 2001. Production of astaxanthin by *Haematococcus pluvialis* in a sequential heterotrophic-photoautotrophic culture. Journal of Applied Phycology 13:395-402.

Heijnen, J.J., Hols, J., van der Lands, R.G.J.M, van Leeuwen, H.L.J.M, Mulder, A., and Weltevrede, R. 1997. A simple hydrodynamic model for the liquid circulation velocity in a full-scale two-and three-phase internal airlift reactor operating in the gas recirculation regime. Chemical Engineering Science 52(15):2527

Hoekema, S., Bijmans, M., Janssen, M., Tramper, J., and Wijffels, R.H. 2002. A pneumatically agitated flat-panel photobioreactor with gas recirculation: anaerobic photoheterotrophic cultivation of a purple nonsulfur bacterium. International Journal of Hydrogen Energy 27:1331-1338.

Hu, Q., Guterman, H., and Richmond, A. 1996. A flat inclined modular photobioreactor for outdoor mass cultivation of phototrophs. Biotechnology and Bioengineering 51:51-60.

Issarapayup, K., Powtongsook, S., and Pavasant, P. 2009. Flat panel airlift photobioreactors for cultivation of vegetative cells of microalga *Haematococcus pluvialis*. Journal of Biotechnology. 142:227-232.

Johnson, E. A. and An, G. H. 1991. Astaxanthin from microbial sources. Critical Review Biotechnology., 11, 297-326.

Kaewpintong, K., Shotipruk, A., Powtongsook, S., and Pavasant, P. 2006. Photoautotrophic high-density cultivation of vegetative cells of *Haematococcus pluvialis* in airlift bioreactor. Bioresource Technology 98(2):288-295.

Kang, C.D., An, J.Y., Park, T.H., and Sim, S.J. 2006. Astaxanthin biosynthesis fromsimultaneous N and P uptake by the green alga *Haematococcus pluvialis* in primary-treated wastewater. Biochemical Engineering Journal 31:234-238.

Katsuda, T., Lababpour, A., Shimahara, and Katoh, K. 2004. Astaxanthin production by *Haematococcus pluvialis* under illumination with LEDs. Enzyme and Microbial Technology 35 : 81–86.

Kobayashi, M., Kakizono, T., and Nagai, S. 1991. Astaxanthin production by green algal, *Haematococcus pluvialis* accompanied with morphological changes in acetate media. Journal of Fermentation and Bioengineering 71(5):335-339.

Kobayashi, M., Kumurira, Y., Kakizono, T. Nishio, N., and Tsuji, Y. 1997. Morphology change in the life cycle of the green alga *Haematococcus pluvialis*. Journal of Fermentation and Bioengineering 84:94-97.

Kobayashi, M., and Sakamoto, Y. 1999. Singlet oxygen quenching ability of astaxanthin ester from the green alga *Haematococcus pluvialis*. Biotechnology Letter 21:265-269.

Krichnavaruk, S., Loataweesup, W., Powtongsook, S., and Pavasant, P. 2005. Optimal growth conditions and the cultivation of *Chaetoceros calcitran* in airlift photobioreactor. Chemical Engineering Journal 105:91-98.

Krichnavaruk, S., Powtongsook, S., and Pavasant, P. 2007. Enhanced productivity of *Chaetoceros calcitran* in airlift photobioreactors. Bioresource Technology 98:2123-2130.

Lee, Y.K. and Soh, C.W. 1991. Accumulation of astaxanthin in H. lacustris (Chlorophyta). Journal of Phycology 27: 575-577.

Lee, Y.K. 2001. Micro algal mass culture system and methods: Their limitation and potential. Journal of Applied Phycology 9:403-411.

Lee, Y.K. and Richmond A. 1998. Bioreactor technology for mass cultivation of photoautotropic microalgae. Environmental Marine Biotechnology 2:271-288.

Lee, C.G., Suh, I.S., Joo, and H.N. 2005. Multi-layered photobioreactor and method of culturing photosynthetic microorganisms using the same. WO/2005/059087

Lee, H.S., Seo, W.W., Kim, H.K., and Lee, C.G. 2006. Determining the best specific light uptake rates for the lumostatic cultures in the bubble column photobioreactors. Enzyme and Microbial Technology 39:447-452.

Lorenz, R.T., and Cysewski, G.R. 2000. Commercial potential for *Haematococcu*s microalgae as a natural source of astaxanthin. Trends in Biotechnology 18(4):160-7.

Mendes-Pinto, M.M., Raposo, M.F.J., Bowen, J., Young, A.J., and Morais, R., 2001. Evaluation of different cell disruption processes on encysted cells of Haematococcus pluvialis: effects on astaxanthin recovery and implications for bio-availability. Journal of Applied Phycology 13: 19–24.

Miki, W. 1991. Biological functions and activities of carotenoids. Pure and Applied Chemistry 63:141-146.

Misawa, N. and Shimada, H. 1998. Metabolic engineering for the production of carotenoids in non-carotenogenic bacteria and yeasts. Journal of Biotechnology 59:169-181.

Monkunsit, S., Powtongsook, S., and Pavasant, P. 2011. Comparison between Airlift Photobioreactor and Bubble Column for *Skeletonema costatum* cultivation. Engineering Journal 15(4):53-64

Olaizola, M. 2000. Commercial production of astaxanthin from Haematococcus pluvialis using 25000-liter outdoor photobioreactors. Journal Applied Phycology. 12:499-506.

Palozza, P., and Krinsky, N.I. 1992. astaxanthin and canthaxanthin are potent antioxidants in a membrane model. Archives of Biochemistry and Biophysics 297:291-295.

Parker, L. 1992. Method is Enzymology: Carotenoid Part A; Chemistry, Separation, Quantitation and Antioxidation. Carifornia:Academic Press: 124-136.

Pruvost, J., Pottier, L., and Legrand, J. 2006. Numerical investigation of hydrodynamic and mixing conditions in a torus photobioreactor. Chemical Engineering Science 61(14):4476-4489.

Ranjbar, R., Inoue, R., Shiraishi, H., Katsuda, T. and Katoh, S. 2007. High efficiency production of astaxanthin by autotrophic cultivation of *Haematococcus pluvialis* in a bubble column photobioreactor. Journal of Biochemical Engineering 39(3):575-580.

Ranjbar, R., Inoue, R., Katsuda, T., Yamaji, H., and Katoh, S. 2008. High efficiency production of astaxanthin in an airlift photobioreactor. Journal of Bioscience and Bioengineering 106(2), 204-207.

Renstrom, B., Borch, G., Skulberg, O.M., and Jensen, S.L. 1981. Optical purity of (3S, 3'S)-astaxanthin from *Haematococcus pluvialis*. Phytochemistry 20:2561-2564.

Richmond, A. 1996. Effect utilization of high irradiance for production of photoautotropic cell mass. Journal of Applied Phycology 8: 381-387.

Rockette, T.R. 1970. The pigment of *praninophyceae* and related organism. Journal of Phytochemistry 9:1835-1842.

Ruen-ngam, D., Wongsuchoto, P., Limpanuphap, A., Charinpanitkul, T., and Pavasant, P. 2008. Influence of salinity on bubble size distribution and gas-liquid mass transfer in airlift contactors. Chemical Engineering Journal.

Sanchez Miron, A., Ceron Garcıa, M.C., Garcıa Camacho, F., Molina Grima, E., and Chisti, Y. 2002. Growth and characterization of microalgal biomass produced in bubble column and airlift photobioreactors: studies in fed-batch culture. Enzyme and Microbial Technology 31:1015-1023.

Schoefs, B., Rmiki, N.E., Rachadi, J., and Lemoine, Y. 2001. Astaxanthin accumulation in *Haematococcus* requires a cytochrome P450 hydroxylase and an active synthesis of fatty acids. FEBS Letters 500:125-128.

Simpson, K.L., Katayama, T. and Chichester, C.O. 1981. Carotenoid in fish feeds. In: J.C. Bauernfeind, Editor, Carotenoids as colorants and vitamin A precursors. Academic Press, Inc, New York, USA 4:463-538.

Smith, G.M. 1950. The Fresh Water Algae of the United States second edition. New York: Mc Grew-Hill Book Company: 39-45.

Spencer, K.G. and Poway, CA 1989. Pigmentation supplements for animal feed compositions. Microbial Resources Inc (US)

Strickland, J.D., Parsons, T.R. 1972. A practical handbook of seawater analysis**.** Fishery Research Board of Canada. Otawa. 310.

Suh, I.S., Joo, H.N., and Lee, C.G. 2006. A novel double-layered photobioreactor for simultaneous *Haematococcus pluvialis* cell growth and astaxanthin accumulation. Journal of Biotechnology 125(4):540-546.

Thimijan, Richard, W., and Rayal, D.H. 1982. Photometric, Radiometric, and Quantum light units of measure: A review of procedures for interconversion. HortScience 18:818-822.

Tjahjono, A.E., Kakizono, T., Hayama, Y., Nishio, N., and Nagai, S. 1994. Isolation of resistant mutants against carotenoid biosynthesis inhibitors for a green alga *Haematococcus pluvialis,* and their hybrid formation by protoplast fusion for breeding of higher astaxanthin producers. Journal of Fermentation and Bioengineering 77(4):352-357.

Tocquin, P., Fratamico, A., and Franck, F. 2011. Screening for a low-cost *Haematococcus pluvialis* medium reveals an unexpected impact of a low N/P ratio on vegetative growth. Journal of Applied Phycology Article in Press, p.p. 1-9

Tredici, M.R., and Materassi, R., 1992. From open ponds to alveolar panels: the italian experience in the development of reactor for the mass cultivation of phototrophic microorganisms. Journal of Phycology 4:221:231.

Tripathi, U., Sarada, R., Rao, S.R., and Ravishankar, G.A. 1999. Production of astaxanthin in *Haematococcus pluvialis* cultured in various media. Bioresource Technology 68 :197-199.

Tung, H.L., TU, C.C., Chang, Y.Y., and Wu, W.T. 1998. Bubble characteristics and mass transfer in an airlift reactor with multiple net draft tubes. Bioprocess Engineering 18:323-328.

Tunthikul, N., Wongsuchoto, P., and Pavasant, P. 2006. Hydrodynamics and mass transfer behavior in multiple draft tube airlift contractors. Korean Journal of Chemical Engineering 23(6):881-887.

Ugwu, C.U., Aoyagi, H., and Uchiyama, H., 2008. Photobioreactors for mass cultivation of algae. Bioresource Technology 99(10):4021-4028

Ugwu, C.U., Ogbonna, J.C., and Tanaka, H. 2003. Design of static mixers for inclined tubular photobioreactors. Journal of Applied Psychology 15:217-223.

Van Nieuwerburgh, L., Wanstrand, I., Liu, J., and Snoeijs, P. 2005. Astaxanthin production in marine pelagic copepods grazing on two different phytoplankton diets. Journal of SEA Research 53:147-160.

Vega-Estrada, J., Montes-Horcasitas, M. C., Dominguez-Bocanegra, A.R., and Canizares- Villanueva, R.O. 2005. *Haematococcus pluvialis* cultivation in split-cylinder internal-loop airlift photobioreactor under aeration conditions avoiding cell damage. Applied Microbiology and Biotechnology 68:31-35.

Vonshak, A. 1997. Outdoor mass production of *spirulina*: The basic concept. Cell Biology and Biotechnology 77-99.

Vonshak, A., and Torzillo, G. 2004. Environmental Stress Physiology. In: Richmond, A. (Ed.), Handbook of Microalgal Culture. Blackwell Publishers, Oxford, pp. 57-82.

Vunjak-Novakovic, G., Kim, Y., Wu, X., Berzin, I., and Merchuk, J.C. 2005. Air-lift bioreactors for algal growth on fuel gas: Mathematical modeling and pilot-plant studies. Industrial & Engineering Chemistry Research 44:6154-6163.

Wang, S., Arimatsu, Y., Koumatsu, K., Furumoto, K., Yoshimoto, M., Fukunaka, K., and Nakao, K. 2003. Gas holdup, liquid circulating velocity and mass transfer properties in a mini-scale external loop airlift bubble column. Chemical Engineering Science 58:3353-3360.

Wongsuchoto, P., Charinpanitkul, T., and Pavasant, P. 2003. Bubble size distribution and gas–liquid mass transfer in airlift contactors. Journal of Chemical Engineering. 92 : 81–90.

Wongsuchoto, P., and Pavasant, P. 2004. Internal liquid circulation in annulus sparged internal. Journal of Chemical Engineering 100:1-9.

Zhang, X.W., Gong, X.F., and Chen, F. 1999. Kinetic models for astaxanthin production by high cell density mixotrophic culture of the microalga *Haematococcus pluvialis*. Journal of Industrial Microbiology and Biotechnology 23:691-696.

Zhang, K., Kurano, N., and Miyachi, S. 2002. Optimized aeration by carbon dioxide gas for microalgal production and mass transfer characterization in a vertical flat-plate photobioreactor. Bioprocess and Biosystems Engineering 25:97-101.

BIOGRAPHY

Mister Kerati Issarapayup was born on 23rd January, 1983 in Nakornratchasrima. He finished his secondary course from Bodindecha (Sing Singhaseni) 2 School in March, 2001. After that, he studied in the major of Biochemistry in Faculty of Science at Chulalongkorn University. He continued his further study for Master's degree in Chemical Engineering at Chulalongkorn University. He participated in the Biochemical Engineering Research Group and achieved his Master's degree in March, 2007. He continued pursuing his Ph.D. degree in the same year. During the Ph.D. program, he was granted by Thailand Graduate Institute of Science and Technology (TGIST) and assistant professor Samir Kumar Khanal, who is a graduate chair of Biochemical Engineering Program at University of Hawaii at Manoa, USA to conduct his research abroad at Department of Molecular Biosciences and Bioengineering, University of Hawaii at Manoa, Hawaii, USA for about a year (November, 2010 to October 2011) as a short term research scholarship. He finally achieved his Ph.D. degree in 2011.